Master of Science in
Electronics and Telecommunication Engineering

Analysis on Simple Feed Microstrip Patch Array Antenna Design for Circular Polarization Diversity and Beam Switching with DOA Estimation

by

Debprosad Das

ID: 19METE024F

This thesis is submitted in partial fulfillment of the requirement for the degree of Master of Science in Electronics and Telecommunication Engineering

Department of Electronics and Telecommunication Engineering
Chittagong University of Engineering and Technology
Chattogram-4349, Bangladesh.
March, 2024

CERTIFICATION

The thesis titled **Analysis on Simple Feed Microstrip Patch Array Antenna Design for Circular Polarization Diversity and Beam Switching with DOA Estimation** submitted by **Debprosad Das**, Roll No. **19METE024F**, Session **2019-2020** has been accepted as satisfactory in partial fulfillment of the requirement for the degree of **Master of Science in Electronics and Telecommunication Engineering** on **25/03/2024**.

BOARD OF EXAMINERS

1. _____

Dr. Md. Azad Hossain — Chairman (Supervisor)
Professor & Head
Department of Electronics and Telecommunication Engineering
Chittagong University of Engineering & Technology (CUET)
Chittagong-4349

2. _____

Dr. Md. Jahedul Islam — Member
Professor
Department of Electronics and Telecommunication Engineering
Chittagong University of Engineering & Technology (CUET)
Chittagong-4349

3. _____

Dr. Md. Saiful Islam — Member
Associate Professor
Department of Electronics and Telecommunication Engineering
Chittagong University of Engineering & Technology (CUET)
Chittagong-4349

4. _____

Dr. Muhammad Asad Rahman — Member (External)
Professor
Department of Electrical and Electronic Engineering
Chittagong University of Engineering & Technology (CUET)
Chittagong-4349

Author Declaration for Electronic Submission of MRP

I hereby declare that I am the sole author of the MRP. This is a true copy of the MRP, including any final revisions, as accepted by my Examiners.

I hereby also declare that the work contained in this Thesis could be uploaded to the repository of the library, Chittagong University of Engineering and Technology after 1 year of submission.

I authorize Chittagong University of Engineering and Technology to land this MRP to other institutions or individuals for the purpose of scholarly research.

I further authorize the Chittagong University of Engineering and Technology to reproduce this MRP by photocopying or by other means, in total or in part, at the request of other institutions or individuals for the purpose of scholarly research.

I understand that my MRP may be made electronically available to the public.

Signature of the Candidate

Debprosad Das
ID: 19METE024F

CANDIDATE'S DECLARATION

It is hereby declared that this thesis or any part of it has not been submitted elsewhere for the award of any degree or diploma.

Signature of the Candidate

Debprosad Das
ID: 19METE024F

APPROVAL by the SUPERVISOR

This is to certify that DEBPROSAD DAS has carried out this research work under my supervision and that he has fulfilled the relevant Academic Ordinance of the Chittagong University of Engineering and Technology so that he is qualified to submit the following Thesis in the application for the degree of MASTER of SCIENCE in ELECTRONICS AND TELECOMMUNICATION ENGINEERING. Furthermore, the Thesis compiles with the PLAGIARISM and ACADEMIC INTEGRITY regulations of CUET.

Signature of the Supervisor

Dr. Md. Azad Hossain
Professor & Head
Department of Electronics and Telecommunication Engineering
Chittagong University of Engineering and Technology
Chittagong-4349

List of Publications

The following publication is a direct consequence of the research carried out during the elaboration of the thesis and gives an idea of the progression that has been achieved.

Journal Articles

1. **Das, D.**, Hossain, M. F., & Hossain, M. A. (2024). A simple feed orthogonal excitation X-band dual circular polarized microstrip patch array antenna. International Journal of Electrical and Computer Engineering (IJECE), 14(2), 1604-1615.

2. Hossain, M. F., **Das, D.**, & Hossain, M. A. (2024). A 5G beam-steering microstrip array antenna using both-sided microwave integrated circuit technology. International Journal of Electrical and Computer Engineering (IJECE), 14(1), 457-468.

3. **Das, D.**, Hossain, M. F., Hossain, M. A., Rahman, M. A., Hossain, M. M., & Hossam-E-Haider, M. (2024). Phase delay through slot-line beam switching microstrip patch array antenna design for sub-6 GHz 5G band applications. International Journal of Electrical and Computer Engineering (IJECE), 14(2), 1625-1633.

4. **Das, D.**, Hossain, M. F., & Hossain, M. A. (2023). Design and characterization of a circularly polarized microstrip-line-fed slot array antenna for S-band applications. Int. J. Electr. Comput. Eng, 13(6), 6399-6409.

Conference Procedings

1. **Das, D.**, Hossain, M. F., & Hossain, M. A. (2023, December). An X-Band Dual Circular Polarized Single Feed Three-Element Microstrip Patch Array Antenna. In 2023 6th International Conference on Electrical Information and Communication Technology (EICT) (pp. 1-6). IEEE.

2. **Das, D.**, Hossain, M. F., & Hossain, M. A. (2023, December). A Four-Element Patch Array Antenna for Direction of Arrival (DOA) Estimation with Beam Switching Applications. In 2023 26th International Conference on Computer and Information Technology (ICCIT) (pp. 1-5). IEEE.

3. **Das, D.**, Hossain, M. A., Rahman, M. A., & Paul, L. C. (2024, April). 1D Beam Switching Four Element Microstrip Patch Array Antenna with Planar 90° Hybrid Circuit. In 2024 3rd International Conference on Advancement in Electrical and Electronic Engineering (ICAEEE) (pp. 1-5). IEEE.

4. **Das, D.**, Hossain, M. A., & Rahman, M. A. (2024, April). Circularly Polarized Single Layer Large Scale Microstrip Patch Array Antenna for Wireless Communications. In 2024 3rd International Conference on Advancement in Electrical and Electronic Engineering (ICAEEE) (pp. 1-5). IEEE.

Dedication

It is a common belief that parents avoid crying in front of their children. There were moments when my parents shed tears for my struggles.

I look forward to witnessing their tears. Tears of happiness.

To that single drop of tear...

Acknowledgment

I am profoundly thankful to God for granting me strength, direction, and blessings during my academic journey. I am wholeheartedly grateful to my supervisor, **Dr. Md. Azad Hossain**, Professor, and Head of the ETE Department at CUET, for his essential mentorship, consistent support, and expert assistance. His support has significantly motivated my academic success.

I would also like to express my gratitude to the members of my oral examination board for their useful feedback and constructive suggestions.

I want to express my gratitude to the teachers and other members of the ETE Department for their knowledge-sharing, encouragement, and dedication to creating a dynamic learning environment.

I would like to express my appreciation to my amazing friend Eftekhar Hossain, a faculty member of ETE, CUET, for assisting me with the formatting of my thesis using LaTex. He has served as a source of inspiration for many, including myself, in terms of academic advancement.

Finally, I want to thank my friends, especially Md. Farhad Hossain, who serves as a faculty member of ETE, and my family, and loved ones for their consistent support, understanding, and encouragement during my academic journey. This achievement is the outcome of collaborative endeavors, and I am thankful to all those who have contributed to my development and accomplishments.

Abstract

The terminal node antenna of a wireless communication device should possess the ability to perform many roles since modern communication necessitates the adoption of advanced approaches to address the rapidly evolving needs of end users. Circular polarization diversity, beam switching, and direction-of-arrival estimation (DOA) are advanced antenna applications that can enhance power efficiency and enable lossless transmission, therefore addressing the demands of the present time. In addition, it is necessary for the devices, especially the antennas, to have lower dimensions, even when considering long-distance communication, which typically requires a large-scale array antenna. Integrating microstrip patch antennas, which have a low profile and are lightweight, into transmitting or receiving devices can resolve the problem. This thesis study focuses on the design and simulation of a microstrip patch array antenna. The purpose is to analyze its applicability in the areas of circular polarization, beam-switching, and DOA estimation. A microstrip patch array antenna is constructed using both-sided microwave integrated circuit (MIC) technology to achieve circular polarization while keeping the feed network simple. A four-element microstrip patch array antenna is constructed, simulated, and validated to determine the feasibility of creating a large extensible array with 256 elements. The antenna utilizes a simple single feed to achieve circular polarization. By making a simple adjustment to the feed line, the formation of a Magic-T junction enables beam switching. Additionally, a simple modification in the design allows for direction of arrival (DOA) estimation. The simulation results demonstrate that the antennas have the capacity to transmit across long distances with circular polarization, achieving a gain of more than 26.15 dBic. Additionally, the antennas can alter their beam direction by up to $\pm 17^{\circ}$. Additionally, they have the capability to determine position by isolating the sum signal and the difference signal by different ports.

Keywords: Array antenna, Beam switching, Both-sided MIC, Circular polarization, DOA estimation, Left-hand circular polarization (LHCP), Magic-T, Microstrip patch, Right-hand circular polarization (RHCP).

Contents

List of Figures

List of Tables

List of Abbreviations

AR	Axial ratio
ARBW	Axial Ratio Bandwidth
BW	Bandwidth
CO-POL	Co Polarization
CP	Circular Polarization
DOA	Direction of Arrival
EMW	Electromagnetic Wave
ESPRIT	Estimation of Signal Parameters via Rational Invariance Techniques
LHCP	Left-Hand Circular Polarization
LP	Linear Polarization
MIC	Microwave Integrated Circuit
MIMO	Multiple Input Multiple Output
MUSIC	MUltiple SIgnal Classification
RFID	Radio Frequency Identification
RHCP	Right-Hand Circular Polarization
UAV	Unmanned Ariel Vehicle
Wi-Fi	Wireless Fidelity
WLAN	Wireless Local Area Network
X-POL	Cross Polarization

Chapter 1

Introduction

Considering the remarkable advancements in wireless communication, it is essential to embrace antenna technology to keep up with the ever-changing demands of modern wireless communication systems. To adapt to the rapid changes in the communication system, antenna technology has evolved to meet the demands of various wireless communication systems like mobile communication, Satellite communication, wireless local area network (WLAN), radio frequency identification (RFID), and radar technology. Considering these applications, antennas need to support various applications like circular polarization (CP) diversity, beam switchability, and source localization and seamlessly integrate them with communication system circuits for improved performance [1, 2].

1.1 Antenna in Wireless Communication

In the year 1886, German physicist Heinrich Hertz pioneered the development of a straightforward dipole antenna, which would go on to become an essential component of the end node of wireless communication systems [3, 4]. Since then antenna research has evolved in various directions as the need for applications in various sectors has increased and various types of antennas have entered into wireless communication systems, for example, horn antennas, parabolic reflector antennas, wire antennas, radar antennas, Satellite antennas, unmanned Ariel vehicle (UAV) antennas, etc [5]. With the passage of time and the development of wireless communication systems, there is an increasing interest in making electromagnetic (EM) wave launchers or antennas more compact so that they may be readily integrated into the system and bring agility to the system. However, there are several traditional antennas that had been evaluated and developed in the time between the two world wars and are still in use today. Although it was initially introduced in 1906 with the goal of directivity to realize clear and

stronger reception at the receiver end of the system over long distances, one of these antennas is an array antenna, which is a set of several individual antennas that collectively operate as an antenna [6].

1.2 Motivation: Microstrip Patch Array

At an early period in the history of antenna development, it became necessary to minimize the overall size of the radiators in order to compensate for the bulkiness that was present in the design of a wireless system. Since we are currently in the midst of a generation in communication technology known as 5G, it has become increasingly important to make the antenna more compact, cost-effective in fabrication, easy to install, and low profile, while also ensuring that it has excellent directivity, source sensing, and beam agility. Given the presence of several factors, including antenna orientation sensitivities and multipath fading, it is essential that the antennas have also the capability to transmit a circularly polarized signal [7]. One of the many types of antennas, the microstrip patch antenna was first conceptualized in 1953 and later implemented in the 1970s when suitable substrate materials became available. Although microstrip patch array antennas have some drawbacks such as narrow bandwidth and lesser radiation efficiency, they are a fruitful consideration for design and implementation due to their remarkable advantages like easy installation, easy fabrication, low profile, cost-effectiveness, and conformal nature, especially considering the above-mentioned applications and factors associated with wireless communication systems. Furthermore, as a result of the numerous methods that were developed by researchers in order to make up for the shortcomings of microstrip patch arrays, they became extremely popular in the communication industry due to the incredible benefits that they offered [8, 9].

1.3 Importance: Multi-application Antenna

The emergence of 5G technology in the communication sector has led to a significant increase in the attention given by antenna engineers to multi-functional array antennas. This is because these antennas are capable of reducing the complexity of the circuits at both the transmitting and receiving ends of a communication system and ensuring a high level of circuit integrity [10, 11]. Figure 1.1 depicts a general communication scenario involving several applications such as circular polarization, beam switching, and direction-of-arrival (DOA) estimation.

Long-distance communication, such as satellite communication, necessitates

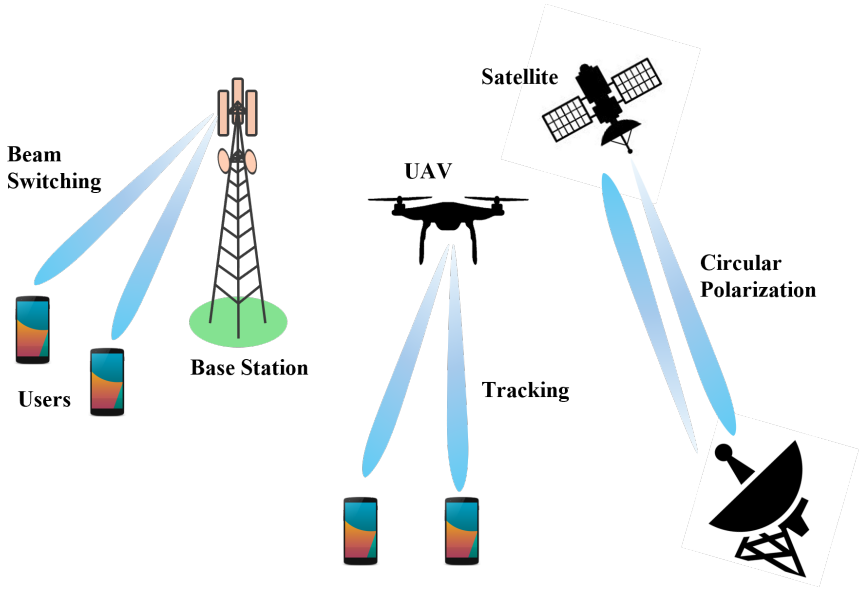

Figure 1.1: A general communication scenario where applications of antennas like circular polarization, beam switching, and direction-of-arrival (DOA) estimation are required.

high-gain, highly directional antennas, achievable by array antennas. The satellite communication signal must be immune to Faraday's rotation effect caused by the ionosphere, which rotates the signal's polarization plane from vertical to horizontal and vice versa, resulting in unsuccessful transmission at the receiving end [12, 13]. For optimal communication in this scenario, the radiating signal should be circularly polarized to minimize the Faraday rotation effect. Circular polarized signals are necessary for communication in urban or rural areas where multipath fading is caused by reflections from trees or buildings, as they are resistant to this type of fading [14].

Modern antennas are required to broadcast their signal in a certain direction and have the ability to alter the beam in order to track the flow of traffic. This is necessary in order to accommodate fast-moving traffic as well as an increasing number of users and ensure proper and dependable transmission. This is something that can be accomplished by beam-switching antennas by adjusting the emitted beam as required. For an antenna radiating in the broadside direction, it is more beneficial to electronically regulate the current propagation path within the antenna or adjust the phase among the radiators of an array, rather than moving or steering it physically to direct the beam in a specific direction [15, 16, 17].

Additionally, for tracking purposes, the antenna should have the capability to tell the location of the source by analyzing the received signal. Therefore, from

the received signal, determining the source, and establishing proper transmission by sending a signal to that particular direction where the source is located, the antenna should perform multiple functions, like the direction of arrival estimation as well as beam switching, to simultaneously build a stable connection between the source and the receiver [18, 19, 20, 21].

Considering these applications and the present communication scenario having an array antenna that can function in a multi-functional manner is essential for enhancing the communication system by integrating the transmission system with ease, improving spectral efficiency, and enhancing multiple-input-multiple-output (MIMO) performance, a recent development in 5G technology originating from the 1970s [22], and providing adaptability in a flexible manner.

1.4 Challenges

Multifunctional antennas, such as frequency reconfigurable antennas, are among the various types of antennas that are capable of functioning at two different resonant frequency bands. When a single antenna is able to handle two different frequency bands for uplink and downlink operations, such as in satellite communication, these antennas are beneficial. They are also useful in situations where more than one antenna is required. There are antenna systems that are able to modify the polarization and pattern in order to meet situations that involve multipath fading, mismatched polarization between the transmitter and the receiver, and the requirement to direct the beam in a particular direction in order to maximize the intensity of the signal. It is possible to find antenna systems that are able to simultaneously detect the source of the signal and direct the beam that is being sent in that direction. However, developing an antenna capable of circular polarization, beam switchability, and direction of arrival estimate concurrently is a tough challenge due to the potential complexity of the required feed network or circuitry. Therefore, the development of an antenna that can be used for a variety of purposes calls for careful study, including the following:

- The design of such an antenna has the potential to enhance the overall circuit's complexity, which is something that should be avoided in a communication system to preserve the integrity of the system, it is essential to keep the antenna functioning uncomplicated.

- It is possible that this kind of application could be practical for a small array; however, for communication systems that are used over long distances, it might be necessary to have a large-scale array. In considering this, it is

of the utmost importance to make certain that the antenna is capable of serving a multitude of applications simultaneously while also being able to accommodate larger-scale activities.

1.5 Objectives

This thesis proposes an analysis of the microstrip patch array antennas that can operate on circular polarization of both senses and can switch the radiated beam accordingly while estimating the direction of the received signal. This work also emphasizes on the fact that the feeding technique remains simple while achieving those applications. The objectives of this thesis work are as follows:

- Analyzing a single-layer microstrip patch array antenna design containing three radiators with a simple feed technique using both-sided MIC technology and simulating the design to achieve circular polarization of both senses that is left-hand circular polarization and right-hand circular polarization. Also, analyzing what factor of the design improves the performance.
- Analyzing a microstrip patch array antenna with four elements on a single layer using both-sided MIC technology and designing it for a larger array of 256 elements using simulation. Additionally, investigate the feasibility of using this antenna for long-distance communication.
- Analyzing single-layer four-element microstrip patch array antenna using both-sided technology with modification in the feeding mechanism while keeping the feeding techniques very simple to realize beam switching applications as well as the direction-of-arrival (DOA) estimation.

1.6 Fabrication Feasibility

In the process of manufacturing a microstrip antenna, it is essential to take into consideration a range of different variables. Considering the wide variety of applications that antennas may serve, it is common practice to install them in outdoor settings that are subject to severe weather conditions or temperatures that are extremely high. In addition, the antenna could be situated in regions that contain high concentrations of chemicals; hence, the choice of materials and substrate for the antenna is of the highest significance [23].

All the antennas proposed and explained in this thesis paper are constructed using copper patches and Teflon Glass Fiber substrates, which exhibit excellent

temperature stability and chemical resistance. Additionally, they possess a non-adhesive quality and feature a smooth surface, hence minimizing friction in the application area [24, 25].

The works that are presented in [26, 27, 28, 29, 30, 31] showcases many microstrip patch array antennas that have been meticulously developed and manufactured for various wireless applications. These antennas utilize Teflon as the substrate material making this thesis work's proposed and designed microstrip patch array antenna, which will be detailed later, viable for production.

1.7 Organization of Thesis

This chapter provides an introduction, the inspiration for the thesis, and a short explanation of the aims of the thesis, along with a comprehensive review of the microstrip patch array antenna, including the practicality of the design methodologies and their production.

Chapter 2 includes some theoretical descriptions of microstrip patch array antennas related to this thesis work, as well as a literature review on recent work done on microstrip patch arrays for circular polarization, beam switching, and direction of arrival estimation.

Chapter 3 describes the design and simulation findings of a three-element microstrip patch array for circular polarization.

Chapter 4-5 describes the design and simulation findings of a four-element microstrip patch array for circular polarization with large extensible array.

Chapter 6-7 describes the design and simulation findings of a four-element microstrip patch array for beam switching and DOA estimation.

Chapter 8 describes the design and simulation findings of two different antennae but with simple feeding techniques for circular polarization and beam-switching applications.

Chapter 9 concludes the thesis.

Chapter 2

Literature Review

This chapter includes a theoretical analysis of circular polarization reconfigurability, beam switching, and Direction of Arrival (DOA) estimations. Additionally, it contains antenna parameters that are relevant to the work being done on the thesis and will be utilized frequently as the report progresses throughout its entirety. This chapter also delves into some recent research on microstrip patch array antennas, which have applications in circular polarization, beam switching, and estimations of the direction of arrival.

2.1 Antenna Parameter

In this section, several fundamental antenna parameters have been described in detail for the purpose of continuing this thesis report. This is because the terminology that is discussed here will be utilized rather frequently in the subsequent portion of this thesis.

2.1.1 Axial Ratio

The term "polarization" refers to the characteristics of electromagnetic waves. The shape and orientation of the tip of the **E** vector, as it evolves with time, is what determines the polarization of an electromagnetic wave [32]. When the vector of the **E** field spins in a circular motion, this phenomenon is referred to as circular polarization. Additionally, the Axial Ratio (AR) is a measurement parameter of an antenna that is used to determine the amount of circularly polarized waves that are radiated by the antenna in the far field zone.

Axial ratio is defined as the ratio of major axis and minor axis of polarization ellipse as shown in Figure 2.1 and can be given by [33],

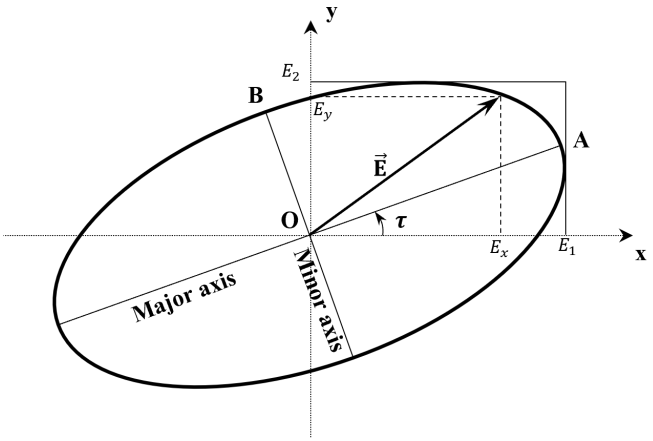

Figure 2.1: Polarization ellipse [32].

$$AR = \frac{OA}{OB}(1 \leq AR \leq \infty) \tag{2.1}$$

The equation (2.10) makes it abundantly evident that the axial ratio must be equal to one for circular polarization to be considered a perfect or special case. However, in actual situations, this parameter is measured in terms of decibels, and the acceptance range for an antenna with a circular polarization has an AR value that is less than 3 dB [34].

Practically, the far field antenna parameter such as axial ratio is measured by placing the antenna under test (AUT) in an anechoic room, facing the boresight direction of an auxiliary antenna, which is a horn antenna as depicted in Figure 2.2. The auxiliary antenna is rotated about its antenna axis, and the received power signal from the AUT (Antenna Under Test) is evaluated using a vector network analyzer.

2.1.2 Co and Cross-Polarization

Co-polarization is the alignment of an antenna's transmitting and receiving elements in the same direction. For instance, when both elements have their electromagnetic waves oscillating in the same horizontal direction, they are considered to be co-polarized.

Cross-polarization refers to the situation where the transmitting and receiving elements of an antenna are positioned at right angles to each other. Consequently, if one element is polarized in a horizontal direction, the second element is polarized in a vertical direction.

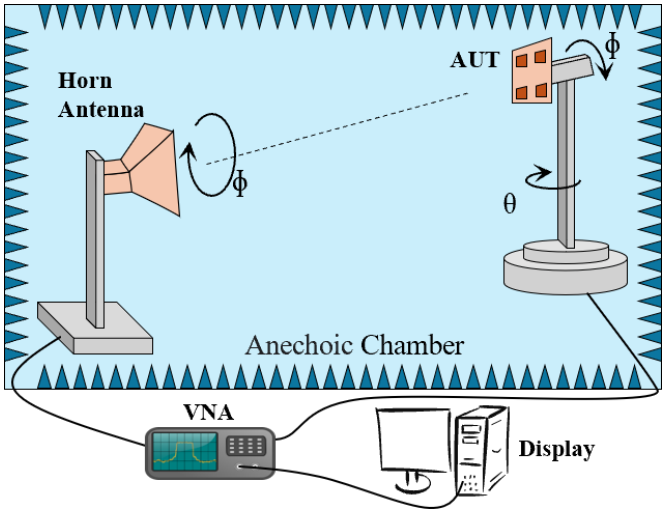

Figure 2.2: A general antenna setup in a standard anechoic chamber for far-field radiation pattern measurement where AUT stands for antenna under test, VNA stands for vector network analyzer, θ means azimuth rotation axis and ϕ means antenna axis rotation and horn antenna is standard gain horn [33].

2.1.3 Relative Power

Relative Power is also a far-field measurement parameter of the antenna defined by the co-polarization and cross-polarization power level difference measured in dB of the propagating field components.

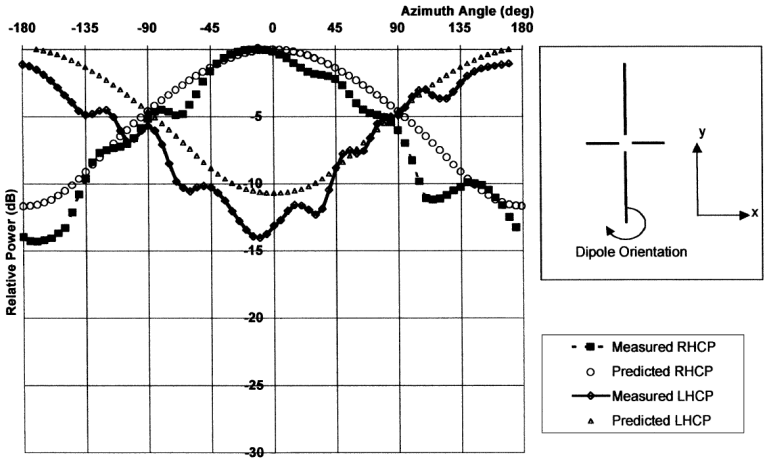

Figure 2.3: Relative power of a circularly polarized dipole antenna. At foresight, the power level difference between co and cross-polarization is greater than -14 dB, and the polarization sense of the antenna reverses at 180° [35].

According to the illustration in Figure 2.3, For an antenna to achieve proper circular polarization, the power level difference between co-polarization and cross-polarization should exceed -15 dB. The diagram illustrates the disparity in power levels between cross-polarizations of a dipole antenna with circular polarization

[35]. In this scenario, the antenna is rotated along its rotation axis to monitor the power levels. From the graphic, it is evident that the power level overlaps beyond ±90° because of the physical rotation of the dipole, and at 180°, the polarization senses reverse, as expected.

2.1.4 Return Loss

The antenna, being the terminal point of a transmitting device, functions as a load and requires efficient power from the input. The effectiveness of power transmission from a transmission line to an antenna input is measured by return loss measured in unit decibels (dB). And, the return loss is defined as [36]

> "(data transmission) (A) At a discontinuity in a transmission system the difference between the power incident upon the discontinuity. (B) The ratio in decibels of the power incident upon the discontinuity to the power reflected from the discontinuity. Note: This ratio is also the square of the reciprocal to the magnitude of the reflection coefficient. (C) More broadly, the return loss is a measure of the dissimilarity between two impedances, being equal to the number of decibels that corresponds to the scalar value of the reciprocal of the reflection coefficient."

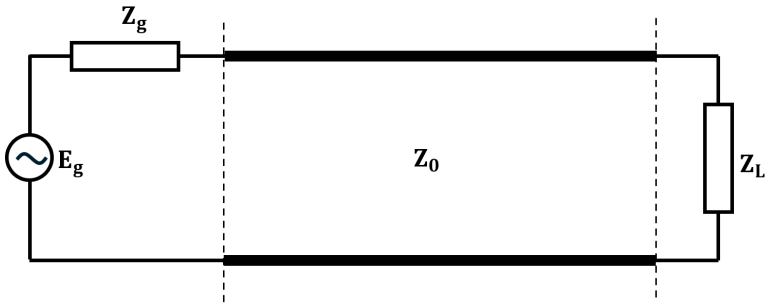

Figure 2.4: A general case of a transmission circuit where, Z_g, Z_0, and Z_L are generator impedance, transmission line impedance, and load impedance respectively [37].

The return loss (RL) equation can be expressed as follows: P_{in} represents the power delivered to the load input from the transmission line, and P_{ref} denotes the power reflected from the load input.

$$RL = 10 \log_{10} \left(\frac{P_{in}}{P_{ref}} \right) dB \tag{2.2}$$

The ratio Pin/P_{ref} in equation (2.2) represents the degree of mismatch between incident and reflected power. However, if the complex reflection coefficient power at the input of load is denoted by ρ, then the equation becomes,

$$RL = 10\log_{10}\left|\frac{1}{\rho^2}\right| dB \tag{2.3}$$

$$= -20\log_{10}|\rho|\, dB \tag{2.4}$$

If a transmission line circuit comparable to the one depicted in Figure 2.4 is taken into consideration, and equation (2.4) is written in terms of impedance rather than the corresponding reflection coefficient, then the return loss is calculated as follows [37]:

$$RL = 20\log_{10}\left|\frac{Z_g + Z_L}{Z_g - Z_L}\right| dB \tag{2.5}$$

Considering the equations and analysis presented above, it is possible to assert that the return loss is the negative of the reflection coefficient. There is also an option of expressing it as the voltage standing wave ratio (VSWR). When stated in terms of voltage standing wave ratio (VSWR), the equation (2.4) becomes,

$$RL = 20\log_{10}\left|\frac{VSWR + 1}{VSWR - 1}\right| dB \tag{2.6}$$

However, for a multi-port network, scattering matrix analysis [38] is done and denoted by the formula of the equation (2.7).

$$\begin{bmatrix} V_1^- \\ V_2^- \\ \vdots \\ V_N^- \end{bmatrix} = \begin{bmatrix} S_{11} & S_{12} & \cdots & S_{1N} \\ S_{21} & \ddots & & \vdots \\ \vdots & & \ddots & \\ S_{N1} & \cdots & & S_{NN} \end{bmatrix} \begin{bmatrix} V_1^+ \\ V_2^+ \\ \vdots \\ V_N^+ \end{bmatrix} \tag{2.7}$$

or

$$\left[V^-\right] = \left[S\right]\left[V^+\right] \tag{2.8}$$

Equation (2.8) can be written as

$$[S] = \frac{[V^-]}{[V^+]} \tag{2.9}$$

where V^+ and V^- are the amplitude of the incident voltage wave and reflected voltage wave respectively. That is [S] matrix, which can be also called an S-

parameter is the ratio of amplitude of the reflected and incident voltage wave at any port of a multi-port network.

2.1.5 Gain and Directivity

Checking the antenna's gain and directivity is a crucial parameter to do in order to acquire an understanding of the antenna's performance. Both gain and directivity are measures that show the amount of power that is emitted in a certain direction.

The term "directivity" refers to the ratio of the antenna's maximum power density to its average value over a sphere in the far field of an antenna.

The gain of an antenna is a description of the amount of input power that the antenna is able to convert into radiated power in a particular direction. Thus, Efficiency is a component of the equation, and it may be expressed as follows [39]:

$$G = \eta \times D \tag{2.10}$$

Where G represents gain, D represents directivity, and η represents the efficiency of the antenna. The efficiency values range from 0 (zero) to 1 (one) where 1 being 100% efficient antenna which in practice is not possible due to some internal loss always being present in the antenna.

2.1.6 Radiation Pattern

The radiation pattern of the antenna as a function of spatial coordinates, either as a mathematical function or as a graphical representation of the behavior of the antenna. The radiation pattern is typically determined in the far-field region and is represented as a function of the directional coordinates [40].

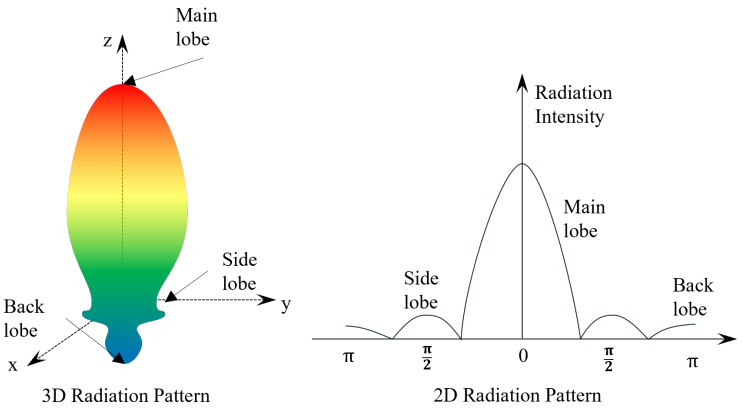

Figure 2.5: 3D and 2D radiation pattern of directive antenna [40].

Figure 2.5 represents both the three-dimensional and two-dimensional radiation pattern of an antenna where the main beam is in the foresight direction.

2.1.7 Other Important Parameters

Some other important antenna parameters are used in antenna performance analysis like impedance bandwidth (BW), axial ratio bandwidth (ARBW), and isolation. These parameters are described as follows:

Isolation: In the case of any network that contains many ports, it is essential to check whether or not there is any interference between the ports, as this might result in a decline in the performance of the signal transmission. Isolation is the phrase that is used to ensure that a multi-port network performs at its maximum potential. Within the context of multi-port devices, an isolation value that is lower than -20 dB at the working frequency is considered to be satisfactory [41].

Impedance Bandwidth: The impedance bandwidth of an antenna is the range of frequencies throughout which it is able to maintain efficient impedance matching. This range of frequencies is often referred to as the antenna's frequency range. Generally speaking, it is defined as the frequency span that extends from resonance values on the S-parameter graph that are lower than -10 dB [42]. Through the use of the equation (2.11), it is possible to ascertain the percentage bandwidth of an antenna.

$$BW = \frac{f_H - f_L}{\frac{f_H + f_L}{2}} \times 100\% \tag{2.11}$$

Where f_H and f_L represent higher and lower frequency bands respectively.

From a practical standpoint, impedance bandwidth is absolutely necessary for ensuring that antennas are capable of transmitting and receiving signals in an effective manner. In order to determine the frequency range in which impedance matching is most successful for signal transfer, it measures the frequency range.

ARBW: One definition of axial ratio is the ratio of the major axis of polarization ellipse to the minor axis. With regard to bandwidth, it is a term that describes the range of frequencies that an antenna is capable of radiating or receiving CP energy in an appropriate manner. The axial ratio bandwidth (ARBW) is a popular measurement that is determined by calculating the ratio of the frequency range to the center frequency. This ratio is produced exactly like the equation shown in (2.11), the difference is the highest and lowest frequency span is the 3dB axial ratio values in dB.

2.2 Theoretical Analysis

The purpose of this section is to provide an overview of the fundamental concepts of circular polarization, beam switching, and direction of arrival, all while keeping in mind the proposal for this thesis report. There is also a brief description has been carried out on microstrip antenna feed types and both-sided microwave integrated circuit (MIC) technology in this section.

2.2.1 Circular Polarization

In the process of wave propagation, the orientation of the electric field is referred to as polarization. When the field line is in the vertical plane along the path of propagation, this phenomenon is referred to as vertical polarization. On the other hand, horizontal polarization refers to the phenomenon in which the electric field oscillates in a direction that is orthogonal to the vertical plane.

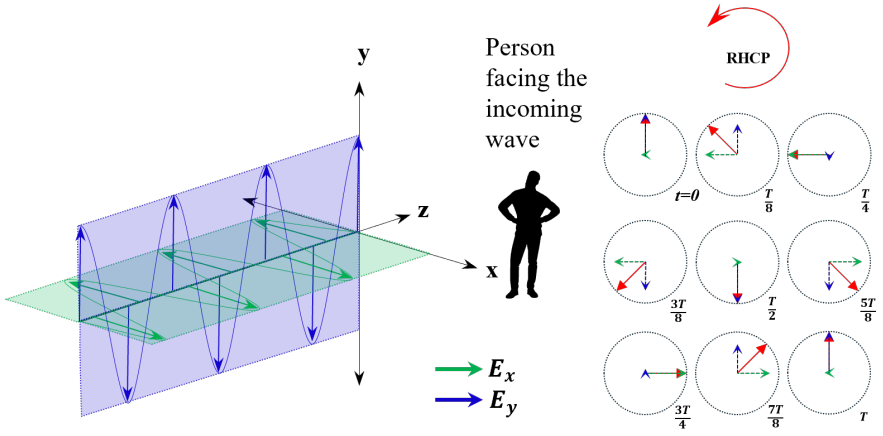

Figure 2.6: A conceptual diagram of right-hand circular polarization (RHCP) where green and blue colored arrow denotes horizontal and vertical electric field lines respectively. The red arrow inside the dotted circle on the right side denotes the rotational resulting field vector.

When the resulting vector rotates in a circular motion while it continues its propagation, this phenomenon is known as circular polarization. Circular polarization requires two orthogonal electric fields to have the same amplitude, but there must be a quarter wavelength phase difference between them. This is the prerequisite for developing circular polarization [43]. In the field of circular polarization, there are two distinct types: the first is known as left-hand circular polarization (LHCP), while the other is known as right-hand circular polarization (RHCP). This is because the rotation direction of the resulting rotating vector as they propagate is the reason they were given their name. If a person is facing the

incoming wave and notices that the rotating vector that results from the wave has a rotation in the opposite direction of clockwise rotation, then this phenomenon is referred to as right hand circular polarization. Figure 2.6 illustrates this phenomenon. Also, the left-hand circular polarization happens for rotation in the clockwise direction as shown in Figure 2.7. The rotating vector that is produced as a result of two orthogonal electric field vectors is represented by the red arrow that is located inside the circle in both graphical representations.

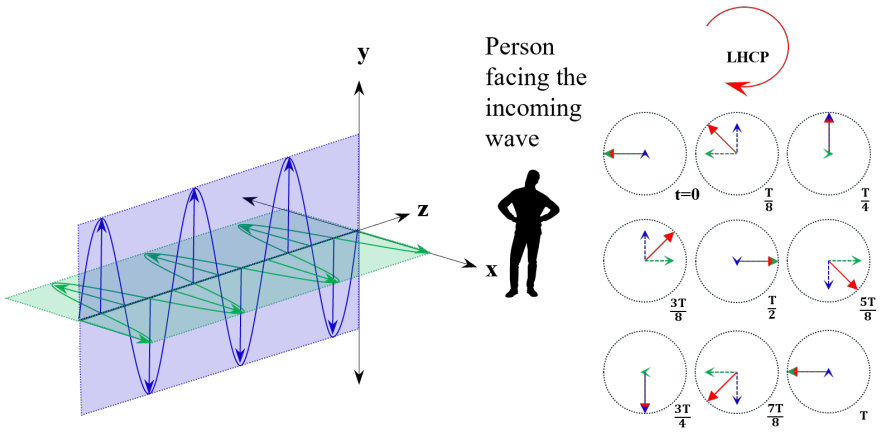

Figure 2.7: A conceptual diagram of left-hand circular polarization (LHCP) where green and blue colored arrow denotes horizontal and vertical electric field lines respectively. The red arrow inside the dotted circle on the right side denotes the rotational resulting field vector.

When looking at the figures (Figure 2.6 and Figure 2.7), it is evident that the red arrow rotates in a circular motion with time, with the clockwise direction for the LHCP and the anti-clockwise direction for the RHCP cases. On both occasions, the red arrow will finish one spin once a length of time denoted by the letter 'T' has passed.

2.2.2 Polarization Mismatch

This subsection demonstrates an overview of the necessity of a circularly polarized signal in the communication medium. Because the environment surrounding the communication medium can be a factor that interferes with a successful transmission, it is essential to take into consideration the environment in which the signal is being transmitted from the transmitter to the receiver to ensure that the transmission is successful. If the signal from the transmitter antenna is transmitted in linear polarization, it is necessary for the receiver antenna also to be linearly polarized to achieve successful reception. The reception antenna must be circularly polarized to receive a signal that features circular polarization. A basic

communication system is one in which the transmitter antenna and the receiver antenna are in line-of-sight (LOS). In this scenario, the transmitter antenna is responsible for transmitting the signal, while the receiver antenna is responsible for receiving it. Nevertheless, even though the antennas are in the line of sight, the transmission is made somewhat more complicated by elements such as buildings, the earth's surface, and trees that come into the scene.

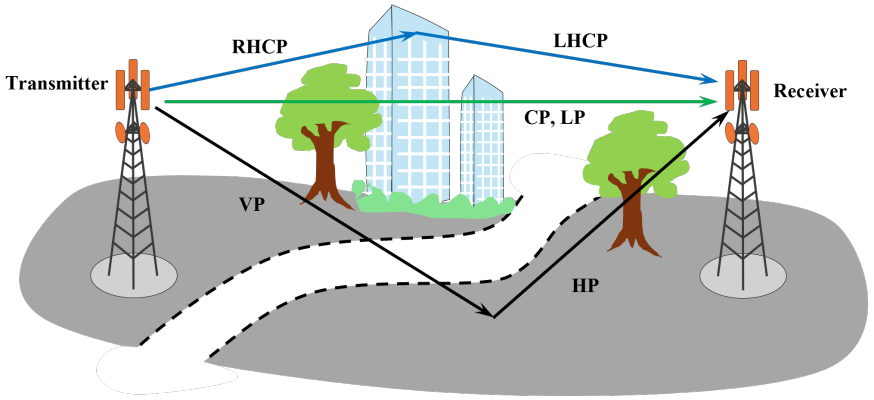

Figure 2.8: A general graphic representation of a communication scenario where polarization mismatch happens and a proper transmission can be hampered.

In a condition similar to Figure 2.8, field polarization changes. If the signal travels in a direct channel and the transmitting signal is linearly polarized, proper reception occurs only when the receiver antenna is aligned with the incoming signal field orientation. This is a disadvantage of linearly polarized antennas. However, if the receiving antenna is circularly polarized and the incoming wave is linearly polarized, there is no problem with reception. Another situation is that the signal will reach the receiver after being reflected by buildings, trees, or the ground. The polarization of the signal will be altered, and the receiver will additionally receive signals with different phases and strengths, resulting in a mismatch at the receiving ends. This phenomenon is known as multi-path fading. To address this issue, the transmitting antenna should likewise be circularly polarized, as a RHCP receiver would reject an LHCP signal and vice versa. As a result, the RHCP receiver will reject a RHCP transmitting signal that has been converted to LHCP via multi-path.

2.2.3 Beam Switching

Beam switching involves directing a radiating beam in a certain direction for better communication. If a user is not facing the broadside of a transmitting device, the user may not receive the full strength of the transmitting signal. A simple method is to point the electronic device or transmitter antenna in the appropriate

direction to achieve optimum signal transmission. Mechanical steering involves rotating or guiding the transmitter antenna in a specific direction which end up requiring external mechanical devices like motors. To compensate for the external rotatory devices, it can be done electronically by arranging several antenna elements in a pattern to operate as one antenna, known as an array antenna, and providing the individual radiators with a phase difference between them. Providing a phase difference among an array's radiators causes the radiating wave to tilt in a direction other than broadside, which can be employed to optimize transmission. Figure 2.9 shows four antenna elements arranged in series, each of

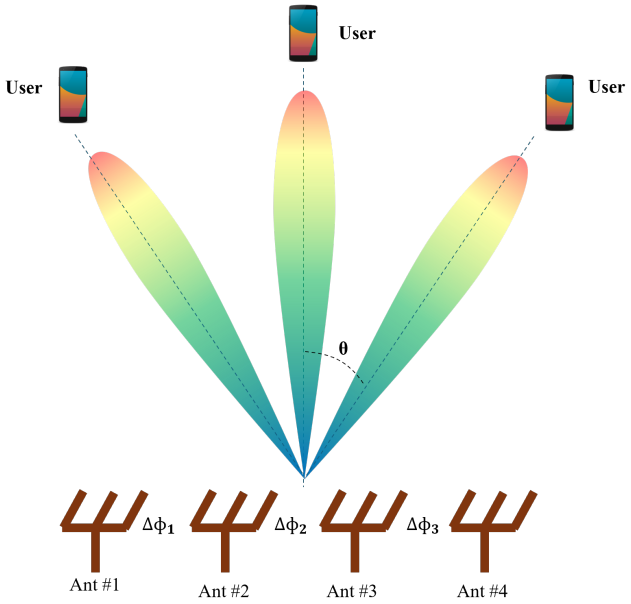

Figure 2.9: A conceptual diagram of beam switching where an array of four radiators is placed in series orientation with several phase differences among them.

which is fed with a phase difference. By regulating the phase difference between radiators, the radiated beam can be regulated and directed to the intended users. The theta symbol in the images represents the inclination angle of the radiated beam with regard to the broadside direction.

2.2.4 Direction-of-Arrival Estimation

The process of calculating the angles from which signals reach an array is referred to as direction-of-arrival (DOA) estimation. This is accomplished through the utilization of complex algorithms that extract directional characteristics from received data despite the presence of noise and a large number of signal sources. Various techniques, including beamforming, Multiple Signal Classification (MUSIC), and monopulse trackers, are utilized in the process of estimating the lo-

cation of the source. It is possible to determine the direction of radiating or reflecting sources with the assistance of these approaches by analyzing the data that is received at an array. One of the techniques is monopulse trackers which

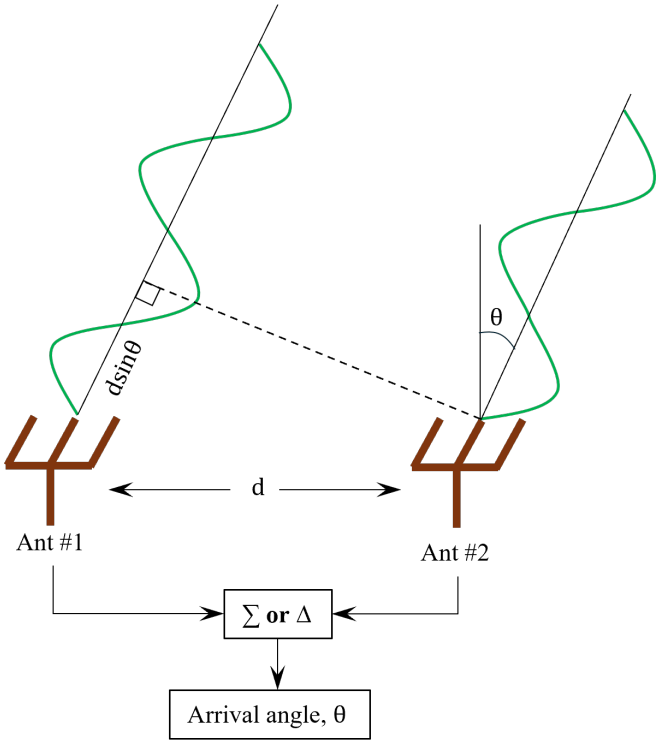

Figure 2.10: A conceptual diagram of the direction of arrival estimation using monopulse technique, where the green colored wave coming towards the antenna with an inclined angle of θ [44].

utilize radio signal encoding to provide accurate directional information. The trackers are used in modern radar systems. They derive both range and direction from a single pulse, thereby avoiding rapid fluctuations in signal intensity. Amplitude monopulse and phase-comparison monopulse were the two classifications of monopulse radars. To obtain accurate directional data, monopulse antennas are an indispensable component of monopulse radar systems. The antennas are designed to generate sum and difference channels from the energy that is flowing in, which enables precise tracking of the targets.

The phase comparison monopluse technique is illustrated in Figure 2.10. This technique involves the extraction of two vector components from an incoming signal, namely the sum signal (Σ) and the difference signal (Δ), and then sending these components to a detector to determine the angle of the wave that is coming in [44]. As seen from the figure, if the antenna element is separated by a distance 'd' and the incoming wave is inclined at an angle θ, The phase difference between the waves denoted as $\Delta\phi$, can be expressed by following the equation, phase

difference = $\frac{2\pi}{\lambda} \times$ path difference as,

$$\Delta\phi = \frac{2\pi}{\lambda} \times dsin\theta \tag{2.12}$$

Therefore, the arrival angle, θ can be calculated using equation (2.12), that is,

$$\theta = sin^{-1}\left(\frac{\lambda\Delta\phi}{2\pi d}\right) \tag{2.13}$$

The $\Delta\phi$ in equation (2.13) is expressed in terms of Δ and Σ signal, then replaced into the equation to determine the direction of arrival estimation.

2.2.5 Microstrip Antenna Feeding Techniques

The feeding of microstrip patch antennas can be accomplished by a variety of approaches, which can be classified as either contacting or non-contacting processes. Contacting methods include microstrip line feed and co-axial feed whereas non-contacting method includes aperture coupled feed [45]. Figure 2.11 illustrates a diagram that describes several strategies for feeding.

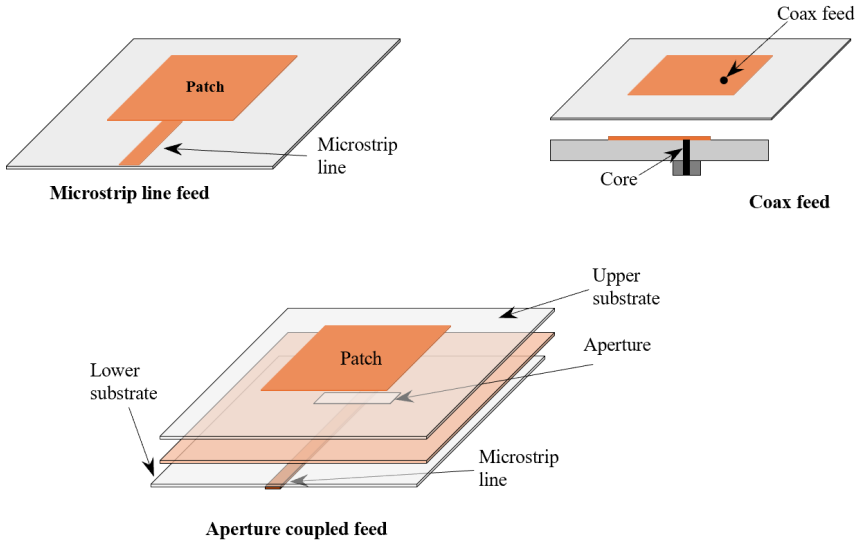

Figure 2.11: Microstrip patch antenna feeding techniques.

Microstrip Line Feed method involves connecting a conducting strip straight to the edge of the microstrip patch. This procedure makes it possible for the feed to be etched on the same substrate, resulting in a planar structure.

A coaxial cable is used to feed the patch, with the inner conductor making contact with the patch and the outer conductor being linked to the ground plane. This type of feed is referred to as a coaxial feed.

An aperture-coupled feed is a type of feed that makes use of two dielectric substrates that are separated by a ground plane and has a slot in the middle of it. This feed provides superior polarization purity and a higher bandwidth.

However, each feeding strategy has a unique set of benefits and drawbacks, which can have an effect on several aspects of the antenna, including its bandwidth, return loss, gain, and impedance matching specifications [46]. To maximize antenna performance following particular criteria, the selection of the feeding technique is of the utmost importance.

2.2.6 Both-sided MIC technology

Microwave integrated circuit (MIC) technology, also known as both-sided MIC technology, is an innovative approach that is applied in the design of antennas. When both sides of the substrate of an antenna are used to integrate a microwave circuit is called both-side MIC or double-sided MIC technology. It has several design flexibilities along with improved antenna performances [47].

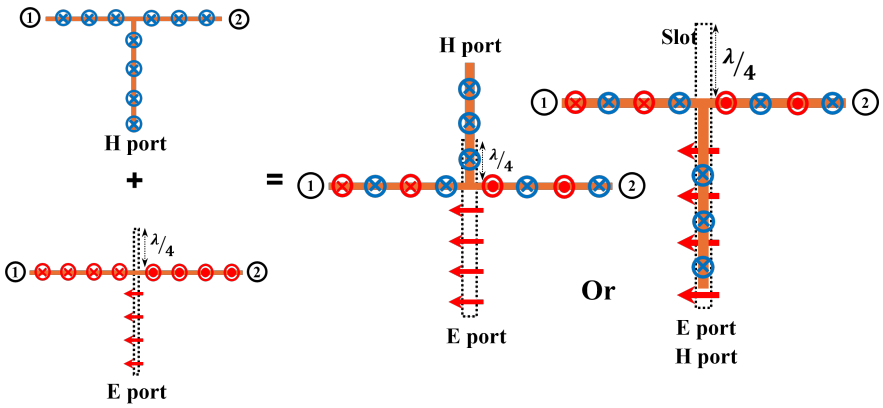

Figure 2.12: Some examples of hybrid dividers (Magic-T). Blue-colored ⊗ and red-colored ⊗ denote in-phase and out-of-phase signals respectively.

Both-sided MIC technology has the capability to form in-phase dividers (**H** port) and out-of-phase dividers (**E** port), and it can combine these two types of dividers to form a hybrid tee that is referred to as Magic-T [48]. This capability is illustrated in Figure 2.12.

2.3 Related Antenna Work

Within this section, a concise overview will be provided of the scientific work that has been conducted on circular polarization, beam switching, and DOA estimating antennas, with a particular focus on microstrip antennas.

2.3.1 Circularly Polarized Antennas

Circularly polarized antennas are a common choice among antenna engineers because they are resistant to the rotation of faradays and have the capacity to correct for interference caused by multi-path fading. The circular polarized microstrip patch has been the focus of research for a considerable amount of time due to its low profile, simplified manufacturing process, cost-effectiveness, and lightweight nature. Moreover, the inherent low gain problem is compensated for by array arrangement, microstrip patch array antenna has been utilized in a variety of wireless applications [49, 50, 51, 52].

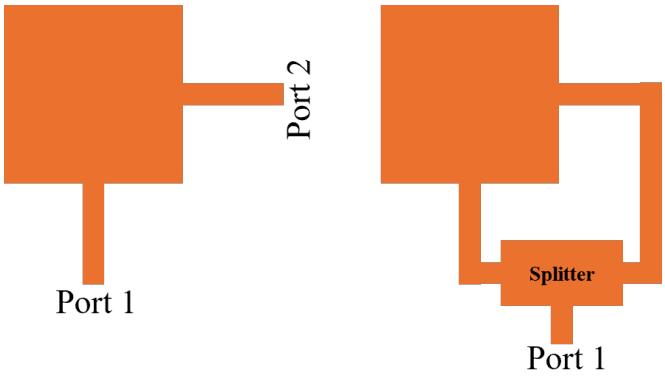

Figure 2.13: Typical circularly polarized square-shaped microstrip patch antenna with dual feed and with single feed associated with an external splitter.

The fundamental TM_{10} resonant mode of a simple microstrip patch is activated when it is fed with a radio frequency signal. This occurs when the patch form is rectangular [53]. A simple microstrip patch radiates along its width. To achieve circular polarization, it is necessary to provide two orthogonal electric fields of equal amplitude, with a phase shift of 90° between them. However, there is only one resonant mode that can be excited by a single microstrip patch with a single feed, which results in either vertical or horizontal polarization [54, 55]. Therefore, to achieve circular polarization through the use of a microstrip patch antenna, it is necessary to stimulate two orthogonal resonance modes. Dual feed, as depicted in the Figure 2.13, is one method that can be utilized to accomplish this. In order to obtain this through a single feed, it is necessary to have an external splitter that has one arm of the splitted microstrip lines that is a quarter wavelength longer than the other arm, as depicted in the pictorial representation [56]. In this way, the microstrip patch is able to excite two orthogonal resonant modes within the patch, which in turn allows it to generate circularly polarized waves. It is possible that the complexity of the design will expand as a result of this external circuit or dual feed arrangement, increasing the total volume of

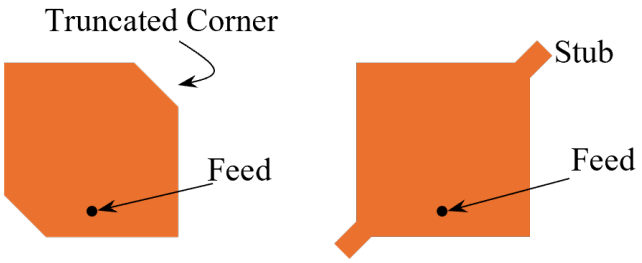

Figure 2.14: Typical single feed circularly polarized square-shaped microstrip patch antenna with corner truncation and with stub extension diagonally.

the design. Therefore, there is another method that involves dividing the fundamental resonant mode of a microstrip patch into two orthogonal degenerative modes in order to acquire circular polarization employing a single feed without the need for an external circuit configuration. This criterion is met when the corner of the patch is cut off and the feed is placed along the center axis near the edge of the patch [57, 58, 59], as depicted in Figure 2.14.

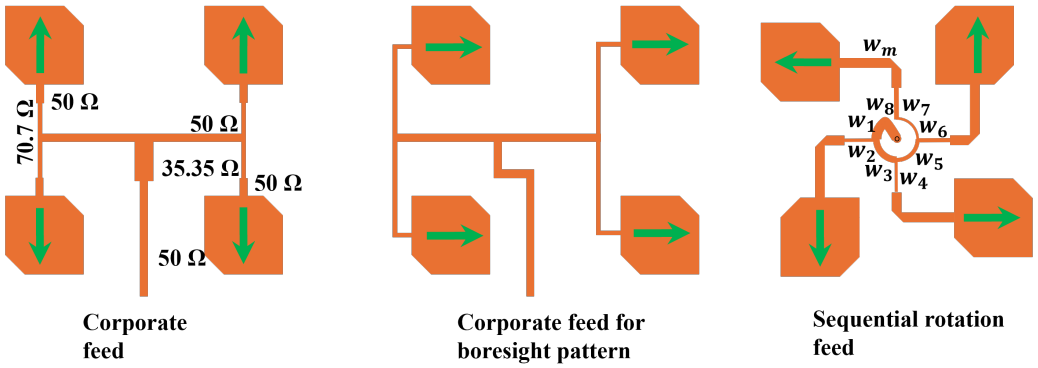

Figure 2.15: Some general examples of circularly polarized microstrip patch array antenna feeding arrangement. The green-colored arrow represents the field lines of the patch when excited.

On the other hand, with a microstrip patch array antenna that is circularly polarized, there is an intuitive way to utilize every individual radiator as circularly polarized by either corner truncation or extending stub and to set up a feeding network to transfer power among individual radiators in an effective manner. The employment of the series feeding method, which is capable of effectively distributing power across radiators, is one of the feeding approaches that may be used for array antennas [60, 61, 62, 63]. One more method for feeding the array is to make use of a parallel or corporate feed network to distribute power across radiators in an effective manner [64, 65, 66, 67]. This feeding necessitates the placement of certain individual radiators in order to achieve the same field

distribution across the elements, as seen in Figure 2.15. If this is not accomplished, the elements will end up with a radiation pattern that is bi-directional and does not have a boresight radiation pattern [68]. Other feeding arrangements, including the sequential rotation feeding method [69] and the series-fed gap coupled feeding [70] technique, are also available for use with the microstrip patch array antenna. The sequential rotation feeding, on the other hand, requires a complicated calculation about the width and length of the feed line, in addition to ensuring that the orientation is symmetrical [71, 72].

Since a microstrip patch antenna is a low gain antenna that makes use of numerous of the feeding techniques stated above in case of array design when gearing up to big-scale array antennas to battle long-distance wireless communication, it becomes fairly complicated to maintain a single-layer simple feed network. Both-sided MIC technology is a concept that can be utilized in the process of array-making [73]. This technology makes the structure very simple to feed efficiently, and it also makes the structure very simple in such a way that it can be easily extended for large-scale arrays. Additionally, it provides design flexibility by allowing for the incorporation of several internal circuits into the design, which enables simple options for polarization diversity [74, 75].

2.3.2 Beam Switching Antennas

In addition to polarization mismatch, it is essential for better communication to be free of interference, to have increased channel capacity, and to prioritize power efficiency, which means achieving maximum power reception at the receiver end. This is especially important in this day and age of rapidly moving and continuously growing traffic. In this particular scenario, it is of the utmost importance to guide a radiated beam emitting from the transmitting antenna in the desired direction without shifting the antenna itself. In this particular circumstance, beam switching or beam steering antennas, which are defined as antennas that are able to steer their radiating beam, have the potential to be successful [76, 77]. It is possible to mechanically guide a radiated beam in a certain direction by continually switching or guiding the antenna into the desired direction [78, 79]. This process needs the use of an external controller, which ultimately results in the complexity of the system. Therefore, beam switching results in benefits when it is carried out electronically [80, 81, 82]. The use of microstrip patch antennas for beam switching is attractive because of the advantages of being lightweight, having a simplified manufacturing process, and having an easier installation [83, 84, 85].

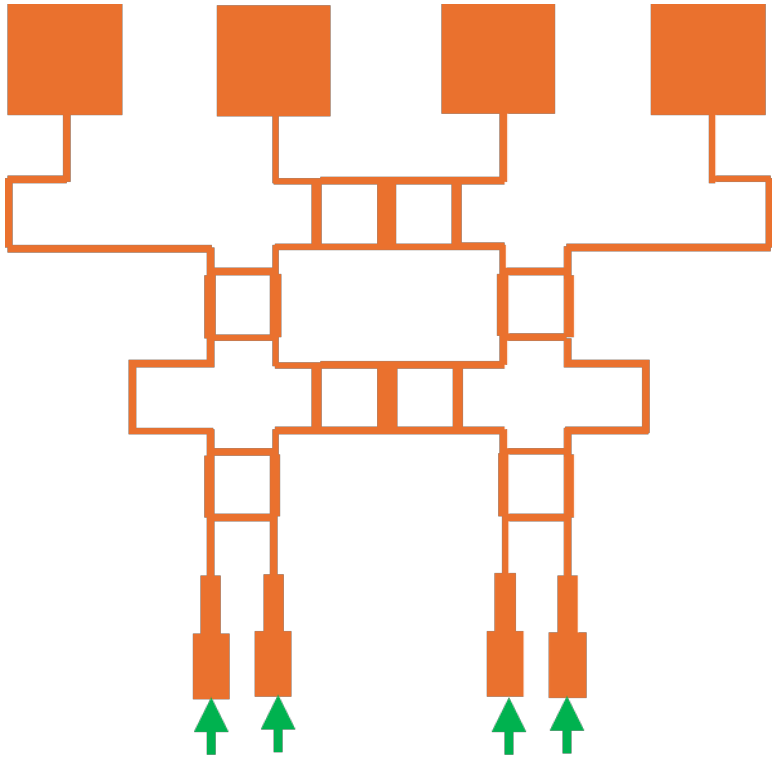

Figure 2.16: A general architecture of switched-beam microstrip patch array antenna with butler matrix in the external circuit. Green arrow indicates the feed point [86].

In the event that an array antenna is taken into consideration, the primary purpose of a switched beam antenna is to implement a phase difference between the radiators. To produce an equi-phase wavefront in the distant zone at a tilted angle with the axis perpendicular to the antenna plane, it is necessary to have a phase difference among the elements of the array. This phase difference causes electromagnetic waves to be emitted with phase differences among the elements. It is possible to do this by providing each radiator of a microstrip patch array with its distinct input port, which comes equipped with its phase signal [87]. However, in order to construct a circuit component that has such capabilities inside the device, it would be too complicated to do so for large-scale arrays. However, in the case of a microstrip patch array antenna, the general method of introducing a phase difference between the components of the array is by employing a phase shifter and diodes into the design [88, 89, 90, 91, 92, 93]. On the other hand, one of the most typical methods for achieving beam switching by means of a microstrip array antenna is to make use of an external butler matrix circuit in order to generate a phase difference among the array radiators [94, 95, 96, 97]. A beam-switching array antenna with a butler matrix is represented in Figure 2.16, which is a schematic illustration of the antenna [86, 98].

One additional method for configuring beam switching in a microstrip array is to make use of switches or diodes in parasitic patches that circulate a centrally driven patch [99]. Controlling the configuration of the diodes results in beam switching to different directions, which is also a complex process when dealing with large-scale arrays. The switch or diode configuration may also be utilized in a single patch, and depending on how they are configured, altering the current flow inside the patch can result in an inclined radiated wave [100]. Also, a single element with a multi-port can switch beams with deviation from the general patch shape like star patch [101]. Nevertheless, since a single patch antenna is a low-gain device that has the potential to fail in long-distance transmission, an array antenna is a more desirable option.

2.3.3 DOA Estimation Antennas

A crucial component of wireless communication, including smart antennas, sonar, radar, and surveillance, is the calculation of the direction of arrival, also known as DOA is an act of determining the direction from which a propagating wave arrives. The monopulse tracker is a technology that is often used to find the direction of arrival (DOA). When compared to other methods, such as MUSIC (MUltiple SIgnal Classification) and ESPRIT (Estimation of Signal Parameters via Rational Invariance Techniques), the monopulse tracker is preferred since it requires less sophisticated computations and offers extremely precise information about the direction of travel [102, 103, 104]. The monopulse concept involves comparing the received signal beam by the components of the receiver antenna array using two different techniques: the pulse monopulse concept and the amplitude monopulse concept [105]. The use of microstrip patch arrays with both-sided microchip technology for the monopulse phase comparison technique is a new area of study that is being focused on in the field of wireless communication. This technology has several advantages, including a low profile, a lightweight construction [106], and the option of incorporating microwave circuits into the whole structure [107, 108].

Recent research has highlighted the effectiveness of microstrip patch antennas in improving the precision and resilience of DOA estimates. As a result, these antennas have emerged as a potentially useful choice for a wide range of applications that require accurate direction-finding capabilities. It was speculated in [109] that a four-element microstrip patch array may be used for DOA estimate; however, the practicality of this array for extensible arrays has been put into doubt due to the fact that the comparator circuit for phase comparison

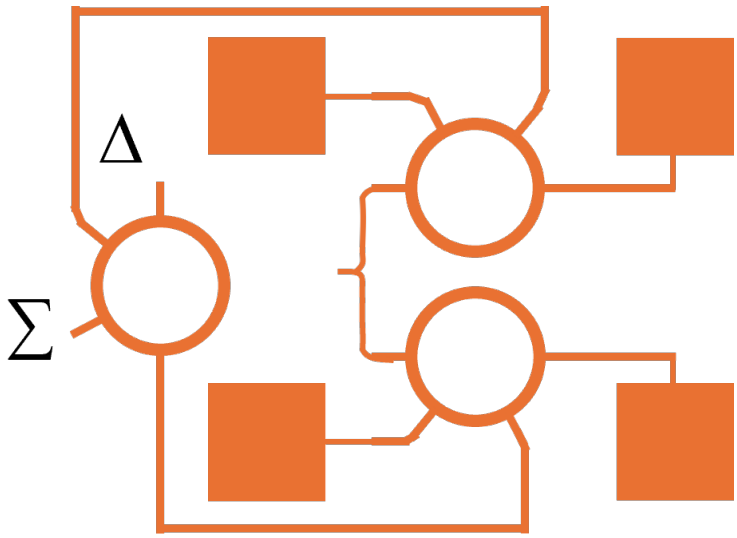

Figure 2.17: A general architecture of DOA estimating microstrip patch array antenna with comparator circuit made of rat-race [109].

is situated around the patch array as shown in Figure 2.17. It is necessary to incorporate a comparator circuit in the middle of the array in order to compensate for this, despite the fact that this results in blockage and raises the sidelobe level [110]. To eliminate blockage and achieve a reduced sidelobe level, a 256-element array for DOA estimation is presented, with a central comparator and four output ports connected to the sum signal, difference signal, and the matching load. However, this antenna suffers from spurious radiation in the sidelobe level, as well as feed network loss [111]. This phenomenon can be addressed by using an RF multiplier and a Magic-T, which is an application of both-sided MIC technology [112, 113, 114].

Chapter 3

Circularly Polarized Three-Element Patch Array

This chapter describes a single-fed, three-element patch array antenna that operates in a linear polarized sense but a simple modification in the quarter wavelength transformer microstrip line enables the antenna to radiate a circularly polarized signal of both senses. The proposed design distributes a single port input signal across three patches. The signal can be routed to each patch by taking advantage of both-sided MIC technology's design flexibility. Element #1 is fed orthogonally, whereas the following patches (Element #2 & #3) are fed in a single direction but with orthogonal orientations. Section 3.1 delves into the design process and includes the materials used, as well as technical specifications and an explanation of how the antenna works. Section 3.2 offers the findings, which validate the concepts' successful application.

3.1 Design Method

3.1.1 Antenna Structure

Figure 3.1 demonstrates the arrangement of three square microstrip patches, labeled #1, #2, and #3, on a Teflon substrate with a relative dielectric constant of $\epsilon_r = 2.15$. These patches are capable of resonating at frequencies within the X-band range. The figure also shows a cross-sectional view of the planned antenna along AA'. To produce the microstrip-to-slot junction and the slot-to-microstrip junction, which function as equal dividers of the input signal from the port, a U-shaped slot line with flared arm ends, measuring 0.2 mm in width, is cut in the ground plane. The microstrip lines that connect the patches and the flared ends of the slot form the slot-microstrip junction. Two signals originating from slot-

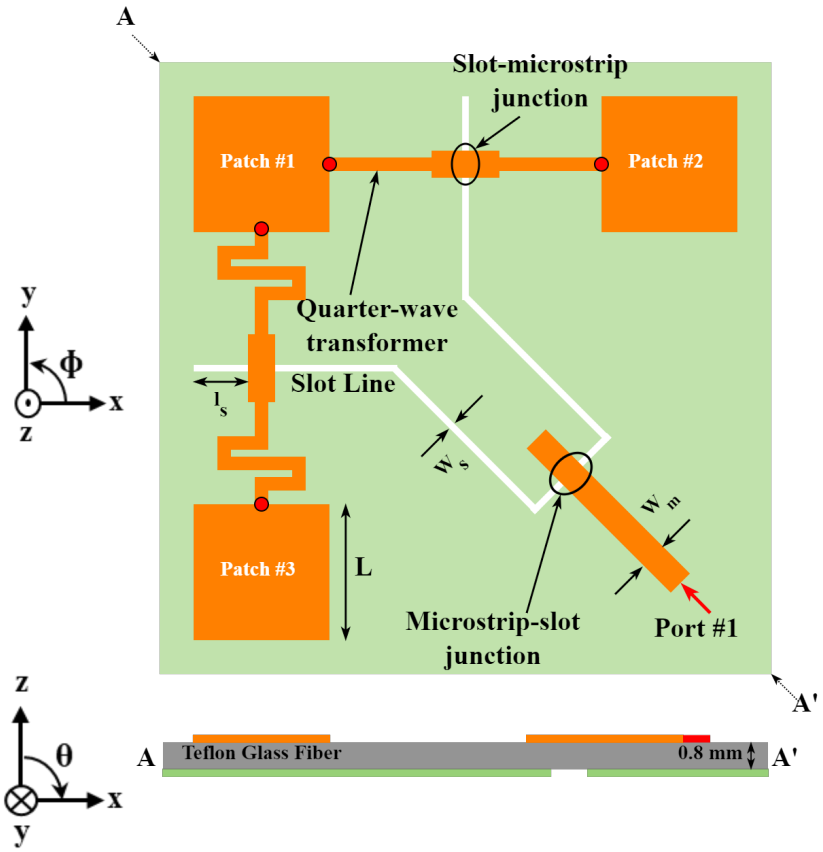

Figure 3.1: Geometry of proposed three-element microstrip patch array antenna.

microstrip junctions are directed towards patch #1 in an orthogonal manner, whereas signals from the same junctions are sent towards patches #2 and #3 through edge feeding. To enhance the isolation of the divided signals from those indicated as l_s in the figure, the slot line in the ground plane was extended by a distance of $\lambda/4$ at the slot-microstrip junction. The size and specifications of the antenna are provided in Table 3.1.

Table 3.1: Design parameters of the proposed microstrip antenna array.

Parameter	Value
Substrate	Teflon Glass Fiber
Relative dielectric constant, ϵ_r	2.15
Patch length, L	9.7 mm
Microstrip line width, w_m	2.1 mm
$\lambda/4$ slot line length, l_s	4.8 mm
Slot line width, w_s	0.2 mm

Four red circles with black boundary lines at the microstrip line's four ex-

tremities serve as ports to measure the feed networks' asserted phase difference. The simulation was run in Advanced Design System (ADS) by putting four ports (Port #2, Port #3, Port #4, and Port #5) at the right spots, as shown in Figure 3.2(a) and Figure 3.2(b).

3.1.2 Antenna Mechanism

The basic operation of the three-element microstrip patch array antenna's feed network without a meander line and with a meander line are shown in Figure 3.2(a) and Figure 3.2(b) respectively. The signal splits into two identical signals at the microstrip-slot junction after passing via the 50 Ω microstrip line from the input port (port #1). On the ground plane, these signals are transferred along the 0.2 mm slot line. Signals split into two equal-amplitude reverse phase signals at the slot-microstrip junction. Signals are sent to the microstrip line's ends via a quarter wavelength transformer.

As shown in Figure 3.2(a), Two electric vectors that are perpendicular to each other and have the same magnitude can be produced from port 2 and port 3. Furthermore, port 4 and port 5 are positioned in an orthogonal direction. Therefore, they can collectively generate two electric field vectors that are perpendicular to each other. However, this orientation results in a phase difference of 0° between the ports. Ultimately, they generate +45° linear polarization.

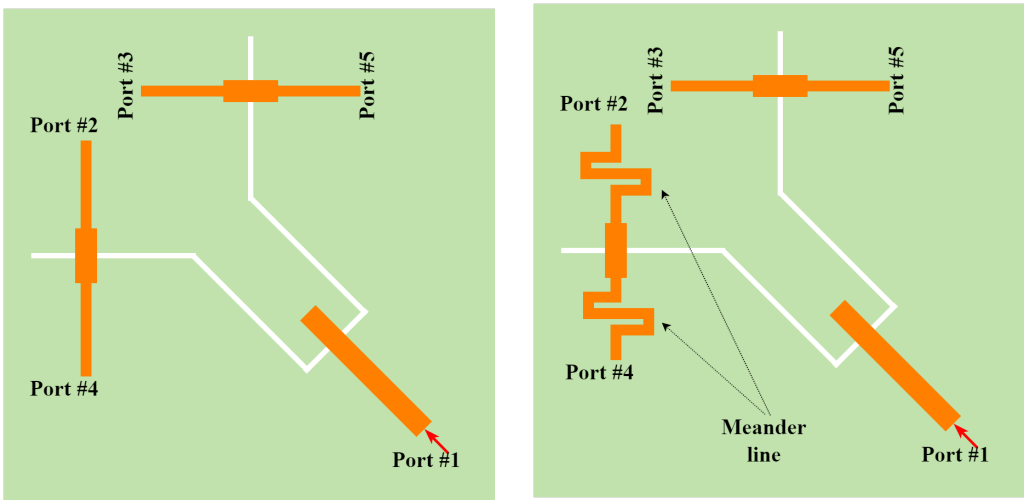

(a) Without meander line (b) With meander line

Figure 3.2: Basic behavior of the feed network of the proposed array antenna without meander line and with meander line.

Figure 3.2(b) depicts the feed network in the design, which includes a meander line. A meander line is incorporated into the design to ensure that there is a

quarter wavelength phase variation between the ports. This allows the patch to be stimulated by two signals of equal amplitude, with a 90° phase difference between them.

3.2 Result Analysis

The findings of the simulation are presented in this section. Initially, an analysis was conducted on the feed network to ascertain the phase difference of the network. This was achieved by substituting pins in place of the patch edge and performing simulations. After inserting the patch, the antenna is simulated and examined to determine its linear and circular polarization, as well as its impedance matching. Ultimately, the radiation pattern for circular polarization (CP) is analyzed, and the impact of varying meander line lengths on CP is investigated.

3.2.1 Phase Difference

Figure 3.3 illustrates the phase difference of the feed network. Four pins were placed at the extremities of the microstrip line, excluding the meander line, and then simulated using ADS. The simulation was rerun after the inclusion of meander lines. From the figure, it is evident that the network does not have any

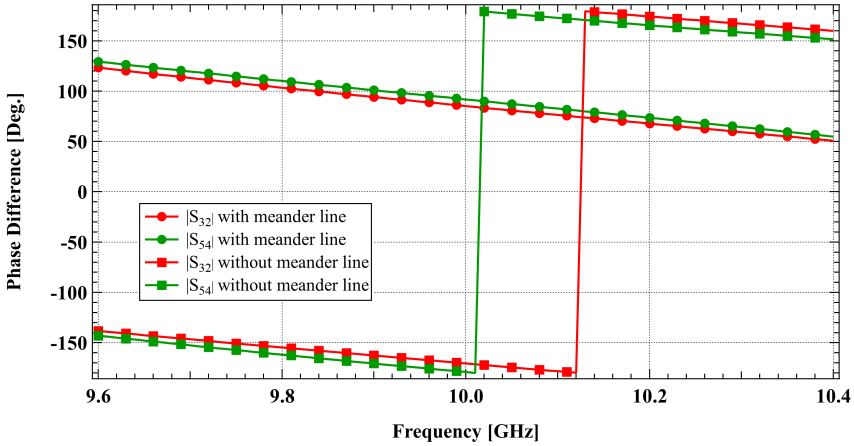

Figure 3.3: Phase difference of the feed network.

meander lines. At around 10 GHz, the phase difference between pins #2 and #3, as well as pins #4 and #5, is precisely zero, when there is no meander line in the design. At a frequency of 10.04 GHz, the phase difference in the network is precisely 90°, when there is a meander line in the design. Consequently, the

assertion of successfully achieving quarter wavelength phase differences across ports is validated.

3.2.2 Return Loss and Axial Ratio

Following analysis of the feed network, particular patches of appropriate length for resonating at the X-band frequency are added to the design. These patches are then simulated and their results analyzed. Figure 3.4 depicts the proposed

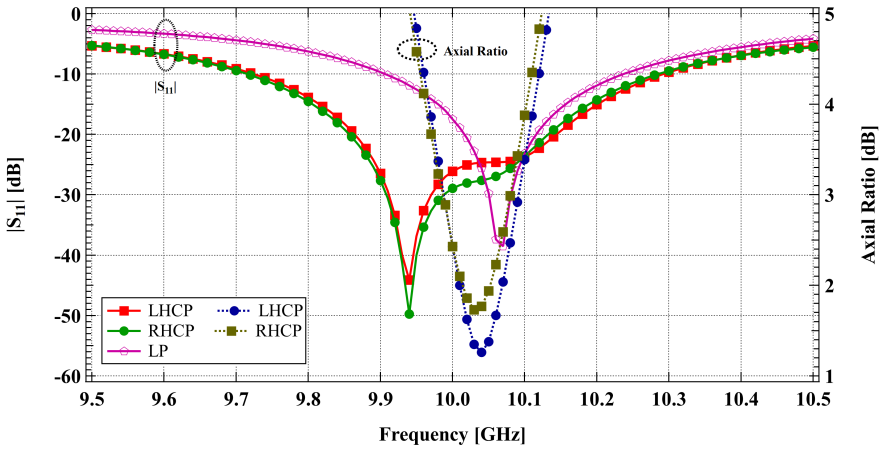

Figure 3.4: Simulated return loss and the axial ratio of the proposed three-element microstrip patch array antenna.

antenna's return loss and axial ratio. The figure clearly shows that the suggested constructed antennas can emit linear polarization (LP) when there is no meander line in the design and circular polarization (CP) in both senses when there is meander line in the design respectively. The reflection coefficient curve in Figure 3.4 shows an increase and drop at 10.04 GHz, showing that the antenna can produce two independent degenerative modes that are orthogonal to one another. Figure 3.5 shows a dip around the value of one on the Smith chart, which indicates the formation of two orthogonal degenerative modes. Figure 6 shows that at a frequency of 10.04 GHz, the axial ratio is less than 3 dB for both clockwise and counterclockwise circular polarization. The antenna has a linear impedance bandwidth of 300 MHz and a circular impedance bandwidth of 600 MHz. The antenna's axial ratio bandwidth (ARBW) measures 112 MHz.

3.2.3 Radiation Pattern

Figure 3.6 shows the antenna's three-dimensional (3D) and two-dimensional (2D) radiation patterns. The measurements show that the antenna produces a highly focused beam in the boresight direction. The 2D radiation pattern represents a

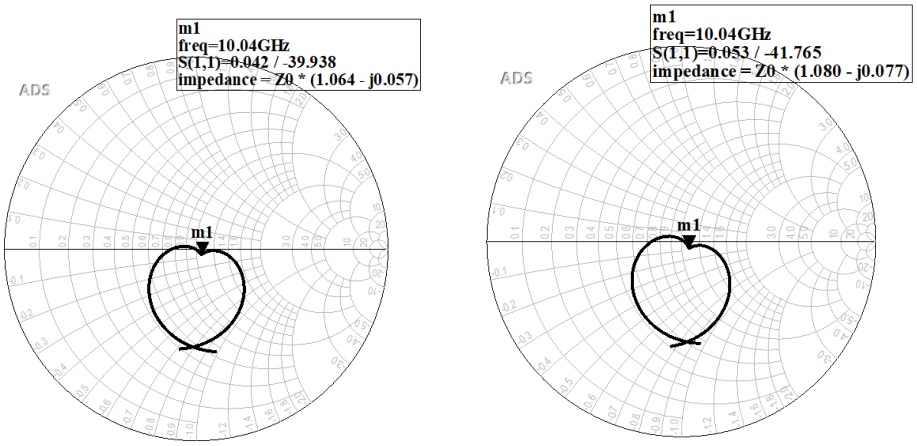

(a) RHCP (b) LHCP

Figure 3.5: Input impedance of the array antenna on Smith chart.

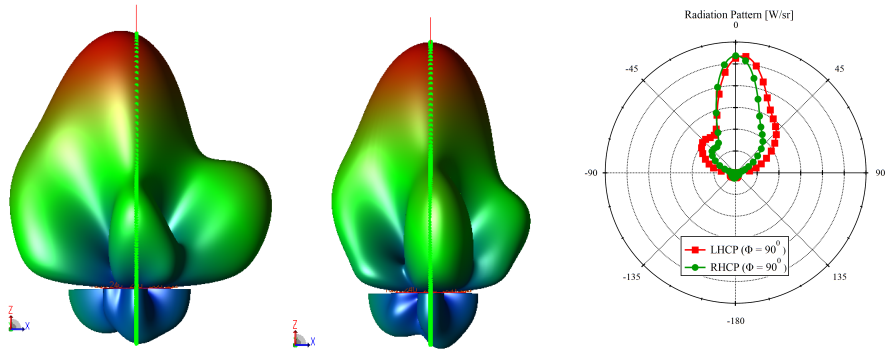

(a) RHCP (b) LHCP (c) 2D radiation pattern

Figure 3.6: Simulated 3D (a and b) and 2D radiation pattern of the proposed three-element patch array antenna.

plane that has been split at a phi angle of 90 degrees. The pattern's maximum strength occurs at zero (0) degrees on the polar plot, indicating that the antenna transmits a strong signal perpendicular to its axis for both left- and right-hand circular polarization.

Figure 3.7 shows the computed gain in decibels (dBic) relative to an isotropic circular radiator at various frequencies, for both senses of circular polarization. The antenna, which has a meander line design, produces a gain of 11.25 dBic for left-hand circular polarization and 11.35 dBic for right-hand circular polarization at the resonance frequency. Furthermore, it achieves a maximum gain of 11.65 dBic for circular polarization over the whole frequency range.

Figure 3.8 shows the cross-polarization level for left- and right-handed circular polarization. The graph's red color represents the LHCP level, whereas the green

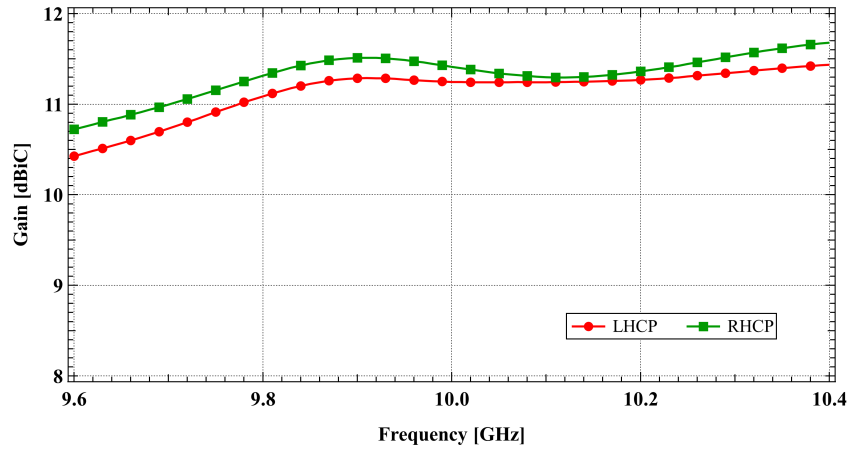

Figure 3.7: The gain of the array antenna for a range in the X-band frequencies.

color represents the RHCP level. The square marking represents left-handed

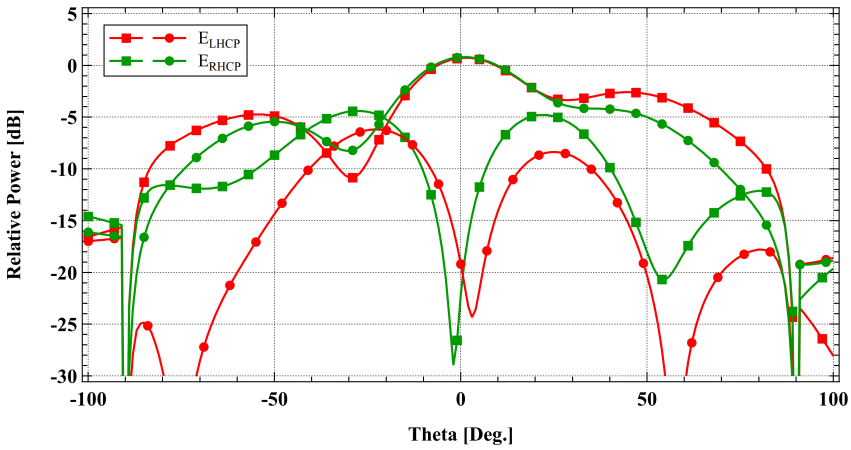

Figure 3.8: Relative power level difference for the antennas operated at LHCP and RHCP mode.

circular polarization, while the circle marker indicates right-handed circular polarization. The statistics demonstrate that the cross-polarization level exceeds 20 dB in all circumstances, ensuring the antenna's capability of circular polarization emission in both senses.

3.2.4 Effect of Meander Line Length

The previous section explained how the design's meander lines provide the requisite quarter-wavelength phase difference between equal amplitude orthogonal signals, resulting in the transmission of circular polarization. As a result, changing the length of the meander line affects the antenna's circular polarization performance in a variety of ways. This can be estimated by looking at the axial

ratio of the proposed antenna. Figure 3.9 shows how changing the length of the

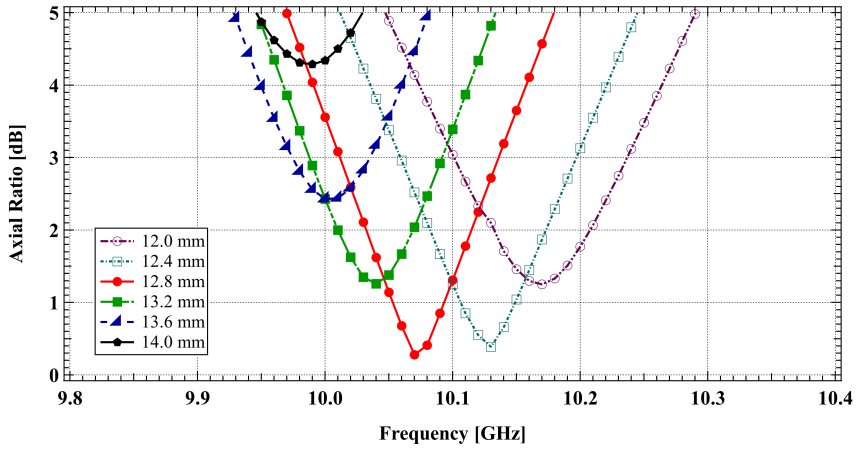

Figure 3.9: Axial ratio performances for different meander line lengths of the antenna operated at LHCP mode.

meander line in the design affects the axial ratio. The graphic shows that including a meander line in the design has a considerable effect on the antenna's CP performance. The axial ratio increases with length, and for line lengths greater than 13.6 mm, it exceeds 3 dB. Reducing the length of the meander line improves the axial ratio. However, when the length is smaller than 12 mm, the axial ratio appears to decrease. As a result, choosing the suitable length assures the correct phase difference between signals, resulting in accurate CP radiation. The antenna has a maximum axial ratio bandwidth of 140 MHz.

3.3 Summary

An antenna with three elements is designed and simulated using ADS software. The antenna utilizes both-sided MIC technology and operates at X-band frequency. The design without a meander line results in a linear polarization of 45 degrees, while the version with a meander line achieves circular polarization. The position of the meander line determines whether the signal is left-hand circularly polarized (LHCP) or right-hand circularly polarized (RHCP). The proposed layout achieves a gain of 11.25 dBic. Using a single input simplifies the structure's feed network, and a Co-pol and X-pol level differential greater than -15 dB indicates excellent circular polarization performance.

Chapter 4

Orthogonal Excitation Four-Element Patch Array

This chapter describes a 2×2 microstrip patch array antenna, in which each patch is excited orthogonally. The aim is to achieve circular polarization using a simple feed mechanism. The microstrip feed line transmits signals to each patch through the structure, employing both-sided MIC technology. The antenna consists of a four-element array, and the diagonal patches propagate in the same polarization direction. The inclusion of the meander line in the modified design effectively resolves the limitation. This chapter is conducted using simulation techniques and is structured in the following manner: it begins with a description of the structure, followed by an analysis of the outcomes.

4.1 Antenna Design Method

4.1.1 Antenna Structure

Figure 4.1(a) shows the design structure of the proposed antenna array. Four microstrip square patches have been etched on top of a 0.8 mm thick Teflon Glass Fiber substrate with a relative dielectric constant of 2.15. A 0.2 mm wide slot line is created in the ground plane. The 50 Ω impedance microstrip line receives an input signal from the port and propagates it to a slot line via a microstrip-slot branch (shown by a solid line circle in the image). The array is energized by two microstrip lines that connect each patch via slot-microstrip junctions.

The illustration shows these intersections as dotted line circles. All the slot-microstrip junctions draw power from the same slot line. The microstrip-slot junction acts as a parallel divider, hence the slot line impedance must be double that of the microstrip line impedance. As a result, the slot line has an impedance

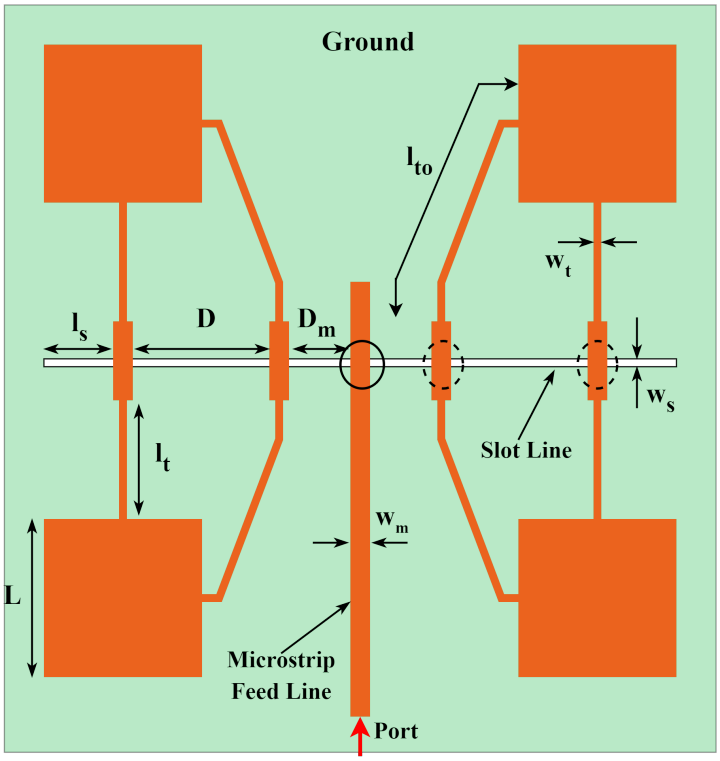

(a) Proposed design

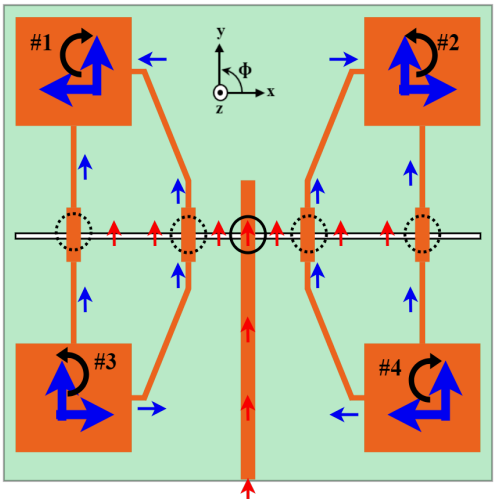

(b) Schematic without meander line

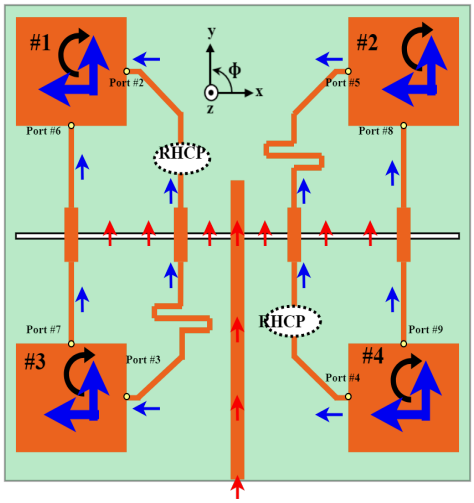

(c) Schematic with meander line

Figure 4.1: Geometry (a) and schematic diagram of the basic behavior of the proposed array antenna (b) without meander line (vertical linear polarization) and (c) with meander line (circular polarization) of the proposed array antenna.

of 100 Ω. The slot-microstrip junction functions as a series divider. The symbol l_s represents a quarter wavelength extension of the slot line. The D variable represents the distance between two slot-microstrip junctions. W_m denotes the width of the microstrip line. The variables l_t and l_{to} denote the lengths of two

orthogonal quarter wave transformers formed at slot-microstrip junctions. And, the relation between l_t and l_{to} can be expressed as, $l_{to} = l_t + \lambda/4$. Table 4.1 shows the design's dimensions parameters and their optimal values.

Table 4.1: Dimension and design parameter of the proposed microstrip antenna array.

Parameter	Value
Patch dimension, L×L	$9.7 \times 9.7\ mm^2$
Copper thickness (ground, patch)	0.018 mm
Slot-line width, w_s	0.2 mm
Microstrip feed line width, w_m	1.6 mm
Quarter-wavelength transformer width, w_t	0.6 mm
Quarter-wavelength transformer length, l_t	7.8 mm
Orthogonal transformer length, l_{to}	15.44 mm
Slot-line stub length, l_s	4.8 mm
Line to line distance, D	10.5 mm
Line to line distance, D_m	4.4 mm

4.1.2 Working Principle

As the signal travels along the microstrip line, it splits into two identical signals with the same phase at the microstrip-slot junction. At the slot-microstrip junction, these signals are divided again into two identical signals with opposite phases (shown by a dotted circle). Figure 4.1(b) shows that the red arrow represents the in-phase signal, while the blue arrow indicates the out-of-phase signal. Two microstrip lines that arise from adjacent slot-microstrip junctions on the same slot line are perpendicularly coupled to each patch. The signals are the same amplitude, but the U-shaped microstrip lines are longer than the other lines, ensuring a 90° phase shift between the two perpendicular signals. As a result, each element of the array can propagate in a circularly polarized manner. Furthermore, the feed network is constructed so that patches #1 and #4, as well as patches #2 and #3, receive the same field distribution. Patches #1 and #4 emit radiation in a counterclockwise direction, while patches #2 and #3 emit radiation in a clockwise circular fashion.

This design approach demonstrates that the antenna can generate both right- and left-handed circular polarization in a single array. However, because they propagate in different directions, this type of propagation is mutually exclusive. This issue can be resolved by properly examining the field lines in the patches. The two arms of the U-shaped microstrip line are in opposite direction to each

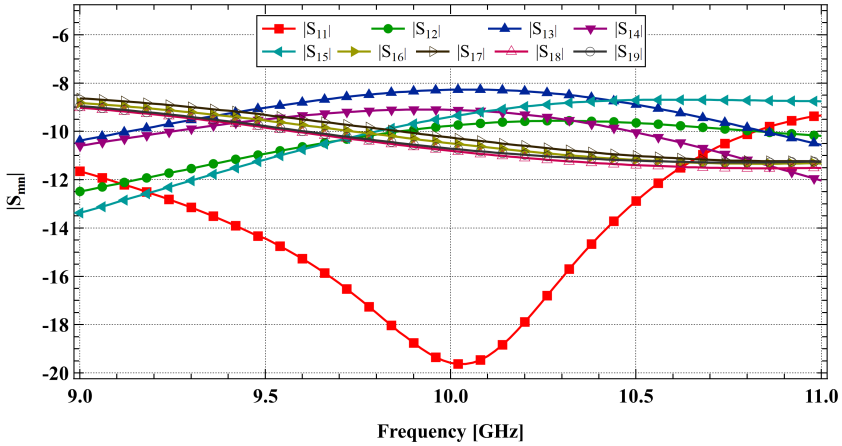

(a) Reflection coefficient of feed network

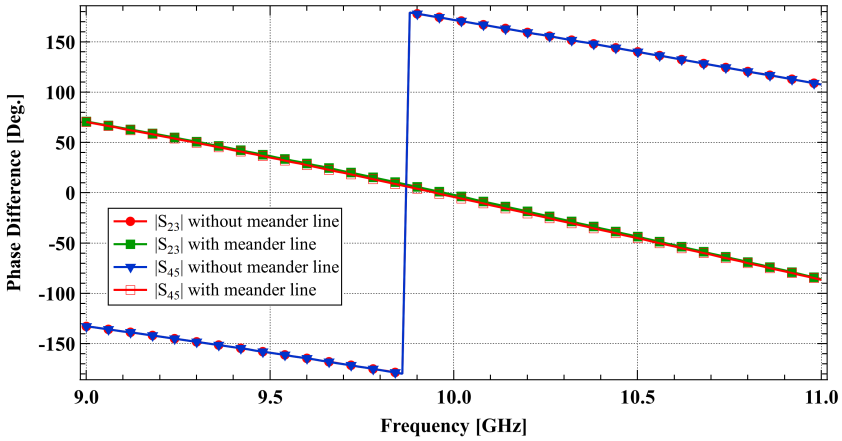

(b) Phase difference of feed network

Figure 4.2: Feed network analysis. (a) Reflection coefficient and transmission coefficient of the feed network. (b) The phase difference between ports of the feed network when the meander line is inserted into the design.

other because they originate at a slot-microstrip junction, as shown in Figure 4.1(b). As a result, the horizontal electric fields E_x in patches #3 and #4 run in opposite directions, as opposed to the horizontal electric fields, E_x, in patches #1 and #2. The feed network's orientation causes the orthogonal patches to emit in two separate polarization senses. Since dual circular polarization is happening due to horizontal electric fields being opposite to each other, the antenna ends up producing only a vertical polarized signal.

Implementing a meandering path may help to alleviate this issue. Figure 4.1(c) shows that the E_x field line is aligned in the same direction for all patches as the meander line has been inserted in the arm of the U-shaped microstrip line. Figure 4.2 shows the impedance matching and phase differences among ports for the feed network. Figure 4.2(a) shows that the input signal is nicely

carried out from the input port as the transmission coefficient are above -10 dB. Also, it is clear from the Figure 4.2(b) that, the meander lines can transform out-of-phase signals to in-phase signals at the U-shaped microstrip line's ends. This simulation was carried out by inserting ports (Ports #2, #3, #4, #5, #6, #7, #8, and #9) in place of a yellow-colored black line circle as shown in Figure 4.2(c). However, A meander line in the arms of the microstrip lines supplying patches #2 and #3 generates left-hand circular polarization (LHCP). But, a meander line in the microstrip lines that feed patches #1 and #4 gives right-hand circular polarization (RHCP). In addition, the U-shaped microstrip line has been extensively adjusted to accommodate the meander line in the design.

4.2 Results and Discussions

In this section a parametric analysis presented which has been carried out for the design without meander line in the design, Once an optimized results has been visualized, meander line has been inserted into the design and rest of the design and results has been speculated.

4.2.1 Parametric Analysis

This study examines the slot stub length (l_s), orthogonal microstrip length (l_{to}), and different lengths for microstrip line spacing (D_m) above the slot line. Figure

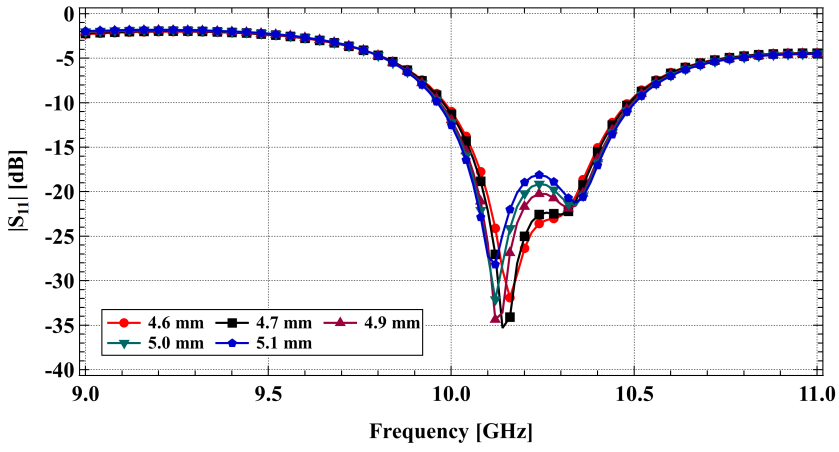

Figure 4.3: Parametric analysis for various stub length, l_s of the proposed four-element microstrip patch array antenna without meander line in the design.

4.3-4.6 illustrates the return losses for different dimensions. Figure 4.3 demonstrates that the changes in quarter wavelength slot line stub length have little effect on the whole array. However, different lengths of the U-shaped microstrip

line which are denoted as l_{to}. have an effect on impedance matching as well as the impedance bandwidth of the array as shown in Figure 4.4. The antenna's circu-

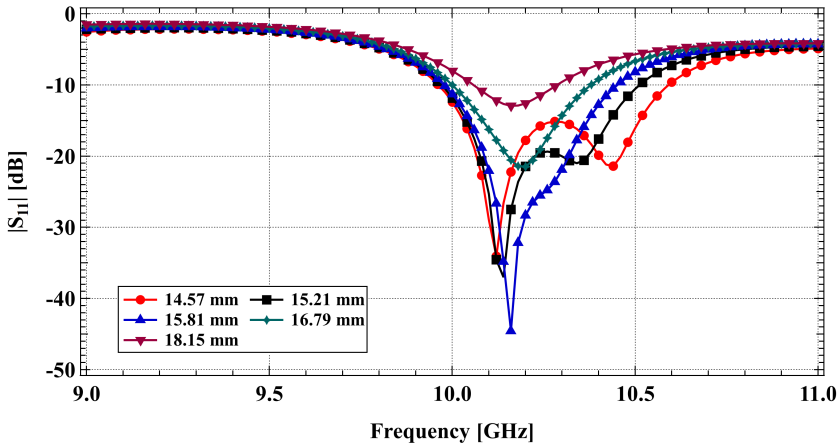

Figure 4.4: Parametric analysis for various stub length, l_{to} of the proposed four-element microstrip patch array antenna without meander line in the design.

lar polarization capability is compromised for U-shaped microstrip line lengths shorter than 15 mm due to its inability to achieve a 90° phase shift. Figure

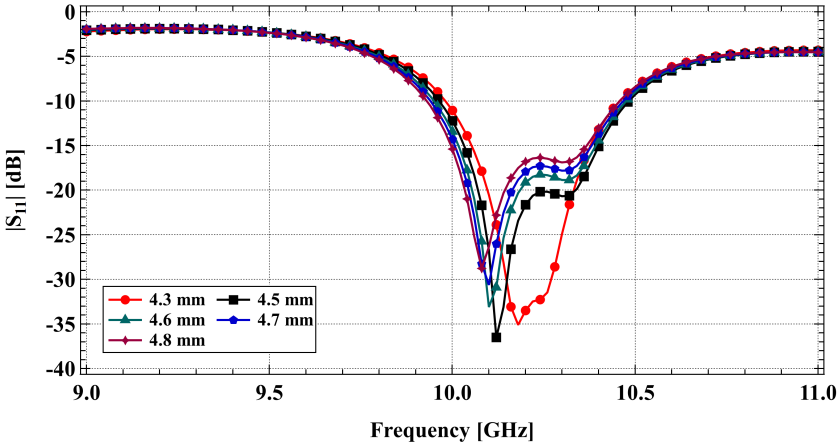

Figure 4.5: Parametric analysis for various distances of D_m of the proposed four-element microstrip patch array antenna without meander line in the design.

4.5 displays the return loss for different spacing lengths between two microstrip lines positioned above the slot line. Furthermore, Figure 4.6 provides return losses for various spacing parameters between microstrip lines. Additionally, presents several microstrip line lengths, l_{to}, that can be used to maintain a square shape for the array. From this analysis, the optimum dimensions for the array are selected and simulated based on these evaluations.

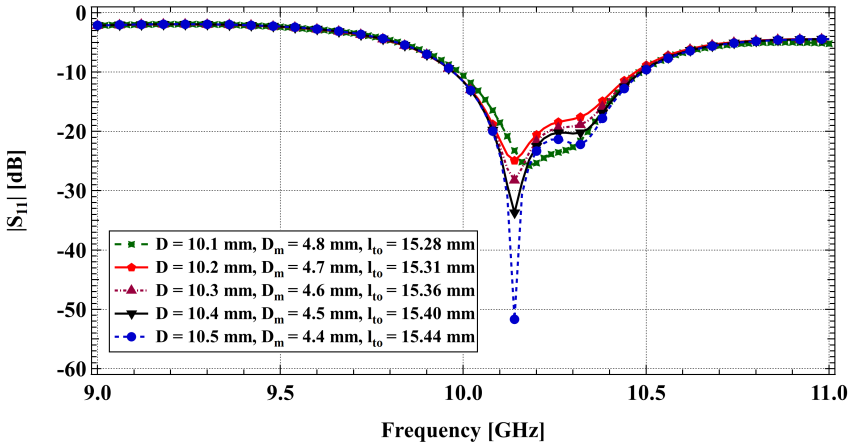

Figure 4.6: Parametric analysis for various parameter variations of the proposed four-element microstrip patch array antenna without meander line in the design.

4.2.2 Optimized Results

By incorporating two meander lines into the arm of the U-shaped microstrip line, the direction of the horizontal electric field can be reversed, resulting in the propagation of the complete array with the same-handed polarization. This section provides the optimized results obtained after the inclusion of a meander line. In addition, a slight adjustment is made to the size of the array to achieve circular polarization at a frequency of 10 GHz. The inclusion of meander lines in the patch array increases its size by 1.2 × 1.2 mm^2, resulting in a total array size of 41 ×41 mm^2.

4.2.2.1 Return Loss, AR, and Gain

Figure 4.7 shows the simulated return loss for the proposed antenna design without a meander line as well as with meander lines with the axial ratio in the frequency band. The data clearly shows that the antenna has outstanding impedance matching in the X-band frequency region, as seen by a return loss of -41.86 dB at 9.88 GHz. The curve's rise and fall around 10 GHz show the presence of two orthogonal modes with closely separated resonance frequencies, which is necessary for circular polarization. The diagram also shows that the antenna has an impedance bandwidth of 460 MHz, with a return loss of -10 dB between 9.72 GHz and 10.18 GHz.

The axial ratio is 0.12 dB as seen from the figure at 10 GHz, which is around the dip regions of the return loss curve. This shows the existence of two separate resonant modes that are perpendicular to one another. As a result, the antenna is capable of producing circularly polarized radiation at a frequency of 10 GHz.

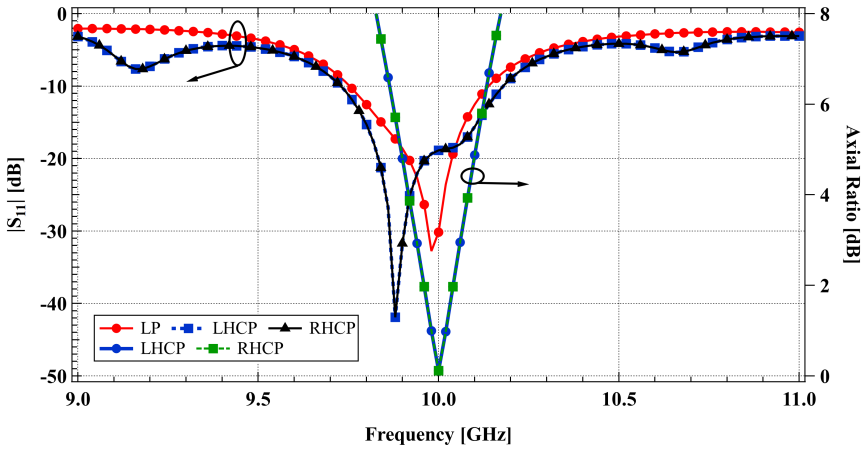

Figure 4.7: Optimized return loss and axial ratio of the proposed four-element microstrip patch array antenna with meander line incorporated into the design.

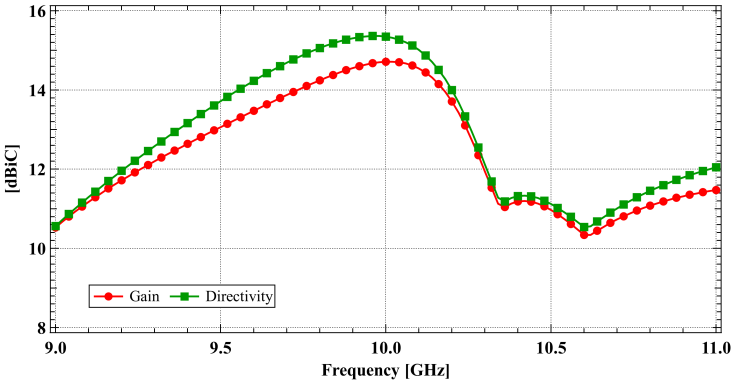

Figure 4.8: Gain and directivity versus frequency for RHCP of the proposed four-element microstrip array antenna.

Figure 4.8 depicts the simulated gain and directivity characteristics of the proposed antenna for right-hand circular polarization (RHCP). The antenna has a directivity of 13.30 dBi and a gain of 12.87 dBi at 10 GHz, which is its resonance frequency.

4.2.2.2 Radiation Pattern

Current distributions of the designed antenna array with the meander line and without the meander line are shown in Figures 4.9-4.10. It is clear from the figure that the meander line in the design helps field lines to reverse and act as one sense of CP. Patches #2 and #3 radiate similarly to #1 and #4. This gives the array antenna right-hand circular polarization. When there are no meander lines in the microstrip line that feed patches #1 and #4, but in the arms of U-shaped lines that feed patches #2 and #3 causes the array to radiate in a

left-hand circular polarized (LHCP) manner. It is also clear from the figure that the surface current for RHCP antennas moves in the opposite direction to that of LHCP antennas as well as the feeding network shows small changes from the design without the meander line. As mentioned earlier these adjustments are made to include the meander line in the design.

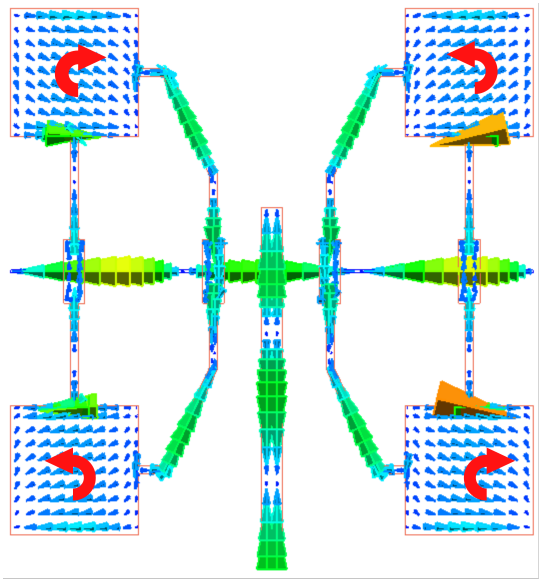

Figure 4.9: Current distribution of the proposed circular polarized microstrip array antenna without meander line operated in linear polarization mode where diagonal patches polarization senses cancel out each other.

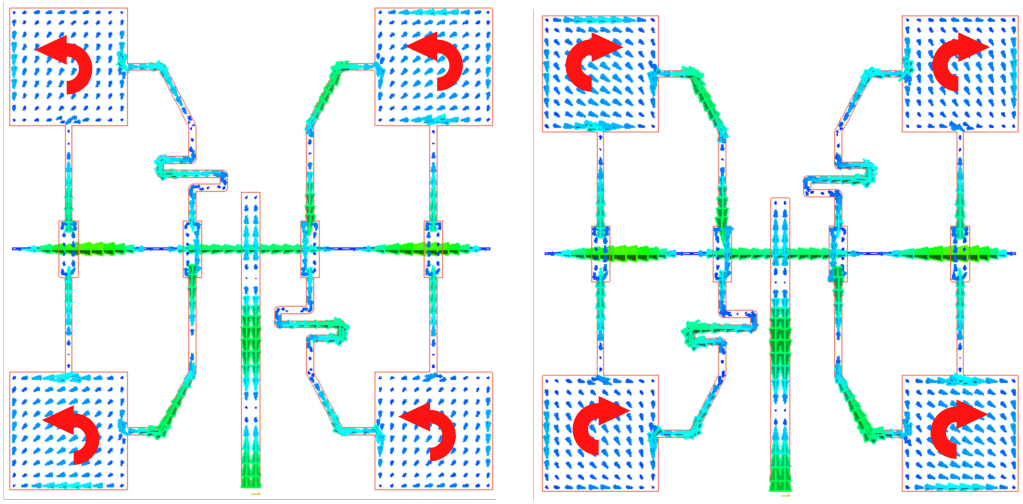

(a) RHCP (b) LHCP

Figure 4.10: Current distribution of the proposed circular polarized microstrip array antennas with meander line operated in RHCP and LHCP mode.

According to Figure 4.11, the cross-polarization level for both right-hand cir-

cular polarization (RHCP) and left-hand circular polarization (LHCP) operation exceeds 42 dB. Hence, it is clear that the proposed circular polarized array an-

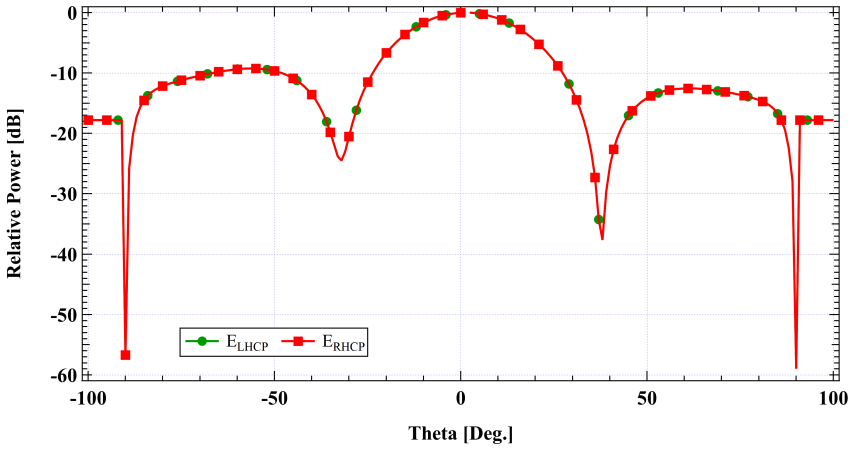

(a) LP

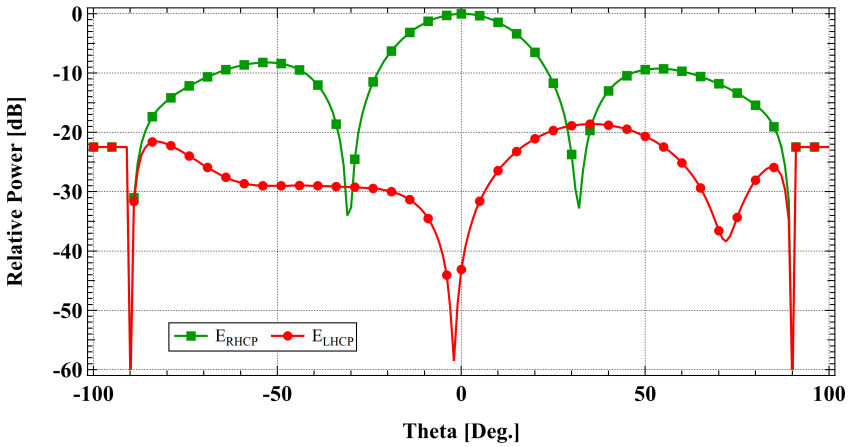

(b) RHCP

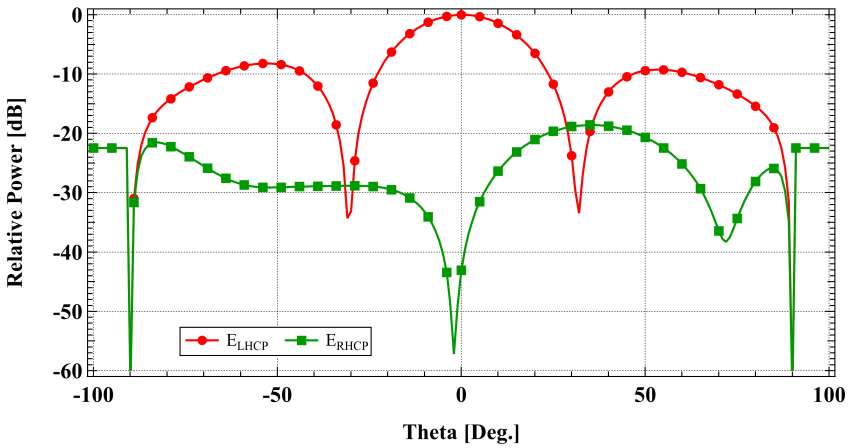

(c) LHCP

Figure 4.11: Radiation pattern of the proposed design for LP, RHCP, and LHCP operation.

tenna has exceptional radiation capabilities for both right-hand circular polarization (RHCP) and left-hand circular polarization (LHCP) operations.

4.2.3 Effect of Meander Line Length

The study found that the meander line in the design is critical for ensuring accurate CP array performance. It can be confidently stated that the length of the meander line has a direct impact on the array antenna's overall CP performance. Figure 4.12 shows how the length of meander lines influences the performance of

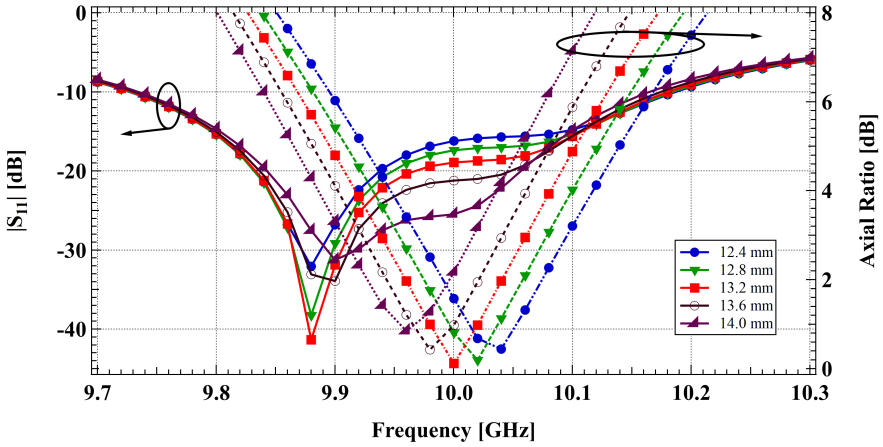

Figure 4.12: Effect of meander line length on the microstrip array antenna operated in LHCP mode.

array antenna circular polarization (CP) and impedance. The graph shows that the antenna performs best in terms of circular polarization (CP) and impedance matching when the meander line length is 13.2 mm. When the line length reaches 14 mm or falls below 12.4 mm, both the CP and impedance performance deteriorate, but the percentage of bandwidth remains constant. The bandwidth of the axial ratio is approximately 140 MHz.

4.3 Summary

This section summarizes this chapter's designed work simulation findings and compares them with previous work. Table 4.2 presents a comparison between the performance of the proposed work as well as of the previous chapter's three-element array antenna and that of other works. The data unequivocally demonstrates that the antenna exhibits significantly superior performance when configured as a three-element array as well as a four-element microstrip patch array antenna. The proposed antenna exhibits a maximum gain of 11.65 dBic for the

three-element array antenna and 15.02 dBic for the four-element microstrip patch array antenna, which surpasses the performance of prior designs. Additionally, it offers a much wider axial ratio bandwidth of 140 MHz.

Table 4.2: Comparison of the proposed 3-element and 4-element circularly polarized microstrip patch array antenna with other works.

[Ref]	No of Elements	No of Ports	Gain	ARBW
[55]	Four(2×2)	Single	8.11 dB	$< 1\%$
[58]	Four(2×2)	Single	4.83 dB	$< 1\%$
[60]	Four(4×1)	Single	10 dBic	0.4%
[62]	Four(2×2)	Dual	4.51 dB	160 MHz
This Thesis	Three	Single	11.65 dBic	140 MHz
	Four(2×2)	Single	15.02 dBic	140 MHz

Chapter 5

Large Scale Circularly Polarized Array

The previous two chapters explore the utilization of both-sided MIC technology in the design of microstrip array antennas. This technology offers flexibility in design and the potential for easy scalability to larger arrays. This chapter explores the potential by using a simple feed single-layer 256-element (16×16) microstrip patch array antenna for circular polarization. This chapter provides a comprehensive explanation of the construction of a large-scale array. The array is constructed using a similar approach as before but with a different arrangement of the feed. Additionally, the simulation data are thoroughly analyzed and discussed.

5.1 Design and Mechanism

In the beginning, a feed network is built and then fine-tuned for a 2×2 array that is running at a central frequency of 5.8 GHz. Once it is complete, four patches are combined in the feed circuit to create a 2×2 array, which is then simulated for additional optimization. The larger arrays are built with the basic array and simulated for optimization. A substrate composed of Teflon with a thickness of 0.8 millimeters and a relative dielectric constant of 2.15 is used in the construction of the antennas. The patches are situated on the surface that is facing upward. Due to the presence of a slot line in the ground plane that is 0.2 millimeters wide, the antenna has the potential to utilize both-sided MIC technology. Because of this, the construction of the feed network is made easier, and it ensures that the amount of power provided to each array is the same. The antenna configuration that is being analyzed is shown in Figure 5.1.

It is essential to have two electric fields that are perpendicular to each other and display a phase difference of one-quarter of a wavelength to achieve circular

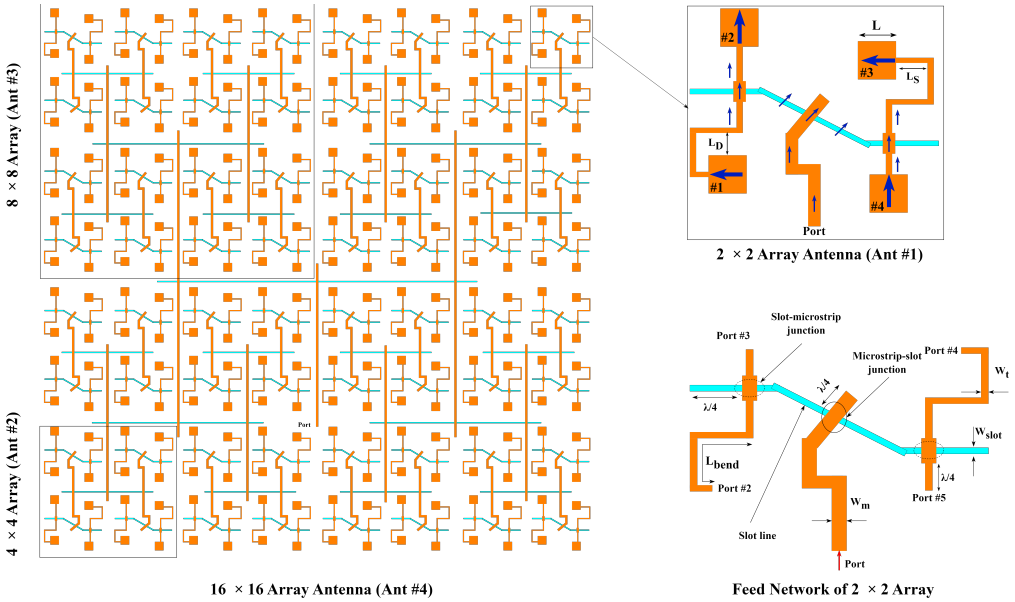

Figure 5.1: Geometry of proposed 256 element microstrip array with the basic feed network. Ant #1 (4), Ant #2 (16), Ant #3 (64), and Ant #4 (256) are the four array antennas (with several numbers of elements).

polarization. This situation must be present in order to achieve circular polarization. In order to accomplish this task by utilizing the proposed 2×2 array, the feed network is created in a manner that enables the bend in the microstrip line that connects patch #1 and patch #3 to be aligned perpendicularly with patch #2 and patch #4. To ensure the manufacture of the necessary 90° phase difference between them, the microstrip line is curved or bent, which assures its production.

5.2 Result and Discussion

5.2.1 Imepedance Matching

The feed network of the antenna is emulated by connecting a 50 Ω microstrip line to the input.

Four ports, namely port#2, port#3, port#4, and port#5, are linked to the microstrip line ends where the patch would be attached. Each port has an impedance of 190 Ω. Figure 5.2 depicts the simulated reflection coefficient and transmission coefficient of the feed network for the 2×2 array. Based on the illustration shown in 5.2(a), it is clear that the input impedance $|S_{11}|$ of the feed network is outstanding as shown by a return loss of less than -40 dB at the central frequency of 5.8 GHz. other scattering parameter value above -10 dB level

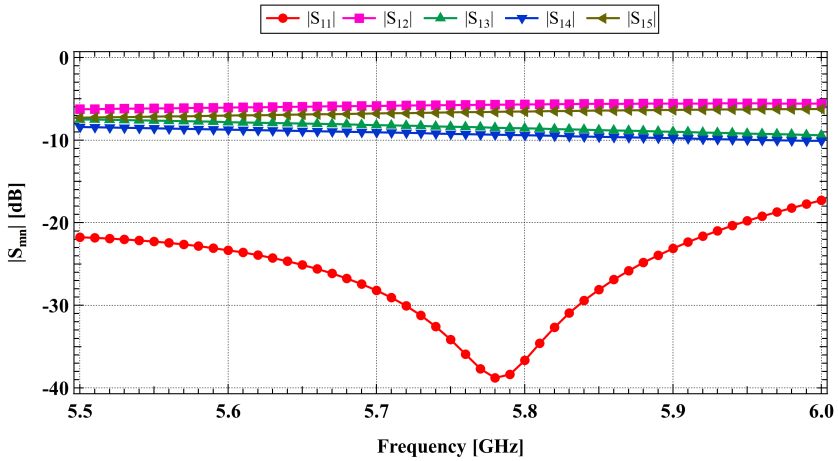

(a) 2×2 feed network impedance

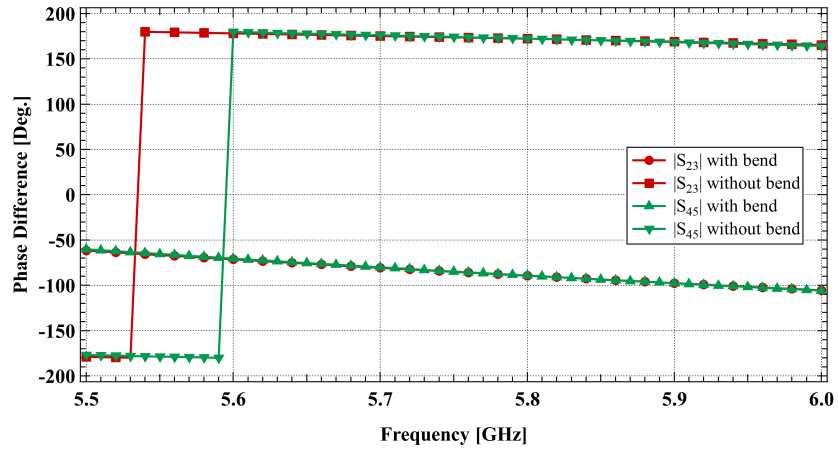

(b) 2×2 feed network phase

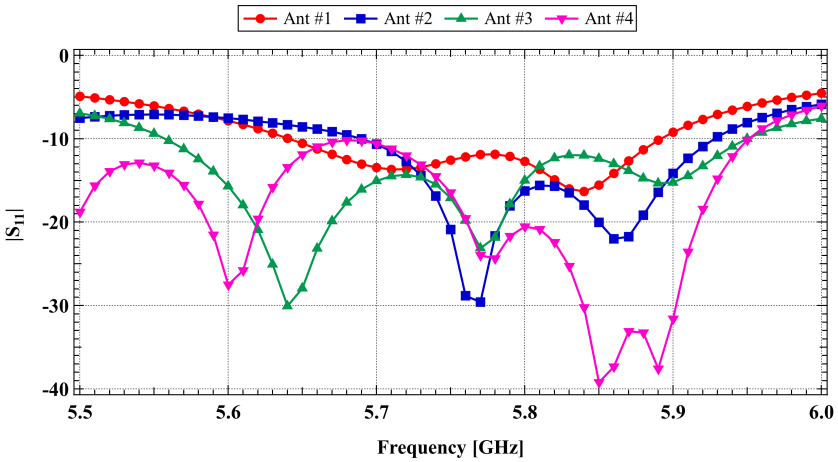

(c) Array antennas' return loss

Figure 5.2: Simulated return loss for the feed network and array antennas' designed for circular polarization.

indicates proper transmission. Figure 5.2(b) shows the phase difference between the microstrip line ends ports. It is clear from the figure that the phase differ-

ence between ports are 180° when there is no bend (L_{bend}) in the microstrip line that is feeding to patches but has a phase difference between ports or 90° when there is a bend in the microstrip line. Figure 5.2(c) depicts the return losses for Ants #1–#4 showing that the antennas efficiently match the input signal, with return loss levels below -10 dB. The simulation findings show that the four antennas have impedance bandwidths of 260 MHz, 380 MHz, 240 MHz, and over 440 MHz, respectively.

5.2.2 Radiation Pattern

The antenna functions with a left-hand circular polarization (LHCP) configuration. Figure 5.3 illustrates the comparative power of the suggested antennas. Based on the image, it is clear that all the antennas (Ant#1- Ant#4) have cross-

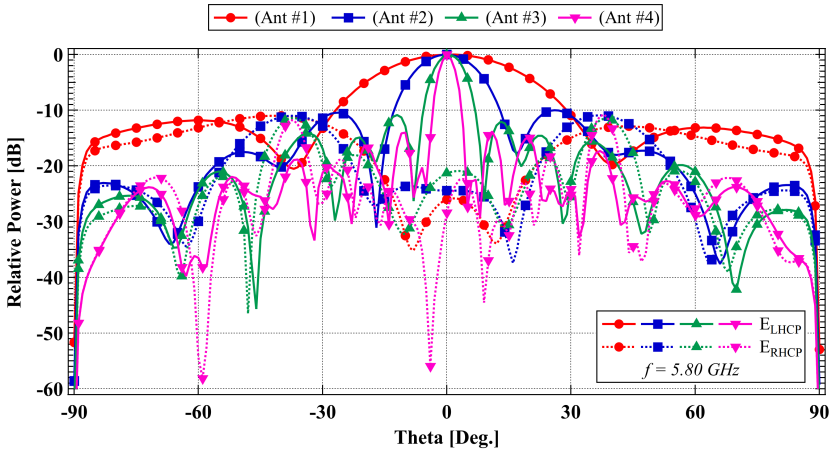

Figure 5.3: Relative power of the proposed circularly polarized microstrip patch array antenna operated in LHCP mode.

polarization power level differences of more than 20 dB, indicating a strong radiation pattern in the LHCP mode.

Figure 5.4 and figure 5.5 demonstrate that the proposed antenna has a high level of gain and directivity, with a side lobe level difference of over 20 dB relative to the main lobe. Additionally, it is capable of efficiently radiating in the circular polarization (CP) sense since the antennas have axial ratios that are well below 3 dB, with the minimum value being 0.70 dB for a 256-element antenna operating at a resonance frequency of 5.79 GHz. The highest directivity of antennas with 2×2, 4×4, 8×8, and 16×16 components is 13 dBic, 18.34 dBic, 23 dBic, and 27 dBic, respectively.

The 3D radiation pattern of the proposed antennas is seen in Figure 5.6. Increasing the size of the array with the radiator number causes the beamwidth

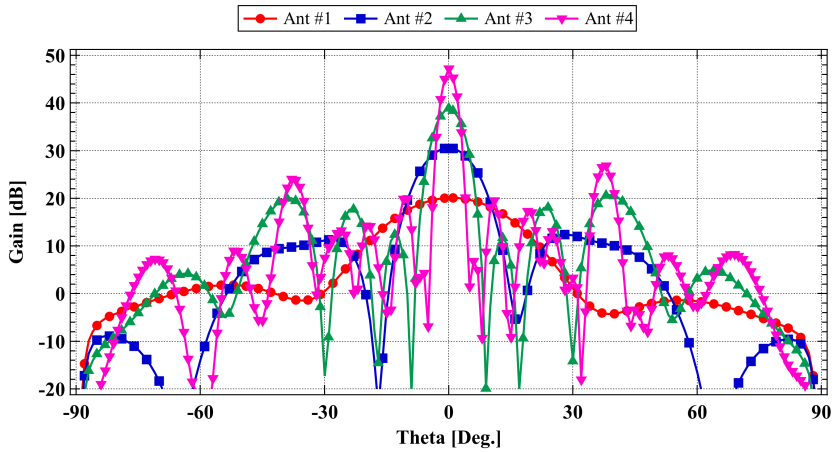

Figure 5.4: Simulated Broadside gain of the proposed circularly polarized antenna.

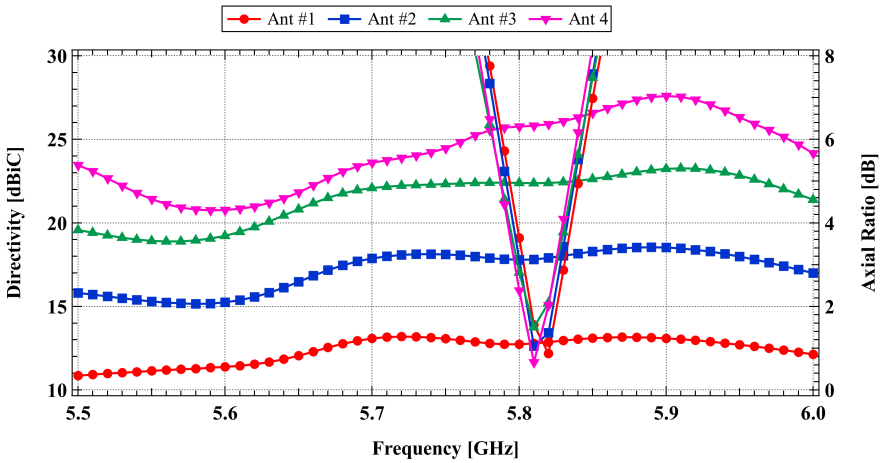

Figure 5.5: Simulated directivity and axial ratio of the proposed microstrip patch array antenna.

of the suggested arrays to become narrower. On top of that, the beam becomes highly focused in the boresight direction. Therefore, it can be concluded that based on the information provided, the 256-element array antenna is suitable for long-range signal transmission with optimal power efficiency.

5.3 Summary

This chapter presents the design and simulation of a 256-element microstrip patch array antenna. The objective is to verify the effectiveness of employing both-sided MIC technology in simplifying the construction of the feed network for large-scale arrays. In addition, a microstrip patch array antenna consisting of 4, 16, and 64 elements was built as part of the process to ultimately construct the 16×16

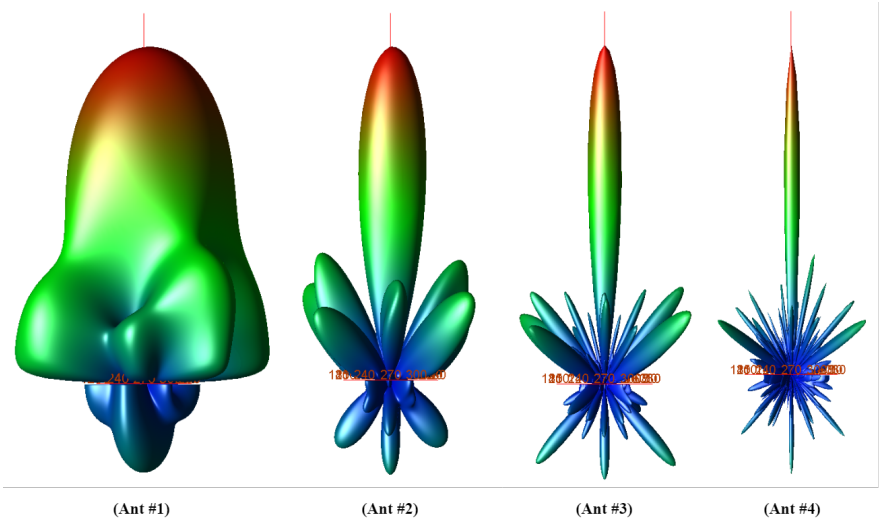

Figure 5.6: Simulated 3D radiation pattern of the proposed microstrip patch array antenna.

array. The presence of a single input port verifies the intended uncomplicated configuration, characterized by a foresight gain of 48 dB and a relative power differential above -20 dB. The axial ratio values of all the antennas were below 3 dB.

Chapter 6

Beam Steering Four-Element Patch Array

This chapter presents a microstrip array antenna with four elements that are used for beam steering operations by utilizing both-sided MIC applications. This chapter also details the inclusion of a planar phase shifter into the design and acheive beam switching with the same array arrangement. The feeding network of the proposed design is quite simple because of the design flexibilty of the both-sided MIC technology. The array antenna is designed to be simulated at the resonance frequency of 3.5 GHz in the sub-6 GHz 5G frequency range, in response to the growing number of smartphone users and the increasing demand for streaming. In the period of widespread 4G usage, it is necessary to make the switch to the next generation of technology to ensure the successful installation of new systems. The sub-6 GHz frequency range is the immediate frequency band used for the efficient implementation of the 5G frequency band.

6.1 Beam Steering as a Concept

6.1.1 Design and Working Mechanism

The microstrip line has an impedance of 50 Ω. The slot impedance in the microstrip-slot branch circuit must be precisely 100 Ω due to its function as a parallel power divider. This device splits the signal into two signals of equal amplitude and in phase. The strip impedance in the slot-microstrip branch circuit must be 50 Ω, as it functions as a series power divider [115]. This divider splits the signal into two signals of equal amplitude that are out of phase with each other. To achieve improved impedance matching, quarter wave transformers are employed, with an impedance of precisely 92.95 Ω, as determined by equation

(6.1).

$$Z = \sqrt{Z_1 \times Z_2} \tag{6.1}$$

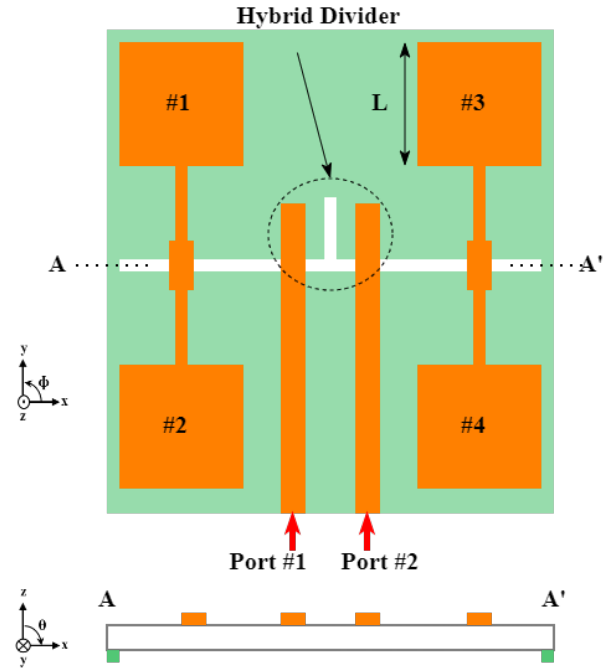

(a) Antenna Structure

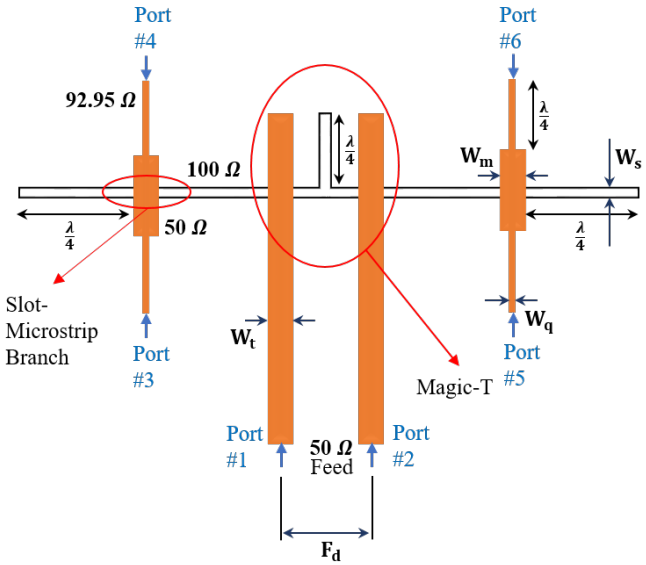

(b) Feed Network

Figure 6.1: Configurations of the proposed array antenna which contains four radiating square patches, microstrip lines, quarter wave transformers, slot line. Where, W_t=W_m=2.6 mm, W_q=0.8 mm, W_s=0.2 mm, F_d =15.2 mm.

The slot line at the slot-microstrip branch extends by a quarter-wavelength to improve the antenna's characteristics. Similarly, the quarter-wavelength microstrip line is also extended at the microstrip-slot branch. Figure 6.1 displays the arrangement of the suggested array antenna, revealing the use of two slot-microstrip branches to connect the four antenna parts. The impedance of a slot-line is equal to double the impedance of a microstrip line. Two input ports with a 50 Ω impedance are connected to two microstrip lines with a width of 2.6 mm. Four additional ports, each having an impedance of 172 Ω, are connected to the terminals of four quarter wave transformers, as seen in Figure 6.1(b). And, F_d, which represents the distance between two input microstrip lines.

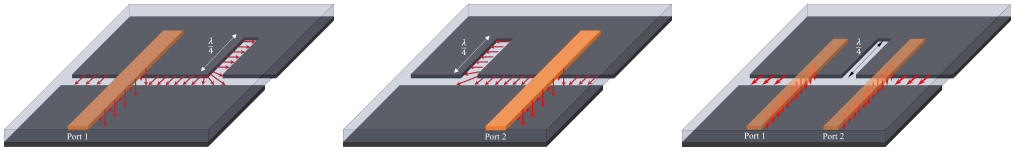

(a) Only port #1 (b) Only port #2 (c) Port #1 & #2 with $\Delta\phi$

Figure 6.2: Hybrid coupler structure with schematic electric fields for several conditions.

The T-type slot line in the ground plane incorporates a quarter wavelength slot, enabling the design to operate in a hybrid divider configuration. Figure 6.2 provides a schematic representation of the behavior of field lines on the slot line and microstrip line, which helps to understand the operation of the proposed antenna's working operation. Two parallel microstrip lines and an inverted T-shaped slot in the ground plane form a hybrid divider, which is a signal division technique that uses both-sided MIC technology to divide a signal into two equal amplitude signals that may be either in phase or out of phase depending on the input signals provided phase. The slot lines allow for the transmission of both in-phase and out-of-phase signals, as depicted in Figure 6.2. The schematic electric field distribution is depicted in Figures 6.2(a) and 6.2(b) when the input signal is applied to ports #1 and #2 individually.

When an input signal is received exclusively by port #1, it travels along the microstrip line and is split into two equal amplitude in-phase signals at the microstrip-slot branch, since the microstrip-slot branch functions as a parallel power divider. The quarter wavelength stub functions to prevent the signal from propagating towards the right side of the slot lines. Consequently, port #1 functions as the **H** port or in phase divider. The signal only travels in the leftward direction along the slot line. When activated separately, port #2 also functions as an **H** port of the divider, as seen in Figure 6.2(b).

When two ports are stimulated concurrently with a phase difference, the hybrid junction functions in a way that two different mode signals travel along the two microstrip lines and reach up to the hybrid junction. This different mode signal is sent then to slot lines, which travel along the slot line and reach the slot-microstrip junction separeatly, as seen in Figure 6.2(c). Since, these different mode signals propagate down the slot line and reach the patches eventually, induce a phase difference between patch #1, #2, and patch #3, #4, resulting in a tilted beam.

6.1.2 Simulation Findings

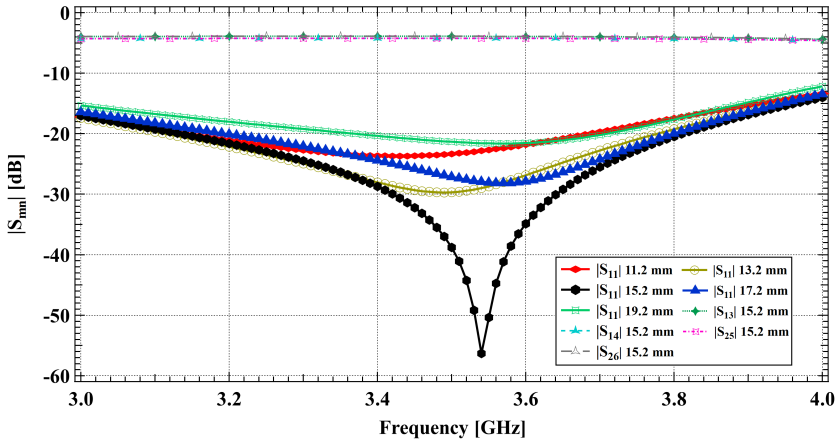

(a) Feed network

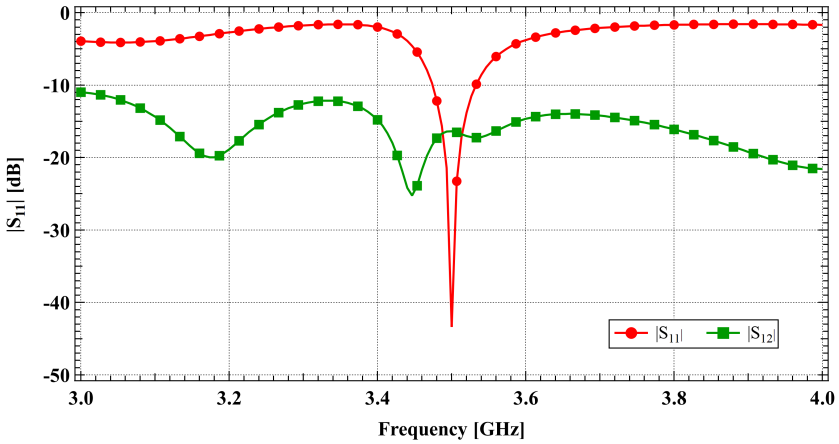

(b) Array antenna

Figure 6.3: Input impedance response of the feed network and the proposed four-element microstrip patch array antenna.

Figure 6.3 illustrates the reflection coefficient of the feed network and the beam steering array antenna. Figure 6.3(a) clearly indicates that the feed network

exhibits optimal performance at a distance of 15.2 mm between input ports, denoted as F_d in the design geometry. Figure 6.3(b) demonstrates the antenna's input impedance response ($|S_{11}|$), revealing a return loss of less than -40 dB at a resonant frequency of 3.5 GHz.

This indicates that the input impedance matching is excellent. The figure indicates that the impedance bandwidth range of -10 dB is between 3.47 GHz and 3.53 GHz. Although this antenna has a narrow bandwidth, it works in the center frequency of the sub-6 GHz frequency band used in 5G. The antenna also exhibits a high level of isolation between its two input ports. Figure 6.3(b) clearly demonstrates that $|S_{12}|$ achieves a return loss of less than -10 dB, which guarantees excellent port isolation. Therefore, it may be concluded that the antenna exhibit excellent impedance matching and superior isolation between them.

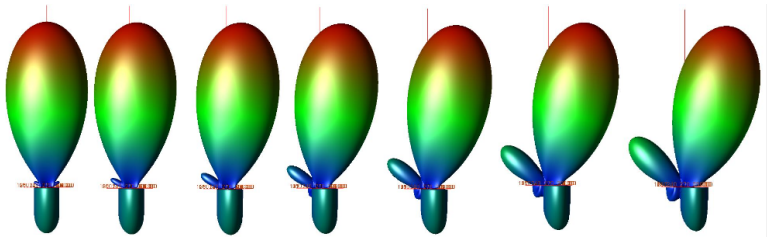

(a) Port #2 phase is varied

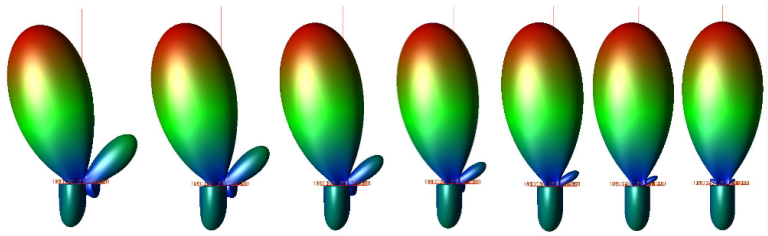

(b) Port #1 phase is varied

Figure 6.4: Simulated 3D radiation pattern of the proposed microstrip array antenna.

Figure 6.4 depicts the 3D radiation pattern of the antenna in two different scenarios while the ports are being fed. Figure 6.4(a) displays the pattern of phase variation for port #2. The phase of port #1 has been retained, while the phase of port 2 has been increased by a step of 15°. Figure 6.4(b) shows the pattern for the second scenario when the phase of port #1 has been increased by a step 15°, but the phase of port #2 has remained unaltered. Both scenarios exhibit a phenomenon where the emitted beam is observed to be inclined at a specific angle. In the first instance, the emitted beam tilts in the opposite direction compared to the second situation. This ensures that the radiation is

directed along the elevation angle, as seen in the illustrations.

Figure 6.5 illustrates the two-dimensional (2D) radiation pattern of an antenna that has been clipped at $\phi = 0°$. Figure 6.5(a) illustrates the radiation pattern that occurs when port #1 is supplied with a signal that has a phase variation of zero degrees and port #2 is supplied with a signal that has a given degree of phase shift. In order to alter the phase of the port #2 signal, an increment of 15° step is effectively utilized. When the phase difference between two

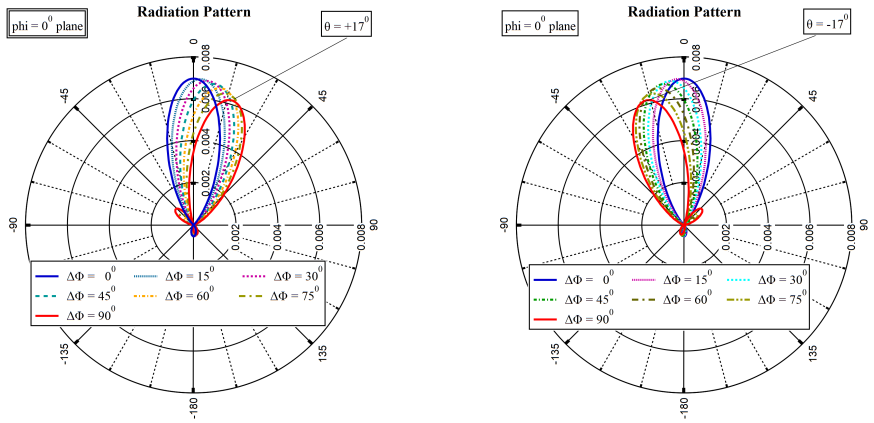

(a) Port #2 phase is varied

(b) Port #1 phase is varied

Figure 6.5: Simulated 2D radiation pattern of the proposed microstrip array antenna.

ports is 90 degrees, the beam tilts an angle of +17°. Figure 6.5(b) illustrates the pattern that takes place when there is a 15° step wise phase shift in port #1, but the signal at port #2 does not exhibit any phase variation. In this particular scenario, the maximum beam tilt angle is −17°. The pattern that is shown by the color blue in both of these representations is the pattern that pertains to a zero-phase difference between two various input signals. The symbol $\Delta\phi$ is used to represent the phase difference that exists between two input signals in the figure.

Figure 6.6 displays the two-dimensional radiation pattern illustrating the broadside gain and directivity of the antenna design being suggested. The Figure exhibits a displacement in the theta axis due to the phase difference between two signals of identical amplitude that are inputted into ports #1 and #2. However, the main lobe's directivity maintains about 25 dB. Figure 6.6(a) demonstrates that the maximum gain and maximum directivity of the main lobe occur at a +17° angle when there is a 90-degree phase difference between two signals, with the signal from port #1 having no phase shift. Figure 6.6(b) shows maximum

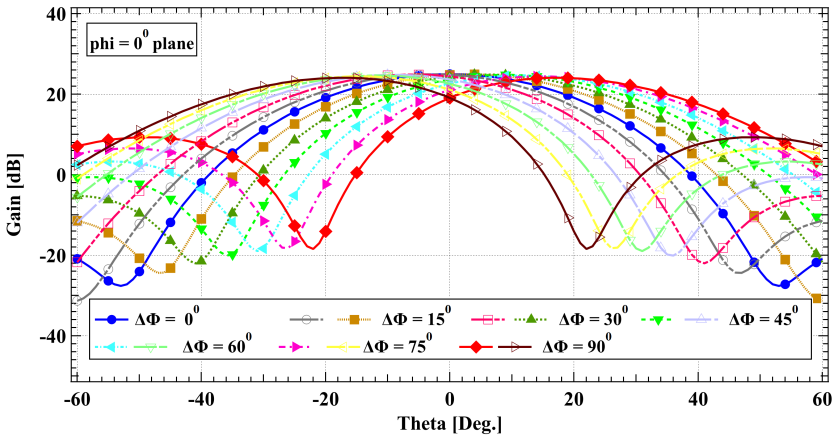

(a) Broadside gain

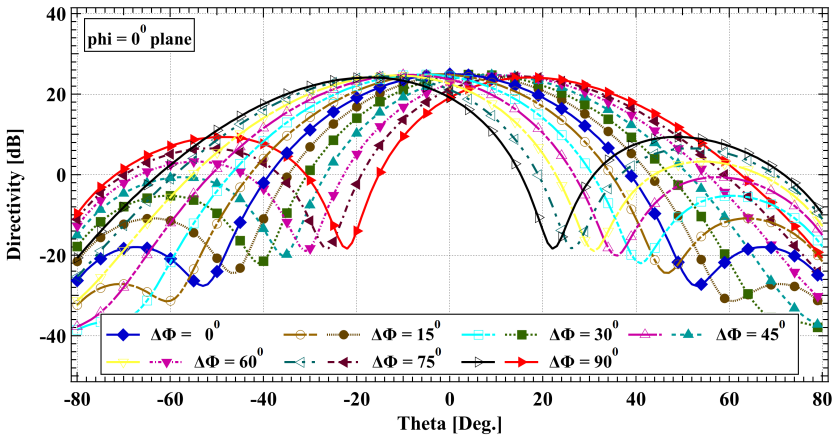

(b) Broadside directivity

Figure 6.6: Broadside gain and directivity of the proposed array antenna for phi=0° plane.

gain and directivity at an angle of −17° when there is a 90-degree phase difference between the two input signals. This occurs when the signal at port #2 has no phase shift, while the signal at port #1 has a gradual rise in phase by 15° increments. It is clear that when the primary beam is slanted, the directivity or gain remains at its maximum with a minimum deviation from the peak.

6.1.3 Simulation Findings

Table 6.1 displays the simulation findings of the radiation pattern, including gain, side lobe (SL) gain, and the maximum angle of beam steering. These parameters are governed by the phase difference between port #1 (ϕ_1) and port #2 (ϕ_2). The array antenna being considered exhibits a gain of around 13 dBi at a resonant frequency of 3.5 GHz, as indicated in the provided table. It is feasible to get a

maximum beam steering range of $-17°$ to $+17°$.

Table 6.1: Radiation pattern data of the array antenna.

ϕ_1	ϕ_2	**Gain (dB)**	**SL Gain (dB)**	θ_{max}
0°	0°	25.111	-16.729	0°
0°	15°	25.089	-10.025	$-3°$
0°	30°	25.023	-4.677	$-6°$
0°	45°	24.903	-0.274	$-9°$
0°	60°	24.704	+2.966	$-11°$
0°	75°	24.436	+6.537	$-14°$
0°	90°	24.090	+9.48	$-17°$
15°	0°	25.089	-10.025	$+3°$
30°	0°	25.023	-4.677	$+6°$
45°	0°	24.903	-0.274	$+9°$
60°	0°	24.704	+2.966	$+11°$
75°	0°	24.436	+6.537	$+14°$
90°	0°	24.090	+9.48	$+17°$

6.2 Beam Switching with Planar Circuit

This portion discusses the ability of the antennas to switch beams when combined with a planar 90 degree phase shifter. The phase shifter's output is linked to the two ports of the design, which has the same construction as described in the previous section.

6.2.1 Design Method with Hybrid Circuit

Figure 6.7 illustrates the process of designing a beam switching antenna that incorporates a 90° phase shifter into the design. At its output terminal, the 90° hybrid coupler generates a signal that has a phase difference of 90°. Taking into consideration the information shown in Figure 6.7(a), if the hybrid circuit's input terminals are ports #1 and #2, then the output terminals are ports #3 and #4. Additionally, the feed network of the design is depicted in the figure when the hybrid coupler is brought into connection with the input of the feeding network. The entire array antenna design is seen in Figure 6.7(b), along with a schematic field that is included in the array and provides an explanation of the method that the array antenna performs. The output of the hybrid coupler is sent to two parallel microstrip lines of the array, which results in the production of two orthogonal modes. These modes then propagate through the slot line to patches using Magic-T. Because of this, the four patches, two on the left and two on the

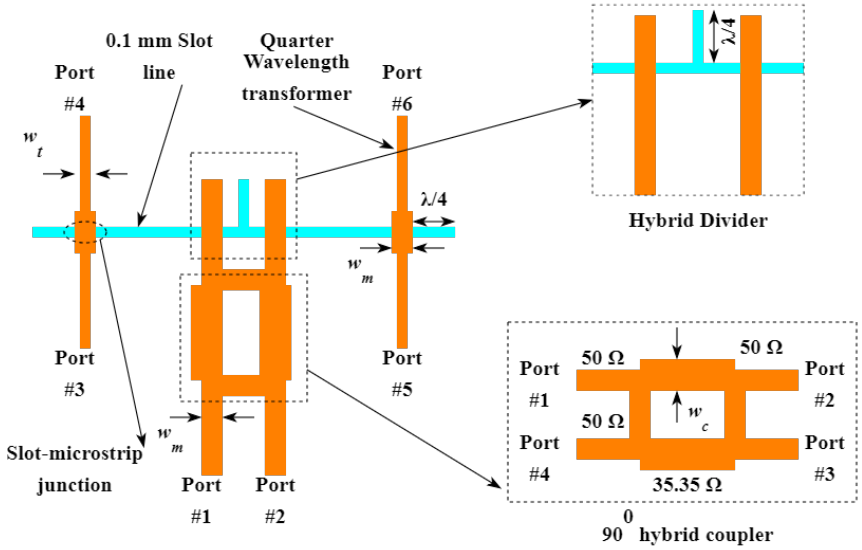

(a) Feed network

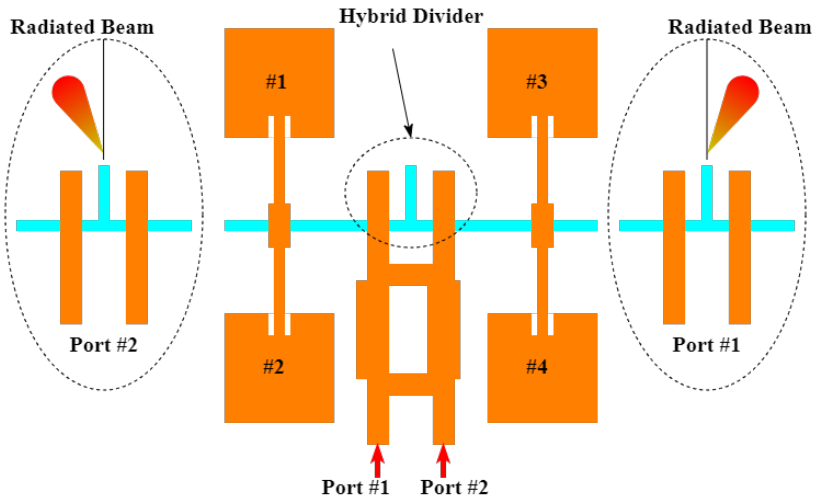

(b) Design with schematic

Figure 6.7: The feed network with hybrid circuit and the proposed microstrip patch array with the schematic diagram.

right become stimulated due to the phase difference that exists between them, which ultimately results in a tilted radiated beam. A summary of the array's design specifications can be found in Table 6.2. The slot line width is 0.1 mm in this design for better performances and better impedance matching which is 0.2 mm for the design without 90° hybrid coupler which has been described in details in the previous section.

Table 6.2: Design specification of the array antenna.

Parameter	Value
Patch length	28.9 mm
$\lambda/4$ transformer width, w_t	0.8 mm
Phase shifter line width, w_c	4.06 mm
Microstrip line width, w_m	2.47 mm
$\lambda/4$ slot line length	19.8 mm
$\lambda/4$ microstrip line length	15.78 mm
Slot line width	0.1 mm

6.2.2 Simulated Outputs

During the design stage, the initial step involves designing and simulating a hybrid coupler using ADS. Next, the hybrid coupler is linked to the feed network of the array antenna and subjected to simulation for the purpose of optimization. Ultimately, the array antenna is subjected to simulation and analysis to uncover observations. Figure 6.8-6.11 display the scattering matrix for both the

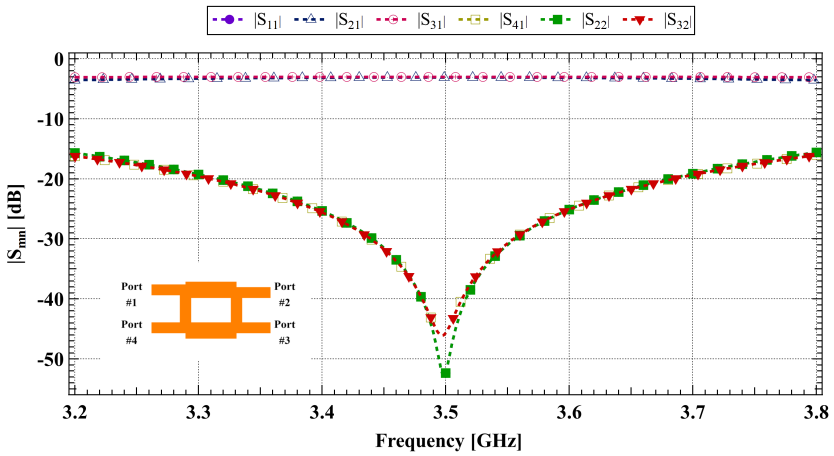

Figure 6.8: Scattering parameter of the proposed array antenna's hybrid coupler.

feed network and the antenna array. The hybrid coupler is highly compatible with the operating frequency of 3.5 GHz and is capable of generating the necessary 90-degree phase difference at the output terminal, as seen in Figures 6.8 and 6.9. The diagram also demonstrates that the antenna's feed network is properly matched in terms of impedance, and the antenna exhibits excellent isolation between its two input ports as seen in Figures 6.10 and 6.11.

An illustration of the three-dimensional radiation pattern is shown in Figure 6.12, which includes a number of feed locations of interest. The beam is oriented at an angle to the right of the broadside direction when it is fed into port #1, as

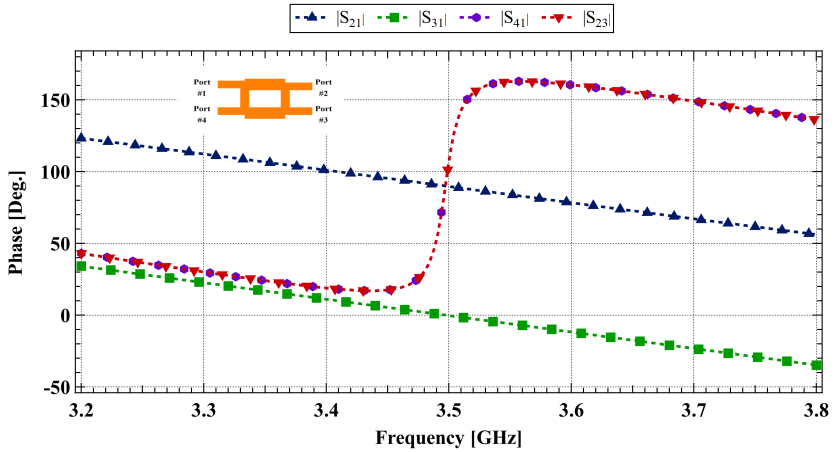

Figure 6.9: Phase of the proposed array antenna's hybrid coupler.

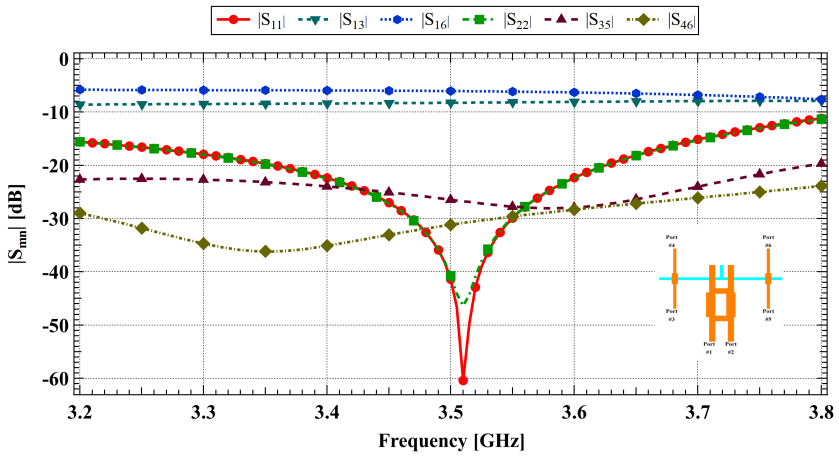

Figure 6.10: Scattering parameter of the proposed array antenna's feed network.

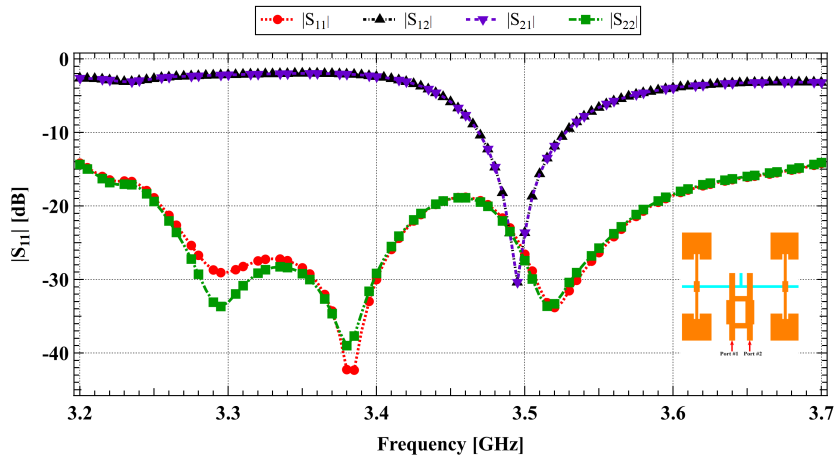

Figure 6.11: Scattering parameter of the proposed array antenna.

illustrated in Figure 6.12(a).

On the other hand, when the signal is inputted into port #2, the radiated

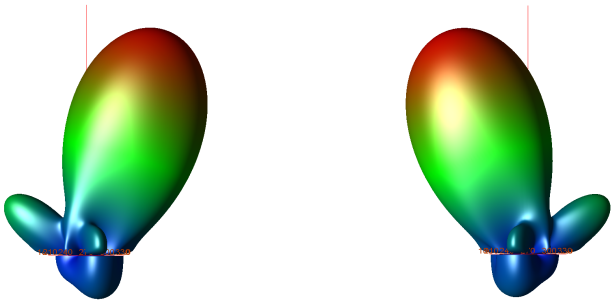

(a) Port #1 (b) Port #2

Figure 6.12: Simulated 3D radiation pattern of the proposed antenna when the input is given to port #1 and port #2 distinctly.

beam is tilted to the left of the broadside direction (as indicated in Figure 6.12(b) along the phi = 0° plane. Additionally, Figure 6.13 that the antenna is well directive with higher efficiency in the operating frequency range.

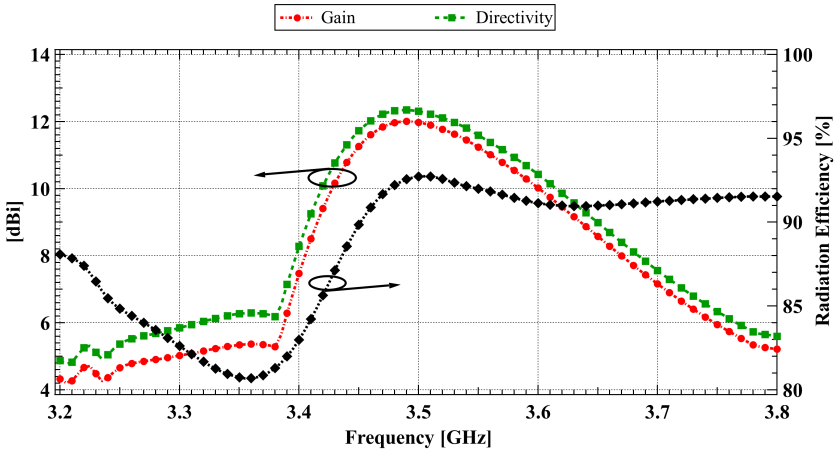

Figure 6.13: Simulated Gain, directivity in dBi, and efficiency of the array antenna versus frequency.

6.3 Summary

This chapter presents the design and analysis of a beam-switching microstrip array antenna employing double-sided MIC technology. The suggested array antenna provides a significant increase in gain and directivity, measuring around 13 dBi. This array antenna achieves a beam switching capacity ranging from −17° to +17°. The antenna exhibits a favorable input impedance at the central frequency of 3.5 GHz inside the sub-6 GHz frequency range.

Chapter 7

DOA Estimation with Beam Switching Array

This chapter focuses on the construction of a four-element multifunctional array that can determine the direction of an incoming signal using the monopulse phase comparison approach. Additionally, it has the capability of switching the radiated beam along two orthogonal planes. This chapter also explores the wide-angle detection capacity of the four-element microstrip patch array antenna.

7.1 Antenna Design

7.1.1 Structure

Four patches, labeled as #1, #2, #3, and #4, have been positioned on a Teflon dielectric substrate with a relative dielectric constant of $\epsilon_r = 2.15$ and a thickness of 0.8 mm. A quarter-wavelength transformer is used to connect Patch #1 and Patch #3, as well as Patch #2 and Patch #4. These patches are then connected to port #1 via a microstrip line. A slot line with a width of 0.2 mm in the ground plane connects the patches to port #2. As shown in Figure **??**, the dotted circle creates two Magic-Ts that allow for the transmission of both sum and difference signals to both ports. Furthermore, the figure also includes a cross-sectional depiction of the antenna that has been created along the AA' axis.

The design incorporates two diodes, D1 and D2, on two microstrip lines connected to port #2 to achieve beam-switching functionality. It is necessary to connect the microstrip lines from port #1 to the quarter wavelength transformer via an air bridge. This is because if the lines from port #2 are not routed through air bridges, they will become interconnected. Port #2 is connected to two microstrip lines by two microstrip-slot junctions and two slot-microstrip junctions.

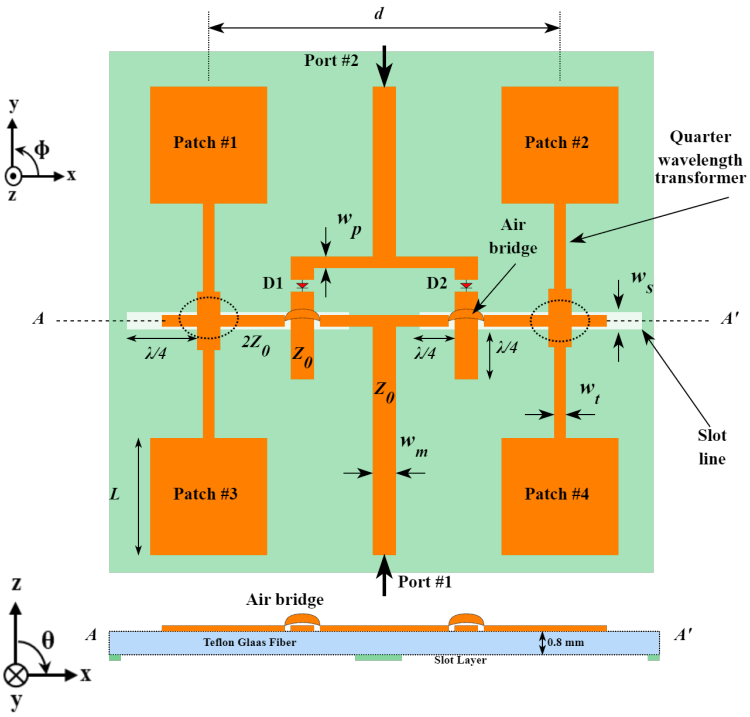

Figure 7.1: Antenna structure of the proposed four-element microstrip patch array antenna.

These connections allow the lines to receive signals from patches through a quarter wavelength transformer or supply signals to the patches. The $\lambda/4$ slot line length extending from the junctions ensures isolation for the junctions. All the antenna design specification and their values as shown in Figure **??**(a) are listed in Table 7.1. Figure **??**(b) illustrates that patch #1 and #2, as well as patch #3

Table 7.1: Several design parameter of the array antenna.

Parameter	Value
Substrate Material	Teflon Glass Fiber
Relative dielectric constant, ϵ_r	2.15
Patch length , L	9.7 mm
Microstrip line width,w_m	2.1 mm
Microstrip line width, $w_p = w_t$	0.8 mm
$\lambda/4$ slot line length	4.8 mm
Slot line width, w_s	0.2 mm
Microstrip line impedance , Z_0	50 Ω
Element to element distance , d	30 mm

and #4, receive signals that are out of phase. These signals propagate over the microstrip line and separate at the Magic-T junction before ultimately reaching port #1 and port #2.

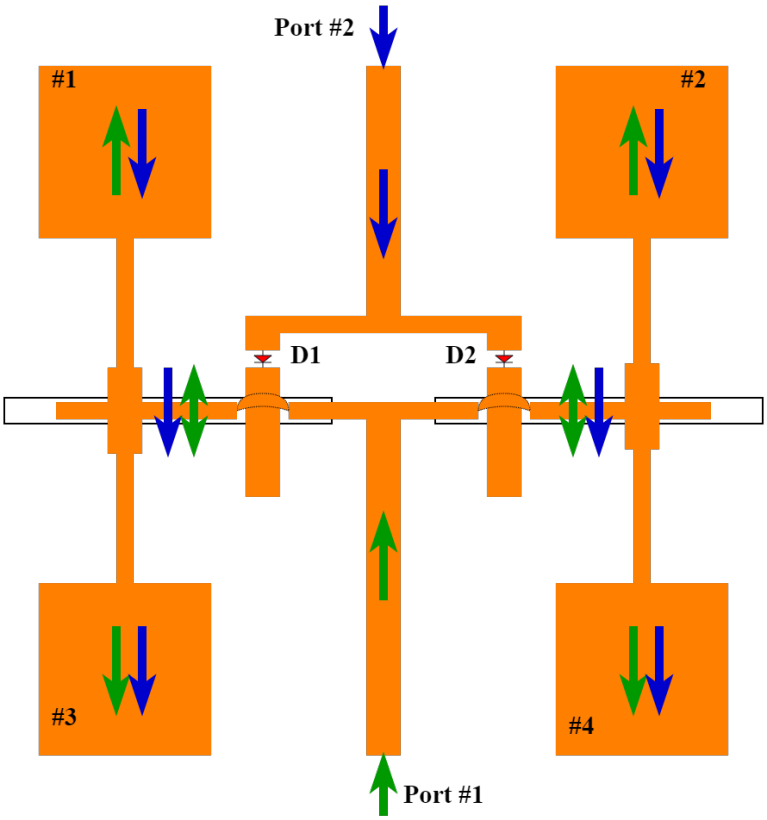

Figure 7.2: Schematic of the proposed four-element microstrip patch array antenna.

7.1.2 Operation

When an antenna detects a signal, based on the mechanism it can split the signal into two parts: the sum (Σ) and difference (Δ) signals. These signals are then sent to a mixer, which uses equation (2.13) [44] to determine the incidence angle. The distance between the antenna elements is represented by the variable d. The Magic-T in this proposed design has the capability to separate in-phase and out-of-phase signals. Figure 7.3 elaborates the Magic-T's working principle of this design.

When doing mode analysis on H-plane signals (even mode) and E-plane signals (odd mode), the primary function of a magic-T is to receive two input ports from a four-port device. In Figure 7.3(a), the slot line and the microstrip line are merged to create a modified coplanar waveguide transmission line. The slot line represents the **E** port, while the microstrip line represents the **H** port. The signals received from Patches #1 or #3 and Patches #2 or #4 are received via the ports labeled as ① and ② in the figure. The vector analysis of the sum and difference signals is shown in Figure 7.3(b), with $\Delta\phi$ representing the angle

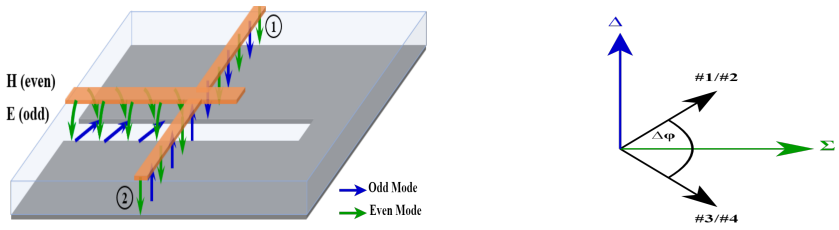

(a) Magic-T principle (b) Vector analysis

Figure 7.3: DOA estimation.

between the receiving signals of the patches. The angle between the sum and difference vectors is specified as $\frac{\Delta\phi}{2}$. Thus, equation (2.13) becomes,

$$\theta = sin^{-1}\left(\frac{\lambda}{\pi d} tan^{-1}\frac{\Delta}{\Sigma}\right) \tag{7.1}$$

Equation (7.1) can be utilized to ascertain the angle at which the incoming signals approach, hence calculating the direction from which they originate.

7.2 Simulation Results

This section details the simulation findings and decorated as impedance matching, DOA estimation, Beam switching and wide angle range detection.

7.2.1 Impedance Matching

Figure 7.4 illustrates the input impedance and port isolation of the proposed antennas. The graph clearly shows that the antenna is correctly matched for both input ports at the resonance frequency. The presence of diodes in the transmission lines causes an imbalance in the microstrip lines, resulting in a little change in the resonance of port #2's input impedance. The return losses for ports #1 and #2 are below -20 dB and below -30 dB, respectively, as indicated by the figure. The signals from the input ports are well isolated, with an isolation of less than -10 dB within the simulated frequency range.

7.2.2 DOA Estimation

Figure 7.5 shows the graph for DOA estimation receive power and radiation pattern. DOA estimation requires the ratio of the difference and sum signals. To achieve this, the suggested antenna retrieves the two signals from two ports and sends them to a mixer. Figure 7.5(a) displays a graph representing the simulated

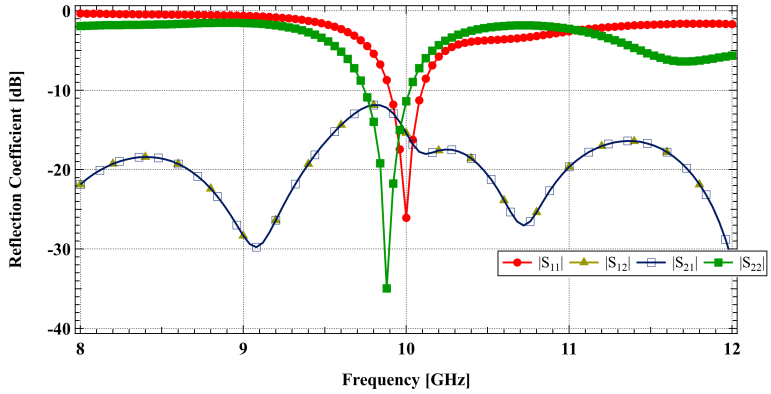

Figure 7.4: Simulated impedance matching and input ports isolation of the proposed design.

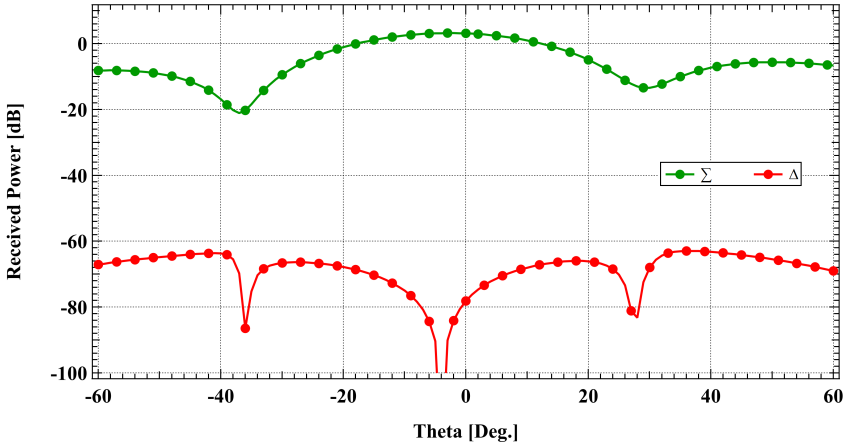

(a) Received power

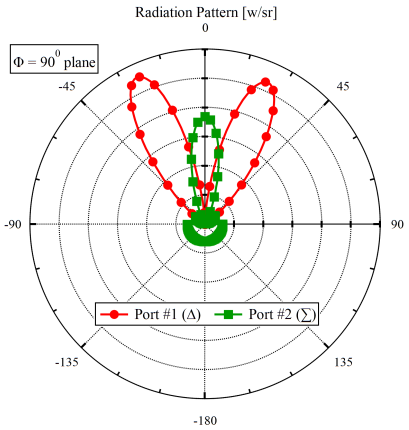

(b) Sum and difference pattern

Figure 7.5: Simulated radiation pattern for sum signal and difference signal.

received power for port #2. The level difference between the two signals exceeds 70 dB, indicating that when port #2 receives sum signals, no difference signal is

received at that port. Therefore, it may be concluded that port #2 is receiving the sum signals, while the other port is receiving the difference signal. The radiation pattern for port #1 and port #2 are shown in Figure 7.5(b). It is clear from the figure that the sum pattern is evident for port #2 and difference pattern for port #1.

7.2.3 Beam Switching

Figure 7.6 shows the 2D radiation pattern of the proposed antenna along two orthogonal palne. Figure 7.6(a) shows the radiation pattern along $\phi = 90°$ plane. When used as a transmitting antenna, the antenna can change its radiated beam to $+17°$ along the $\phi = 90°$ plane if two simultaneous signals to its two input ports with no phase difference is supplied. When the two input signals have a 90-degree phase difference between them, the beam changes to $-17°$ along the same plane.

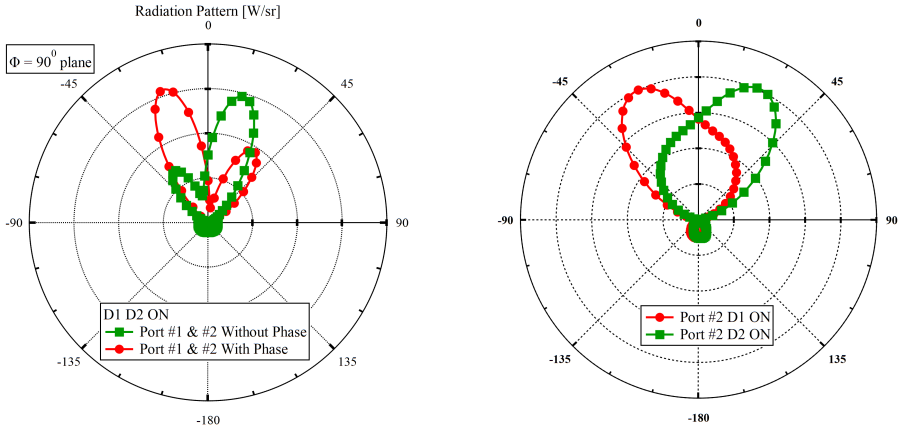

(a) $\phi = 90°$ plane (b) $\phi = 0°$ plane

Figure 7.6: 2D radiation pattern of the proposed four-element patch array antenna along two orthogonal planes.

When only port #2 receives the input signal, the antenna may radiate in the $\phi = 0°$ plane due to the ON and OFF states of the diodes. The diodes ON and OFF state is done by short and open circuit analysis on the ADS software. Figure 7.6(b) shows the antenna's capability to tilt its radiated beam by approximately 30 degrees along the $\phi = 0°$. Hence, the antenna can change its radiating beam to four directions ($\theta = -17°$, $+17°$, $-30°$, and $+30°$) along a two-dimensional plane ($\phi = 0°$ and $90°$), as shown in the figures.

7.2.4 Directivity and Gain

Figure 7.7 shows the directivity and gain of the proposed antenna. The antenna has a scanning range of $-45°$ to $+45°$ for the $\phi = 90°$ plane and $-60°$ to $+60°$ for the $\phi = 0°$ plane if directivity of greater than 10 dB is considered as shown in Figure 7.7(a). Therefore, while operating at the X-band frequency, the antenna is capable of scanning a substantial area. The patch array antenna is a flexible and efficient antenna that offers substantial gain across a wide range of frequencies. Figure 7.7(b) illustrates the results of the study, where the antenna reaches a gain of over 8 dBi over the X-band frequency spectrum, peaking at a maximum gain of 13.67 dBi.

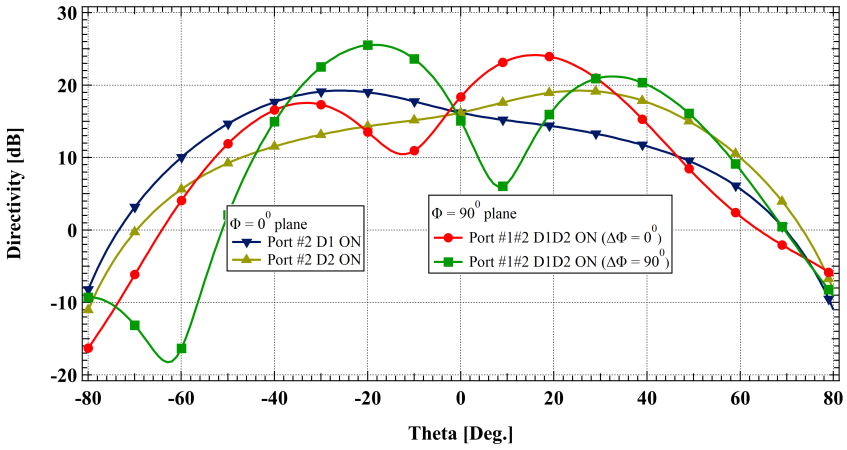

(a) Broadside directivity

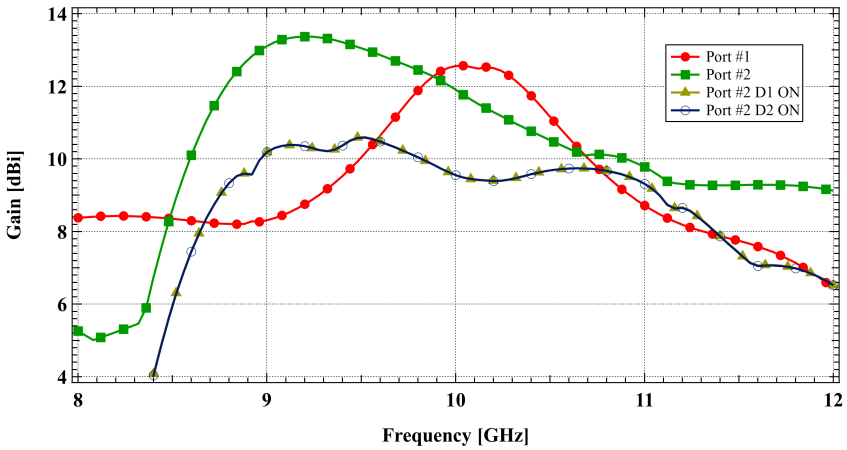

(b) Gain in dBi

Figure 7.7: Simulated broadside directivity and dBi gain for different configurations of the array antenna.

7.3 Summary

The conclusion of this chapter is that it is possible to achieve beam switching by utilizing both-sided MIC technology. The presence of two parallel microstrip lines and an inverted T-shaped cut in the ground layer creates a unique divider that allows for beam switching, as demonstrated in the preceding chapter. Additionally, making further adjustments to the microstrip line allows for a direction of arrival (DOA) estimation with beam switching, as demonstrated in this chapter. Incorporating diodes in the feed line enables the ability to switch the beam in two dimensions. The design's simulation findings of this chapter as well as the previous chapter are compared with some other recent efforts as shown in 7.2.

Table 7.2: Comparison of the proposed 4-element beam switching microstrip patch array antenna with other works.

[Ref]	**No of Elements**	**Use of diodes**	θ_{max}
[88]	Four(1×4)	Yes	14°
[89]	Four(2×2)	Yes	30°
[90]	Four(1×4)	Yes	15°
[91]	Four(2×2)	Yes	13°
[92]	Two(1×2)	No	15°
[93]	Four(2×2)	Yes	8°
[98]	Four(1×4)	No	10°
This Thesis	Four(2×2)	No	17°
	Four(2×2)	Yes	17° ($\phi = 0°$)
			30° ($\phi = 90°$)

Chapter 8

Simple Feed Slot Array and Beam Switching Patch Array

This chapter provides a concise overview of two simple feed antennas. One of the antennas is a microstrip-line-fed slot array antenna designed and simulated for circular polarization at S-band frequencies. The other antenna is a patch array antenna designed for beam-switching applications in the sub-6GHz 5G frequency band. The phase delay among the elements of the beam-switching antenna is achieved through a slot line in the ground plane. Although these antennas are constructed with a simple feed mechanism, they are not single-layer antennas. Instead, they are two-layer antennas, and increasing layers made their feeding much simpler. This chapter is divided into two sections: one for slot array antenna and another for beam switching array antenna. Both sections include their perspective design and simulation outcome.

8.1 Circularly Polarized Slot Array

8.1.1 Design

Figure 8.1 illustrates the structural arrangement of a cross-slot with both single feed and dual feed, as well as a slot array with a simple feed. Initially, a cross-slot with a single microstrip line in the shape of an L is developed. This design consists of a single substrate layer composed of Teflon Glass Fiber material, with a copper microstrip line on top. The slot layer is positioned below the substrate layer. The single cross-slot antenna is also designed using the dual-feed approach. The structure for the dual feed technique consists of two layers of substrate. There is a microstrip line located on the top of the upper substrate, while another microstrip line is positioned beneath the lower substrate. The slot

array is ultimately created utilizing these two feeding techniques. In order to maintain a simple feeding network, the design necessitates the use of two Teflon substrates, each with a thickness of 0.8 mm.

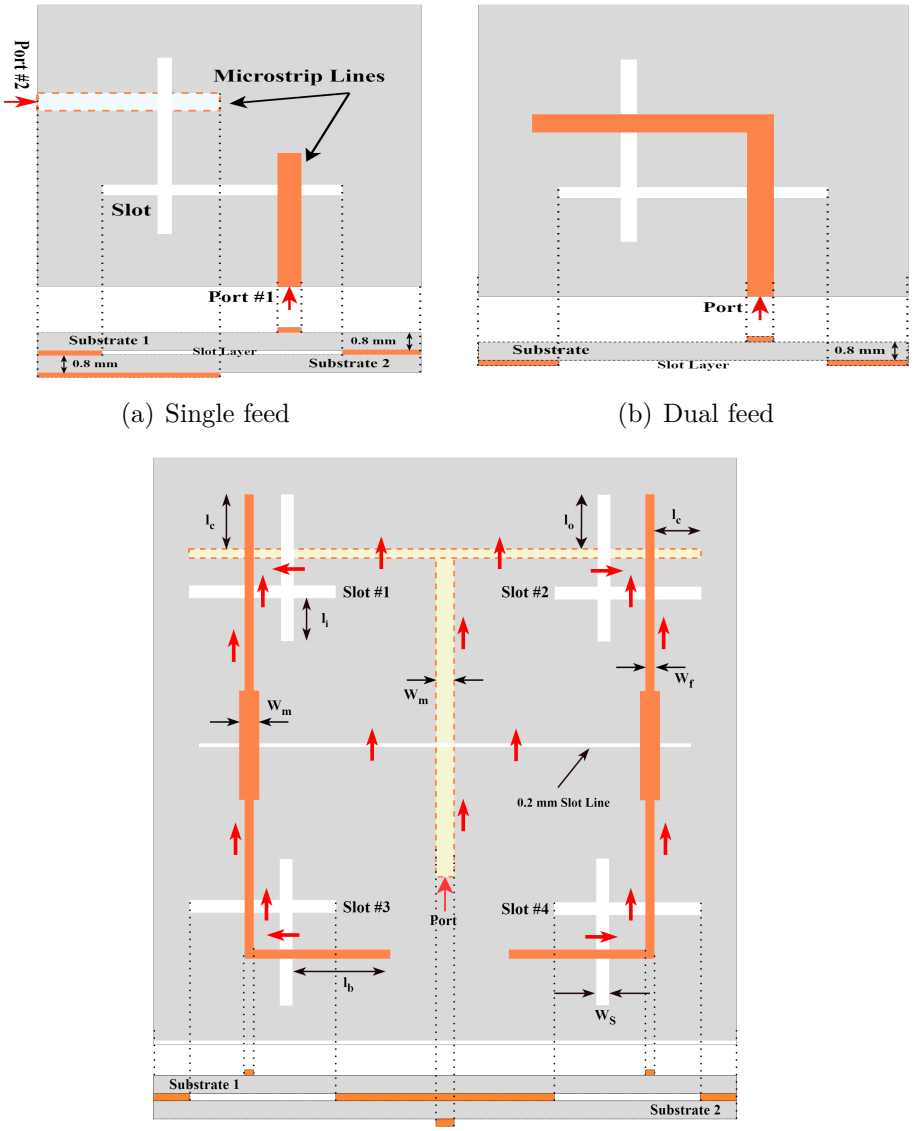

(a) Single feed

(b) Dual feed

(c) Single feed slot array

Figure 8.1: Proposed slot array antenna with single cross slot of single feed and dual feed configuration.

The red arrow in the representation of the slot array antenna represents the electric field distribution of the antenna. The diagram clearly demonstrates that each cross slot of the antenna can be stimulated by a simple feed point, and all of them are positioned in an orthogonal orientation. Therefore, the antenna generates circular polarization. Table 8.1 shows the optimized design specification of the cross-slot array.

Table 8.1: Design parameter with their optimized values of the slot array antenna.

Parameter	Value
Microstrip line length, l_c	12.3 mm
Outer slot length, l_o	16 mm
Inner slot length, l_i	17 mm
Perpendicularly bent patch length, l_b	23.3 mm
Microstrip line width,W_m	2.4 mm
Microstrip line width,W_f	0.8 mm
Slot line width	0.2 mm
Slot width,W_S	1.3 mm
Microstrip line thickness	0.018 mm
Input impedance	50 Ω
Substrate thickness	0.8 mm
Relative dielectric constant, ϵ_r	2.15

8.1.2 Outcome

Figure 8.2 displays the predicted return loss of the single cross-slot antenna for single-feed, dual-feed, and slot array configurations. The data indicates that the single feed element antenna exhibits a return loss of -42.19 dB at a resonance frequency of 2.47 GHz. Additionally, it maintains a return loss of -10 dB within

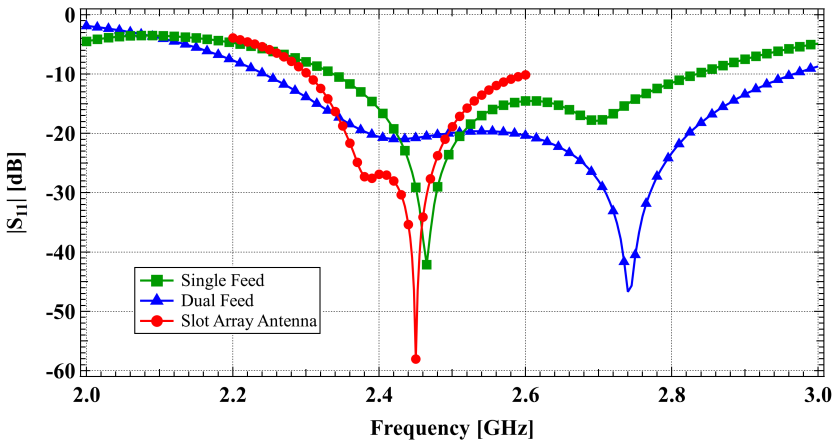

Figure 8.2: Simulated impedance matching and input ports isolation of the proposed design.

the frequency range of 2.34 to 2.83 GHz, making it well-suited for S-band applications. The dual-feed single cross-slot antenna has an impedance bandwidth of 27.76% and a return loss of -46.71 dB at a resonance frequency of 2.74 GHz. The figure illustrates that the slot array antenna exhibits a return loss of -58.017 GHz at its resonance frequency of 2.45 GHz. This return loss remains within a

-10 dB range of 2.3 to 2.6 GHz, indicating an impedance bandwidth percentage of 12.14%. The return loss value represents the optimized value for the slot array. Additionally, the graph exhibits a rise and a fall at 2.4 GHz, indicating the presence of two perpendicular modes at that specific frequency.

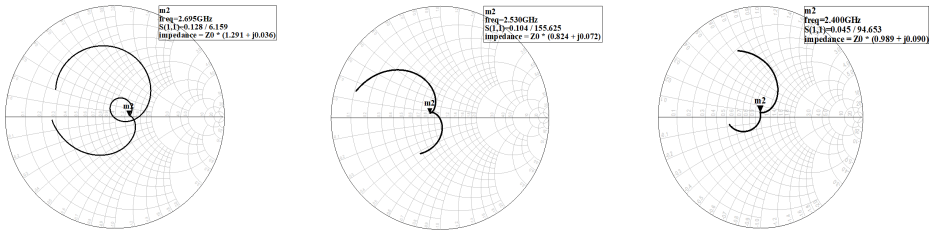

(a) single feed (b) Dual feed (c) Slot array

Figure 8.3: Simulated input impedance of the proposed antenna.

Figure 8.3 displays the input impedance of the suggested antennas. From the image, it is evident that the Smith chart exhibits a dip near 1 (one) at a frequency range of the S-band. This indicates that all the designs have the ability to generate two degenerative orthogonal modes, which is the requirement for circular polarization.

8.2 Phase Delay through Slot-line Beam Switching

8.2.1 Design

Figure 8.4 displays both a top view and a cross-sectional view of the proposed 1×2 microstrip patch array antenna. The antenna is built in such a way that both

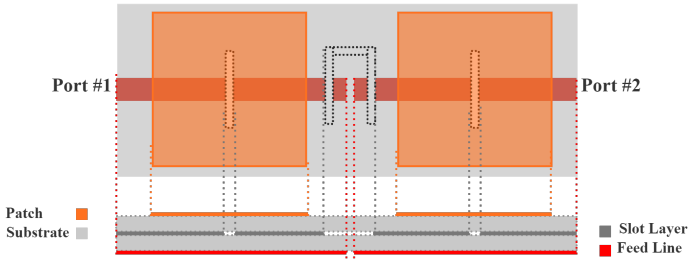

Figure 8.4: Basic structure of the proposed beam steering 1×2 array antenna.

patches of the proposed array can use the aperture-coupled feeding mechanism. The antenna consists of two substrates made of Teflon glass fiber, each with a

relative dielectric constant of 2.15. Both substrates have a height of 0.8 mm and are separated by a ground plane, which contains the aperture slot. The microstrip feed line is connected beneath the bottom substrate, while the square microstrip patches are positioned above the upper substrate. The phase delay between the patches is determined by the slot line that has been carried out on the ground plane between the two substrates. The slot line is formed by cutting a C-shaped pattern on the ground plane. This C-shaped slot line gives the necessary phase delay between elements of the array. The array antenna has also been designed for four-element, eight-element, and sixteen-element arrays using a general corporate feed network.

8.2.2 Outcome

Figure 8.5 displays the two-dimensional (2D) radiation pattern of the array antennas for port #1 and port #2, respectively. The figure clearly shows that for

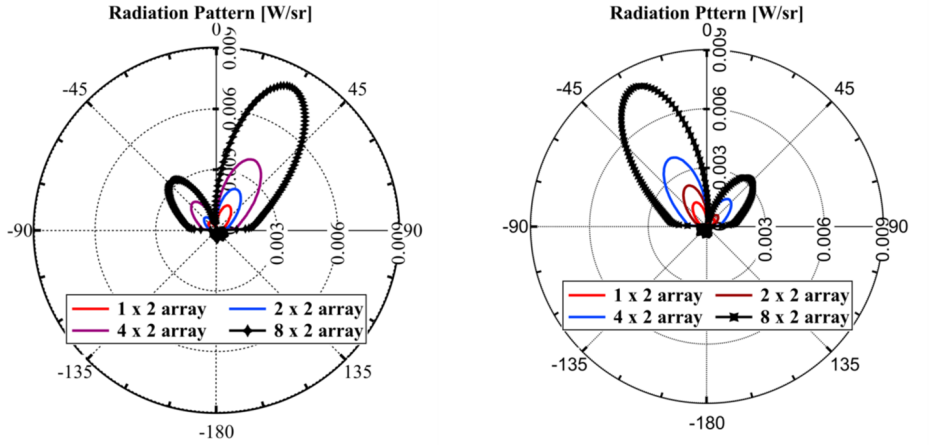

(a) Port #1 (b) Port #2

Figure 8.5: Simulated 2D radiation pattern of the proposed beam steering antenna for $\phi = 90°$ plane.

port #1, the emitted beam is redirected along $\phi = 90°$ for $\theta = +28°$. Figure 8.5(b) displays the two-dimensional deflection of the beam for port #2 of the array antennas. The radiation beam is inclined oppositely compared to the beam for port #1. The antennas may reach a steering angle of $\theta = -28°$ when the signal is sent through port #2. The antennas can achieve a maximum beam switching of $\pm 28°$.

8.3 Summary

This chapter only examines the notion of utilizing a straightforward feeding strategy to produce circular polarization and beam switching, highlighting the possibility of employing alternative arrangements or techniques. A slot array with a simple feed mechanism is developed and simulated to examine the effects of circular polarization. The simulation results demonstrate the slot array antenna's capacity to rotate its emitted beam in a circular motion, as seen by the dip around one (1) on the Smith chart in the results section. Additionally, several microstrip patch array antennas are specifically developed and simulated for the purpose of beam switching, utilizing simple feeding procedures. The simulation results demonstrate that the antenna has the ability to adjust its emitted beam within a range of $\pm 28^{\circ}$. It is important to mention that both antennas have a dual-layer design, unlike the single-layer antennas covered in prior chapters.

Chapter 9

Conclusion

This thesis provides microstrip patch array antenna design and simulation findings with a simple feeding mechanism for many applications such as circular polarization, beam steering, beam switching, and DOA estimation. All the antennas described in this study utilize a Teflon Glass Fiber substrate with a thickness of 0.8 mm and the simulation results for these antennas demonstrate remarkable performance for their intended applications. The reflection coefficient of all the antennas was below -10 dB at their respective resonance frequencies. Table 9.1 displays a comprehensive list of array antennas, including their types, orientations, and applications. In this table, "BS" stands for beam switching, "CP" is for circular polarization, and "DOA" refers to the direction of arrival.

Table 9.1: Antenna type and their orientation in design with outcomes.

Ant. type	**Orientation**	**Applications**	**Outcomes**
Microstrip patch array	3-element	CP	LP, RHCP, LHCP
Microstrip patch array	2×2	CP	RHCP, LHCP
Microstrip patch array	16×16	CP	RHCP, LHCP
Microstrip patch array	2×2	BS	$\theta = \pm 17°$
Microstrip patch array	2×2	BS, DOA	$\theta = \pm 17°(\phi = 90°)$ $\theta = \pm 30°(\phi = 0°)$
Slot array	2×2	CP	RHCP, LHCP
Microstrip patch array	2×8	BS	$\theta = \pm 28°$

In the absence of a meander line in the design, the 3-element microstrip patch array is capable of generating 45° linear polarization. Circular polarization is achieved by including a meander line in the design, which creates the necessary quarter wavelength phase difference between two perpendicular equal excitations. The placement of the meander line in the microstrip line determines whether it exhibits right-hand circular polarization or left-hand circular

polarization. The 3-element microstrip patch array, which utilizes both-sided MIC technology, achieves a relative power difference of over -20 dB and a gain of 11.25 dBic through effective impedance matching. However, the 4-element microstrip patch array antenna independently stimulates each patch in an orthogonal manner and emits circular polarization in both senses. The 4-element microstrip patch array antenna exhibits a relative power level differential of almost -40 dB due to the separate excitation of each patch through the feed configuration. The utilization of double-sided MIC technology facilitates the design of the feed network and enables the effortless construction of large-scale arrays. And, for that case, a 256-element microstrip patch array is built to achieve circular polarization with a relative power difference exceeding -20 dB and a directivity surpassing 27 dBic.

By implementing both-sided MIC technology, a minor adjustment to the feeding arrangement can create a unique hybrid divider junction. This junction has the capability to separate in-phase and out-of-phase signals along the same slot line, utilizing the shape of the slot line in the ground plane. This arrangement ensures that the patches receive signals with equal amplitude but with varying phase differences, resulting in the generation of a tilted beam. The modeling results indicate that the configuration can achieve a maximum beam tilting of $\pm 17^{\circ}$. However, by making further adjustments and including diodes into the microstrip feed line, it becomes possible to achieve two-dimensional beam switching while also estimating the direction of arrival.

The other two arrangements of antenna one being slot array antenna use simple feeding techniques to achieve circular polarization but with dual-layer structure.

9.1 Future Recommendation

The antennas for circular polarization presented in this study are capable of configuring three specific polarization states: linear polarization, left-hand circular polarization, and right-hand circular polarization. A potential future recommendation for this thesis work is to adapt the suggested antenna design to acquire not only horizontal and vertical polarization, but also $\pm 45^{\circ}$ linear polarization. The antenna design for Direction of Arrival (DOA) estimation with beam switching applications was not specifically optimized for circular polarization. In addition to DOA and beam switching, including circular polarization in the antenna design might be a potential area for future development.

Also, the 4-element circular polarized antenna which uses orthogonal excita-

tion for each patch, and the slot array antenna with simple feed techniques can be further optimized by simulation.

9.2 Implications

Circularly polarized and Direction of Arrival (DOA) antennas with beam switching have an impact on adaptive antenna array performance. These antennas are essential for optimizing transmission efficiency. Wireless Fidelity (Wi-Fi) employs circularly polarized switching beam antennas for pattern diversity. These antennas enhance wireless communication by permitting beam switching and pattern variation, resulting in more effective signal transmission and reception. RF energy recovery applications benefit from circularly polarized antennas that can accurately detect arrival direction. Beyond 5G networks can benefit from electrically steerable small antenna systems, making them more adaptable and smarter than present networks. Since the proposed designs' simulation findings are quite fascinating, the proposed design can be of good use in case of applications where circular polarization, beam switching as well as DOA are required.

9.3 Limitations

The 3-element microstrip patch array antenna and 4-element orthogonal excitation microstrip patch array antenna are capable of generating linear polarization, left-hand circular polarization, and right-hand circular polarization. The polarization sensing for both antennas may be obtained only by altering the feed configuration. There were no inherent mechanisms capable of concurrently modifying the polarization states to meet the specific needs of real-world applications. In order to provide continuous beam steering for the proposed beam-switching antenna, it is necessary to have the ability to continually vary the phase between the two input ports. The utilization of a phase shifter in the external circuit results in the generation of just two distinctively directed radiated beams.

Bibliography

[1] S. S. Gao, Q. Luo, and F. Zhu, *Circularly polarized antennas.* John Wiley & Sons, 2014.

[2] O. H. Karabey, *Electronic beam steering and polarization agile planar antennas in liquid crystal technology.* Springer Science & Business Media, 2013.

[3] H. J. Visser, *Array and phased array antenna basics.* John Wiley & Sons, 2006.

[4] G. C. Corazza, "Marconi's history [radiocommunication]," *Proceedings of the IEEE*, vol. 86, no. 7, pp. 1307–1311, 1998.

[5] H. Wong, K.-M. Luk, C. H. Chan, Q. Xue, K. K. So, and H. W. Lai, "Small antennas in wireless communications," *Proceedings of the IEEE*, vol. 100, no. 7, pp. 2109–2121, 2012.

[6] J. Ramsay, "Highlights of antenna history," *IEEE Communications Magazine*, vol. 19, no. 5, pp. 4–8, 1981.

[7] W. L. Stutzman, *Polarization in electromagnetic systems.* Artech house, 2018.

[8] R. Garg, *Microstrip antenna design handbook.* Artech house, 2001.

[9] L. C. Godara, *Handbook of antennas in wireless communications.* CRC press, 2018.

[10] T. Brandão, H. Filgueiras, and S. A. Cerqueira, "Multitask Antenna Array for 5G NR handsets," in *GLOBECOM 2022-2022 IEEE Global Communications Conference.* IEEE, 2022, pp. 6529–6534.

[11] A. Deligiannis, M. Amin, G. Fabrizio, and S. Lambotharan, "Sparse subarray design for multitask receivers," in *2018 IEEE Radar Conference (RadarConf18).* IEEE, 2018, pp. 0742–0747.

[12] J. Chen, J. Xie, Y. Gu, S. Li, S. Fu, Y. Wan, and K. Lu, "Long-range and broadband aerial communication using directional antennas (ACDA): Design and implementation," *IEEE Transactions on Vehicular Technology*, vol. 66, no. 12, pp. 10 793–10 805, 2017.

[13] A.-M. Dinius, *GPS antenna multipath rejection performance.* Citeseer, 1995.

[14] E. Arnieri, L. Boccia, G. Amendola, and G. Di Massa, "A compact high gain antenna for small satellite applications," *IEEE Transactions on Antennas and Propagation*, vol. 55, no. 2, pp. 277–282, 2007.

[15] J. H. Winters, "Smart antennas for wireless systems," *IEEE Personal Communications*, vol. 5, no. 1, pp. 23–27, 1998.

[16] A. Derneryd and B. Johannisson, "Adaptive base-station antenna arrays," *ERICSSON REV(ENGL ED)*, vol. 76, no. 3, pp. 132–137, 1999.

[17] V. P. Kodgirwar, S. B. Deosarkar, and K. R. Joshi, "Design of beam steering-switching array for 5G S-band adaptive antenna applications–part-I and part-II," *IETE Journal of Research*, vol. 68, no. 4, pp. 2909–2921, 2022.

[18] T. Matsumoto and Y. Kuwahara, "2D DOA estimation using beam steering antenna by the switched parasitic elements and RBF neural network," *Electronics and Communications in Japan (Part I: Communications)*, vol. 89, no. 9, pp. 22–31, 2006.

[19] W.-J. Liao, S.-H. Chang, H.-C. Liu, L.-K. Li, C.-Y. Hsieh, and C.-C. Yao, "A beam switching array antenna for direction-of-arrival applications," *Microwave and Optical Technology Letters*, vol. 53, no. 7, pp. 1601–1606, 2011.

[20] K. A. Gotsis, K. Siakavara, and J. N. Sahalos, "On the direction of arrival (DoA) estimation for a switched-beam antenna system using neural networks," *IEEE Transactions on Antennas and Propagation*, vol. 57, no. 5, pp. 1399–1411, 2009.

[21] S. Maddio, M. Passafiume, A. Cidronali, and G. Manes, "A closed-form formula for RSSI-based DoA estimation with Switched Beam Antennas," in *2015 European Microwave Conference (EuMC)*. IEEE, 2015, pp. 1363–1366.

[22] J. Kim and I. Lee, "802.11 WLAN: history and new enabling MIMO techniques for next generation standards," *IEEE Communications Magazine*, vol. 53, no. 3, pp. 134–140, 2015.

[23] N. Herscovici, "New considerations in the design of microstrip antennas," *IEEE Transactions on Antennas and Propagation*, vol. 46, no. 6, pp. 807–812, 1998.

[24] M. Samsuzzaman, M. Islam, J. Mandeep *et al.*, "Parametric analysis of a glass-micro fibre-reinforced PTFE material, multiband, patch-structure antenna for satellite applications," *Optoelectronics and Advanced Materials*, vol. 7, pp. 760–769, 2013.

[25] F. Huang, Y. Yuan, Z. Jiang, B. Tang, and S. Zhang, "Microstructures and properties of glass fiber reinforced PTFE composite substrates with laminated construction," *Materials Research Express*, vol. 6, no. 7, p. 075305, 2019.

[26] S.-S. Qian, K.-L. Sheng, S.-Z. Zhou, X.-P. Long, Z.-Y. Zong, and W. Wu, "A wideband cylindrical conformal microstrip mimo antenna array," *Electronics Letters*, vol. 59, no. 21, p. e13008, 2023.

[27] T. Seki, N. Honma, K. Nishikawa, and K. Tsunekawa, "High efficiency multi-layer parasitic microstrip array antenna on TEFLON substrate," in *34th European Microwave Conference, 2004.*, vol. 2. IEEE, 2004, pp. 829–832.

[28] ——, "Millimeter-wave high-efficiency multilayer parasitic microstrip antenna array on teflon substrate," *IEEE Transactions on Microwave Theory and Techniques*, vol. 53, no. 6, pp. 2101–2106, 2005.

[29] J. Gao, K. Li, and H. Harada, "Wideband stacked microstrip patch antenna on thin PTFE substrate for millimeter-wave personal area network (mmWPAN)," in *2010 IEEE antennas and propagation society international symposium*. IEEE, 2010, pp. 1–4.

[30] L. Yao, M. Jiang, D. Zhou, F. Xu, D. Zhao, W. Zhang, N. Zhou, Q. Jiang, and Y. Qiu, "Fabrication and characterization of microstrip array antennas integrated in the three dimensional orthogonal woven composite," *Composites Part B: Engineering*, vol. 42, no. 4, pp. 885–890, 2011.

[31] H. Lee, "Pattern reconfigurable micro-strip patch array antenna using switchable feed-network," in *2010 Asia-Pacific Microwave Conference*. IEEE, 2010, pp. 2017–2020.

[32] G. E. Evans, "Antenna measurement techniques," *Norwood*, 1990.

[33] B. Li, "Axial ratio measurements of circularly polarised antennas based on polarisation rotation," *IET Microwaves, Antennas & Propagation*, vol. 12, no. 15, pp. 2379–2382, 2018.

[34] W. L. Langston and D. R. Jackson, "Impedance, axial-ratio, and receive-power bandwidths of microstrip antennas," *IEEE transactions on antennas and propagation*, vol. 52, no. 10, pp. 2769–2774, 2004.

[35] B. Y. Toh, R. Cahill, and V. F. Fusco, "Understanding and measuring circular polarization," *IEEE Transactions on Education*, vol. 46, no. 3, pp. 313–318, 2003.

[36] T. S. Bird, "Definition and misuse of return loss [report of the transactions editor-in-chief]," *IEEE Antennas and Propagation Magazine*, vol. 51, no. 2, pp. 166–167, 2009.

[37] C. Camacho-Penalosa and J. Banos-Polglase, "On the definition of return loss [measurements corner]," *IEEE Antennas and Propagation Magazine*, vol. 55, no. 2, pp. 172–174, 2013.

[38] D. M. Pozar, *Microwave engineering*. John wiley & sons, 2011.

[39] C. A. Balanis, *Antenna theory: analysis and design*. John wiley & sons, 2016.

[40] W. L. Stutzman and G. A. Thiele, *Antenna theory and design*. John Wiley & Sons, 2012.

[41] M. Seyyedesfahlan, A. Uzun, A. K. Skrivervik, and I. Tekin, "Wideband multiport antennas," *Sensors*, vol. 20, no. 23, p. 6960, 2020.

[42] A. D. Yaghjian and S. R. Best, "Impedance, bandwidth, and Q of antennas," *IEEE Transactions on Antennas and Propagation*, vol. 53, no. 4, pp. 1298–1324, 2005.

[43] G. Hurd, "IEEE standard test procedures for antennas," *Electronics and Power*, vol. 26, no. 9, p. 749, 1980.

[44] H. Sakai, E. Nishiyama, and I. Toyoda, "Direction of arrival estimating array antenna," in *2012 International Symposium on Antennas and Propagation (ISAP)*. IEEE, 2012, pp. 1124–1127.

[45] A. Bansal and R. Gupta, "A review on microstrip patch antenna and feeding techniques," *International Journal of Information Technology*, vol. 12, pp. 149–154, 2020.

[46] H. K. Varshney, M. Kumar, A. Jaiswal, R. Saxena, and K. Jaiswal, "A survey on different feeding techniques of rectangular microstrip patch antenna," *International Journal of Current Engineering and Technology*, vol. 4, no. 3, pp. 1418–1423, 2014.

[47] M. Aikawa and H. Ogawa, "Double-sided MICs and their applications," *IEEE transactions on microwave theory and techniques*, vol. 37, no. 2, pp. 406–413, 1989.

[48] M. Aikawa and E. Nishiyama, "Compact MIC magic-T and the integration with planar array antenna," *IEICE transactions on electronics*, vol. 95, no. 10, pp. 1560–1565, 2012.

[49] K. Kumari, R. K. Jaiswal, and K. V. Srivastava, "A compact triple band circularly polarized planar antenna for wireless application," *Microwave and Optical Technology Letters*, vol. 62, no. 7, pp. 2611–2617, 2020.

[50] I. Khan, Q. Wu, I. Ullah, S. U. Rahman, H. Ullah, and K. Zhang, "Designed circularly polarized two-port microstrip MIMO antenna for WLAN applications," *Applied Sciences*, vol. 12, no. 3, p. 1068, 2022.

[51] J. K. D. Gunaram, V. Sharma *et al.*, "Dual band circular polarized printed dipole antenna for S and C band wireless applications," *Progress in Electromagnetics Research C*, vol. 105, pp. 129–146, 2020.

[52] S. Ullah, C. Ruan, M. S. Sadiq, T. U. Haq, and W. He, "Microstrip system on-chip circular polarized (CP) slotted antenna for THz communication application," *Journal of Electromagnetic Waves and Applications*, vol. 34, no. 8, pp. 1029–1038, 2020.

[53] K.-L. Wong and W.-S. Chen, "Compact microstrip antenna with dual-frequency operation," *Electronics Letters*, vol. 33, no. 8, pp. 646–647, 1997.

[54] Q. Liu and L. Zhu, "A compact wideband filtering antenna on slots-loaded square patch radiator under triple resonant modes," *IEEE Transactions on Antennas and Propagation*, vol. 70, no. 10, pp. 9882–9887, 2022.

[55] R. Rajitha, K. Nishitha, R. M. Mandeep, and G. L. Priya, "Design of coaxial fed synchronous microstrip patch antenna array with circular polarization," in *2019 IEEE International Conference on Innovations in Communication, Computing and Instrumentation (ICCI)*. IEEE, 2019, pp. 8–11.

[56] M. Haneishi and S. Yoshida, "A design method of circularly polarized rectangular microstrip antenna by one-point feed," *Electronics and Communications in Japan (Part I: Communications)*, vol. 64, no. 4, pp. 46–54, 1981.

[57] M. A. Sonkusale and S. Khade, "Design of wideband circularly polarized antenna with corner truncated patch," in *2020 International Conference on Emerging Trends in Information Technology and Engineering (ic-ETITE)*. IEEE, 2020, pp. 1–4.

[58] Z. Muludi and B. Aswoyo, "Truncated microstrip square patch array antenna 2× 2 elements with circular polarization for s-band microwave frequency," in *2017 International Electronics Symposium on Engineering Technology and Applications (IES-ETA)*. IEEE, 2017, pp. 87–92.

[59] A. A. Odhekar and A. A. Deshmukh, "Variations of slot cut and stub loaded square microstrip antenna for circular polarization," *Wireless Personal Communications*, vol. 111, pp. 661–677, 2020.

[60] P. D. H. Re, D. Comite, and S. K. Podilchak, "Single-layer series-fed planar array with controlled aperture distribution for circularly polarized radiation," *IEEE Transactions on Antennas and Propagation*, vol. 68, no. 6, pp. 4973–4978, 2019.

[61] T.-Y. Han *et al.*, "Series-fed microstrip array antenna with circular polarization," *International Journal of Antennas and Propagation*, vol. 2012, 2012.

[62] K.-B. Kim, B. C. Jung, and J.-M. Woo, "A compact dual-polarized (cp, lp) with dual-feed microstrip patch array for target detection," *IEEE Antennas and Wireless Propagation Letters*, vol. 19, no. 4, pp. 517–521, 2019.

[63] L. Alatan, "Design of a series fed circularly polarized microstrip patch array," in *IEEE Antennas and Propagation Society International Symposium (IEEE Cat. No. 02CH37313)*, vol. 2. IEEE, 2002, pp. 212–215.

[64] T. Khalifa, N. Ramli, and N. Sahar, "Microstrip Array Antenna using Series-Corporate Feed for Navigation System," *Indonesian Journal of Electrical Engineering and Informatics (IJEEI)*, vol. 8, no. 3, pp. 517–524, 2020.

[65] V. Prakasam, P. Sandeep, and K. A. LaxmiKanth, "Rectangular micro strip patch array antenna with corporate feed network for wireless communication applications," in *2020 5th International Conference on Communication and Electronics Systems (ICCES)*. IEEE, 2020, pp. 311–316.

[66] S. Ogurtsov and S. Koziel, "On alternative approaches to design of corporate feeds for low-sidelobe microstrip linear arrays," *IEEE Transactions on Antennas and Propagation*, vol. 66, no. 7, pp. 3781–3786, 2018.

[67] K. H. Lu and T.-N. Chang, "Circularly polarized array antenna with corporate-feed network and series-feed elements," *IEEE transactions on antennas and propagation*, vol. 53, no. 10, pp. 3288–3292, 2005.

[68] P. Hall and C. Hall, "Coplanar corporate feed effects in microstrip patch array design," in *IEE Proceedings H (Microwaves, Antennas and Propagation)*, vol. 135, no. 3. IET, 1988, pp. 180–186.

[69] Y.-J. Hu, W.-P. Ding, and W.-Q. Cao, "Broadband circularly polarized microstrip antenna array using sequentially rotated technique," *IEEE Antennas and Wireless Propagation Letters*, vol. 10, pp. 1358–1361, 2011.

[70] T. Chang and J. Jiang, "Enhance gain and bandwidth of circularly polarized microstrip patch antenna using gap-coupled method," *Progress In Electromagnetics Research*, vol. 96, pp. 127–139, 2009.

[71] Y. Shen, S.-G. Zhou, G.-L. Huang, and T.-H. Chio, "A compact dual circularly polarized microstrip patch array with interlaced sequentially rotated feed," *IEEE Transactions on Antennas and Propagation*, vol. 64, no. 11, pp. 4933–4936, 2016.

[72] P. Hall, "Application of sequential feeding to wide bandwidth, circularly polarised microstrip patch arrays," in *IEE Proceedings H (Microwaves, Antennas and Propagation)*, vol. 136, no. 5. IET, 1989, pp. 390–398.

[73] K. Kodama, E. Nishiyama, and M. Aikawa, "Slot array antenna using both-sided MIC technology," in *IEEE Antennas and Propagation Society Symposium, 2004.*, vol. 3. IEEE, 2004, pp. 2715–2718.

[74] Y. Ushijima, T. Sakamoto, E. Nishiyama, M. Aikawa, and I. Toyoda, "5.8-GHz integrated differential rectenna unit using both-sided MIC technology with design flexibility," *IEEE transactions on antennas and propagation*, vol. 61, no. 6, pp. 3357–3360, 2013.

[75] M. del Castillo Velazquez-Ahumada, J. Martel, and F. Medina, "Design of compact low-pass elliptic filters using double-sided MIC technology," *IEEE Transactions on microwave theory and techniques*, vol. 55, no. 1, pp. 121–127, 2007.

[76] V. Va, T. Shimizu, G. Bansal, and R. W. Heath, "Beam design for beam switching based millimeter wave vehicle-to-infrastructure communications," in *2016 IEEE International Conference on Communications (ICC)*. IEEE, 2016, pp. 1–6.

[77] V. Va, X. Zhang, and R. W. Heath, "Beam switching for millimeter wave communication to support high speed trains," in *2015 IEEE 82nd Vehicular Technology Conference (VTC2015-Fall)*. IEEE, 2015, pp. 1–5.

[78] W. Hong, Z. H. Jiang, C. Yu, J. Zhou, P. Chen, Z. Yu, H. Zhang, B. Yang, X. Pang, M. Jiang *et al.*, "Multibeam antenna technologies for 5G wireless communications," *IEEE Transactions on Antennas and Propagation*, vol. 65, no. 12, pp. 6231–6249, 2017.

[79] C. A. Fernandes, R. C. Martins, T. Radil, P. M. Ramos, E. B. Lima, C. R. Medeiros, and J. R. Costa, "Low-cost mechanically steered millimeter-wave lens antenna system for indoor LANs," in *2010 International Workshop on Antenna Technology (iWAT)*. IEEE, 2010, pp. 1–4.

[80] D. Jahagirdar and K. S. Rao, "Design and development of electronic beam switching antenna for point-to-multi-point long range data link applications," in *2017 IEEE International Conference on Antenna Innovations & Modern Technologies for Ground, Aircraft and Satellite Applications (iAIM)*. IEEE, 2017, pp. 1–4.

[81] M. R. Kamarudin, P. S. Hall, F. Colombel, and M. Himdi, "Electronically switched beam disk-loaded monopole array antenna," *Progress In Electromagnetics Research*, vol. 101, pp. 339–347, 2010.

[82] L. Han, G. Cheng, G. Han, R. Ma, and W. Zhang, "Electronically beam-steering antenna with active frequency-selective surface," *IEEE Antennas and Wireless Propagation Letters*, vol. 18, no. 1, pp. 108–112, 2018.

[83] R. Waterhouse, "Microstrip patch antennas," in *Handbook of Antennas in Wireless Communications*. CRC Press, 2018, pp. 6–1.

[84] K.-F. Lee and K.-F. Tong, "Microstrip patch antennas—basic characteristics and some recent advances," *Proceedings of the IEEE*, vol. 100, no. 7, pp. 2169–2180, 2012.

[85] I. Singh, V. Tripathi *et al.*, "Micro strip patch antenna and its applications: a survey," *Int. J. Comp. Tech. Appl*, vol. 2, no. 5, pp. 1595–1599, 2011.

[86] S. Lee, Y. Lee, and H. Shin, "A 28-GHz switched-beam antenna with integrated Butler matrix and switch for 5G applications," *Sensors*, vol. 21, no. 15, p. 5128, 2021.

[87] D. Delaune, K. Ito, I. Ida, and H. Yoshimura, "A simple circularly polarized beam-switching patch array antenna for satellite communication," in *IEEE Antennas and Propagation Society International Symposium. 2001 Digest. Held in conjunction with: USNC/URSI National Radio Science Meeting (Cat. No. 01CH37229)*, vol. 4. IEEE, 2001, pp. 776–779.

[88] M. Jusoh, M. Jamlos, M. Kamarudin, M. Salimi, F. Malek, and M. Jais, "A beam steering patch array antenna for WiMAX application," in *2013 7th European conference on antennas and propagation (EuCAP)*. IEEE, 2013, pp. 924–927.

[89] H. Errifi, A. Baghdad, A. Badri, and A. Sahel, "Electronically reconfigurable beam steering array antenna using switched line phase shifter," in *2017 International Conference on Wireless Networks and Mobile Communications (WINCOM)*. IEEE, 2017, pp. 1–6.

[90] C. Ding, Y. J. Guo, P.-Y. Qin, T. S. Bird, and Y. Yang, "A defected microstrip structure (DMS)-based phase shifter and its application to beamforming antennas," *IEEE transactions on antennas and propagation*, vol. 62, no. 2, pp. 641–651, 2013.

[91] H. Errifi, A. Baghdad, A. Badri, and A. Sahel, "Directive beam-steering patch array antenna using simple phase shifter," in *Proceedings of the Mediterranean Conference on Information & Communication Technologies 2015: MedCT 2015 Volume 1*. Springer, 2016, pp. 17–25.

[92] R. Pandhare, P. Zade, and M. Abegaonkar, "Beam-steering in microstrip patch antenna array using DGS based phase shifters at 5.2 GHz," in *2015 International Conference on Information Processing (ICIP)*. IEEE, 2015, pp. 239–243.

[93] M. Katoch, M. Abegaonkar, A. Basu, and S. K. Koul, "Compact microstrip phase shifter for beam steering antenna," in *2016 Asia-Pacific Microwave Conference (APMC)*. IEEE, 2016, pp. 1–5.

[94] S. Orakwue and R. Ngah, "Two dimensional switched beam antenna based on cascaded butler matrix beamforming network," *Nigerian Journal of Technology*, vol. 38, no. 4, pp. 1003–1009, 2019.

[95] J. Lee and K. Chang, "Dual-band switched beam array fed by dual-band Butler matrix," *Electronics letters*, vol. 47, no. 21, pp. 1164–1165, 2011.

[96] G. Sharifi, Y. Zehforoosh, T. Sedghi, and M. Takrimi, "A high gain pattern stabilized array antenna fed by modified Butler matrix for 5G applications," *AEU-International Journal of Electronics and Communications*, vol. 122, p. 153237, 2020.

[97] P. Baniya and K. L. Melde, "Switched-Beam Endfire Planar Array With Integrated 2-D Butler Matrix for 60 GHz Chip-to-Chip Space-Surface Wave Communications," *IEEE Antennas and Wireless Propagation Letters*, vol. 18, no. 2, pp. 236–240, 2019.

[98] C. Liu, S. Xiao, Y.-X. Guo, M.-C. Tang, Y.-Y. Bai, and B.-Z. Wang, "Circularly polarized beam-steering antenna array with butler matrix network," *IEEE Antennas and Wireless Propagation Letters*, vol. 10, pp. 1278–1281, 2011.

[99] E. Nishiyama, R. Hisadomi, and M. Aikawa, "Beam controllable microstrip antenna with switching diode," in *2006 IEEE Antennas and Propagation Society International Symposium.* IEEE, 2006, pp. 2337–2340.

[100] P. Ngamjanyaporn and M. Krairiksh, "Switched-beam single patch antenna," *Electronics Letters*, vol. 38, no. 1, p. 1, 2002.

[101] A. Mehta, D. Mirshekar-Syahkal, P. Massey, and H. Nakano, "A switched beam star patch antenna," in *2008 IEEE Antennas and Propagation Society International Symposium.* IEEE, 2008, pp. 1–4.

[102] P. K. Eranti and B. D. Barkana, "An overview of direction-of-arrival estimation methods using adaptive directional time-frequency distributions," *Electronics*, vol. 11, no. 9, p. 1321, 2022.

[103] X. Zhang, Y. Li, X. Yang, L. Zheng, T. Long, and C. J. Baker, "A novel monopulse technique for adaptive phased array radar," *Sensors*, vol. 17, no. 1, p. 116, 2017.

[104] Y.-X. Zhang, Q.-F. Liu, R.-J. Hong, P.-P. Pan, and Z.-M. Deng, "A novel monopulse angle estimation method for wideband LFM radars," *Sensors*, vol. 16, no. 6, p. 817, 2016.

[105] W. Kederer and J. Detlefsen, "Direction of arrival (DOA) determination based on monopulse concepts," in *2000 Asia-Pacific Microwave Conference. Proceedings (Cat. No. 00TH8522).* IEEE, 2000, pp. 120–123.

[106] K. F. Lee, K. M. Luk, and H. W. Lai, *Microstrip patch antennas.* World Scientific, 2017.

[107] M. Olyphant Jr and T. E. Nowicki, "Microwave substrates support MIC technology. I," *Microwaves*, vol. 19, pp. 74–76, 1980.

[108] M. A. Hossain, A. H. Murshed, M. A. Rahman, E. Nishiyama, and I. Toyoda, "A novel dual-band slot-ring array antenna using both-sided MIC technology for polarization detection," *International Journal of RF and Microwave Computer-Aided Engineering*, vol. 32, no. 11, p. e23373, 2022.

[109] C. M. Jackson and J. Newman, "Low cost, Ka-band microstrip patch monopulse antenna," *Microwave Journal*, vol. 30, p. 125, 1987.

[110] B. Andrews, T. Moore, and A. Niazi, "Millimeter wave microstrip antenna for dual polar and monopulse applications," in *3rd Int. Conf. Antennas and Propagation, ICAP*, vol. 83, 1983, pp. 12–15.

[111] H. Wang, D.-G. Fang, and X. Chen, "A compact single layer monopulse microstrip antenna array," *IEEE Transactions on antennas and propagation*, vol. 54, no. 2, pp. 503–509, 2006.

[112] R. Tanaka, E. Nishiyama, and I. Toyoda, "A mono-pulse DOA estimation antenna integrated with RF amplifiers and detection circuits," in *2014 IEEE Antennas and Propagation Society International Symposium (APSURSI).* IEEE, 2014, pp. 1833–1834.

[113] R. Rashid, E. Nishiyama, and I. Toyoda, "A planar extended monopulse DOA estimation antenna integrating an RF multiplier," *Progress In Electromagnetics Research C*, vol. 81, pp. 53–62, 2018.

[114] ——, "A 5.8-GHz planar beam tracking antenna using a magic-T," *Progress In Electromagnetics Research C*, vol. 76, pp. 159–170, 2017.

[115] K. Egashira, E. Nishiyama, and M. Aikawa, "Planar array antenna using both-sided MIC's feeder circuits," *Electronics and Communications in Japan (Part I: Communications)*, vol. 87, no. 7, pp. 23–30, 2004.